# The osteology and phylogenetic position of the loricatan (Archosauria: Pseudosuchia) *Heptasuchus clarki,* from the? Mid-Upper Triassic, southeastern Big Horn Mountains, Central Wyoming (U.S.A.)

**Sterling J Nesbitt** [Corresp., 1], **John M Zawiskie** [2, 3], **Robert M Dawley** [4]

[1] Department of Geosciences, Virginia Tech, Blacksburg, Virginia, United States

[2] Cranbrook Institute of Science, Bloomfield Hills, Michigan, United States

[3] Department of Geology, Wayne State University, Detroit, Michigan, United States

[4] Department of Biology, Ursinus College, Collegeville, Pennsylvania, United States

Corresponding Author: Sterling J Nesbitt
Email address: sjn2104@vt.edu

Loricatan pseudosuchians (known as “rauisuchians”) typically consist of poorly understood fragmentary remains known worldwide from the Middle Triassic to the end of the Triassic Period. Renewed interest and the discovery of more complete specimens recently revolutionized our understanding of the relationships of archosaurs, the origin of Crocodylomorpha, and the paleobiology of these animals. However, there are still few loricatans known from the Middle to early portion of the Late Triassic and the forms that occur during this time are largely known from southern Pangea or Europe. *Heptasuchus clarki* was the first formally recognized North American “rauisuchian” and was collected from a poorly sampled and disparately fossiliferous sequence of Triassic strata in North America. Exposed along the trend of the Casper Arch flanking the southeastern Big Horn Mountains, the type locality of *Heptasuchus clarki* occurs within a sequence of red beds above the Alcova Limestone and Crow Mountain formations within the Upper Chugwater Group. The age of the type locality is poorly constrained to the Middle – early Late Triassic and is likely similar to or just older than that of the Popo Agie Formation assemblage from the western portion of Wyoming. The holotype consists of associated cranial elements found in situ, and the referred specimens consist of crania and postcrania. Thus, about 30% of the osteology of the taxon is preserved. All of the pseudosuchian elements collected at the locality appear to belong to *Heptasuchus clarki* and the taxon is not a chimera as previously hypothesized. *Heptasuchus clarki* is distinct from all other archosaurs by the presence of large, posteriorly directed flanges on the parabasisphenoid and a distinct, orbit-overhanging postfrontal. Our phylogenetic hypothesis posits a sister-taxon relationship between *Heptasuchus clarki* and the Ladinian-aged *Batrachotomus*

*kupferzellensis* from current-day Germany within Loricata. These two taxa share a number of apomorphies from across the skull and their phylogenetic position further supports 'rauisuchian' paraphyly. A minimum of three individuals of *Heptasuchus* are present at the type locality suggesting that a group of individuals died together, similar to other aggregations of loricatans (e.g., *Heptasuchus*, *Batrachotomus*, *Decuriasuchus*, *Postosuchus*).

# The osteology and phylogenetic position of the loricatan (Archosauria: Pseudosuchia) *Heptasuchus clarki,* from the? Mid-Upper Triassic, southeastern Big Horn Mountains, Central Wyoming (U.S.A.)

Sterling J. Nesbitt[1], John M. Zawiskie[2] and Robert M. Dawley[3]

[1]Department of Geosciences, Virginia Tech, Blacksburg, VA 24061, U.S.A.
[2]Cranbrook Institute of Science, 39221 Woodward Ave, Bloomfield Hills, MI 48303 and Department of Geology Wayne State University, Detroit, MI 48202, U.S.A.
[3]Department of Biology, Ursinus College PO Box 1000 Collegeville, PA 19426, U.S.A.

Corresponding Author:
Sterling J. Nesbitt[1]
926 W. Campus Dr. Derring Hall, Virginia Tech, Blacksburg, VA, U.S.A.
Email address: sjn2104@vt.edu

## Abstract

Loricatan pseudosuchians (known as “rauisuchians”) typically consist of poorly understood fragmentary remains known worldwide from the Middle Triassic to the end of the Triassic Period. Renewed interest and the discovery of more complete specimens recently revolutionized our understanding of the relationships of archosaurs, the origin of Crocodylomorpha, and the paleobiology of these animals. However, there are still few loricatans known from the Middle to early portion of the Late Triassic and the forms that occur during this time are largely known from southern Pangea or Europe. *Heptasuchus clarki* was the first formally recognized North American “rauisuchian” and was collected from a poorly sampled and disparately fossiliferous sequence of Triassic strata in North America. Exposed along the trend of the Casper Arch flanking the southeastern Big Horn Mountains, the type locality of

*Heptasuchus clarki* occurs within a sequence of red beds above the Alcova Limestone and Crow Mountain formations within the Upper Chugwater Group. The age of the type locality is poorly constrained to the Middle – early Late Triassic and is likely similar to or just older than that of the Popo Agie Formation assemblage from the western portion of Wyoming. The holotype consists of associated cranial elements found in situ, and the referred specimens consist of crania and postcrania. Thus, about 30% of the osteology of the taxon is preserved. All of the pseudosuchian elements collected at the locality appear to belong to *Heptasuchus clarki* and the taxon is not a chimera as previously hypothesized. *Heptasuchus clarki* is distinct from all other archosaurs by the presence of large, posteriorly directed flanges on the parabasisphenoid and a distinct, orbit-overhanging postfrontal. Our phylogenetic hypothesis posits a sister-taxon relationship between *Heptasuchus clarki* and the Ladinian-aged *Batrachotomus kupferzellensis* from current-day Germany within Loricata. These two taxa share a number of apomorphies from across the skull and their phylogenetic position further supports 'rauisuchian' paraphyly. A minimum of three individuals of *Heptasuchus* are present at the type locality suggesting that a group of individuals died together, similar to other aggregations of loricatans (e.g., *Heptasuchus*, *Batrachotomus*, *Decuriasuchus*, *Postosuchus*).

## Introduction

During the Middle and Late Triassic, a variety of large pseudosuchian archosaur predators appeared across Pangea. These forms included long-snouted phytosaurs (Stocker and Butler 2013), sailed-back poposauroids (Nesbitt 2003; 2005; 2011; Butler et al. 2011; Nesbitt et al. 2011), short-faced ornithosuchids (von Baczko and Ezcurra 2013), and quadrupedal, large headed 'rauisuchians' – a group that has been traditionally classified together (Nesbitt et al. 2013a). 'Rauisuchians' have been found in nearly every well-sampled Middle to Upper Triassic deposit, but the anatomy and the relationships of these

pseudosuchians remains debated (Gower 2000; Brusatte et al. 2008; 2010; Nesbitt 2011; Nesbitt et al. 2013a). Namely, it is not clear if these 'rauisuchians' represent a natural group (traditional hypothesis; Brusatte et al. 2008; 2010), a grade leading to crocodylomorphs (Nesbitt 2011), or a combination of subclades and grades spread across Pseudosuchia (Nesbitt 2011; Nesbitt et al. 2013a). Luckily, over the past 20 years, huge headway has been made in uncovering their anatomy and relationships through the discovery of new taxa (e.g., *Batrachotomus kupferzellensis*; Gower 1999; Gower and Schoch 2009; *Postosuchus alisonae*, Peyer et al. 2008; *Decuriasuchus quartacolonia*, França et al. 2011; 2013; *Viveron haydeni*, Lessner et al. 2016; *Mandasuchus tanyauchen*, Butler et al. 2018), or new specimens of previously named taxa (e.g., *Arizonasaurus babbitti*, Nesbitt 2003; 2005; *Prestosuchus chiniquensis*, Roberto-Da-Silva et al. 2018; Mastrantonio et al. 2019; *Poposaurus gracilis,* Schachner et al. 2019) and revised and detailed descriptions (e.g., *Rauisuchus tiradentes*, Lautenschlager and Rauhut 2015; *Postosuchus kirkpatricki*, Weinbaum 2011; 2013; *Luperosuchus fractus*, Nesbitt and Desojo 2017; *Prestosuchus chiniquensis*, Desojo et al. 2020; *Ticinosuchus ferox*, Lautenschlager and Desojo 2011).

'Rauisuchians' from western central Pangea (now the western portion of North America) have been instrumental in helping untangle the relationships of 'rauisuchians' particularly and pseudosuchians in general. Remains of 'rauisuchians' occur through the Chinle Formation and Dockum Group (Long and Murry 1995) and now it is clear that nearly all of those taxa or unnamed forms can be sorted into two major groups, the Poposauroidea (*Poposaurus gracilis* and numerous shuvosaurids) and the rauisuchids (*Postosuchus kirkpatricki* and similar forms such as *Viveron haydeni*). To date, these two groups represent highly derived forms within Pseudosuchia and western North America is clearly lacking early diverging paracrocodylomorphs (e.g., *Mandasuchus tanyauchen* from Tanzania), early diverging loricatans (South American or Africa forms like *Prestosuchus chiniquensis*), or more 'middle' loricatan forms like *Batrachotomus kupferzellensis* (from Germany). Out of all of the forms from

current-day western North America, only one possible taxon fits into this gap *Heptasuchus clarki*, was the first formally recognized ‘rauisuchian’ in North America, but was only briefly described when named (Dawley et al. 1979). Moreover, *Heptasuchus clarki* occurs in Triassic sediments of central Wyoming, a place that few vertebrates of this age have been found. Since its naming, Long and Murry (1995) reevaluated parts of its anatomy and considered the taxon as a possible synonym of *Poposaurus,* whereas it has been mentioned as a ‘rauisuchian’, but not formally described or placed into a phylogenetic context.

In this paper, we fully detail the osteology of *Heptasuchus clarki* by describing the holotype skull and associated postcranial material from the type locality bone bed, provide details on a revised geologic setting and age for the taxon and evaluate its evolutionary affinities with other pseudosuchians.

## Methods

The holotype and original material collected during the original excavation were collected under with Bureau of Land Management permission. The TMM *Heptasuchus clarki* material was collected under a Bureau of Land Management permit (BLM Survey and Limited Surface Collection Permit PA09-WY-177) facilitated by Dale Hansen and additional help from Brent Breithaupt.

## Geological Setting: locality, regional, age, and associated assemblage

The *Heptasuchus clarki* type locality (= Clark Locality of Dawley et al. 1979) occurs within a sequence of red beds near the Red Wall Valley on the southeastern flank of the Big Horn Mountains in central Wyoming (Natrona County) within the Chugwater Group (Fig. 1). The *Heptasuchus clarki* bonebed occurs in a sequence of highly calcareous intraformational conglomerates, thin ripple marked highly bioturbated sandstone beds, silty micrites and reddish

brown to dusky red and intercalated green mudstones. All in situ material of *Heptasuchus clarki* (e.g., partial skull, some postcrania) (see below) was derived from 2 to 30 cm thick red mudstone / weathered red regolith (Fig. 1), which is exposed across the bonebed. All cranial elements were found in situ and disarticulated, but closely associated in a one-half square meter (Fig. 2) area in this red mudstone (Fig. 1). Nearly all of the surface collected specimens of *Heptasuchus clarki* and the associated assemblage were collected from the weathered red regolith. With the exception of a lungfish tooth (UW 11567) and a small centrum, no other bones were found below the red mudstone in the underling green mudstone, thin limestone, or conglomerate.

The depositional setting at the locality is inferred to have been a vegetated distal floodplain environment, periodically experiencing sheet floods and the development of ephemeral ponds and lakes. The sheet floods generated the intraformational conglomerates with calcareous nodules and mudstone clasts scoured from soils on the flood plain sediments. The limestone microconglomerates at the *Heptasuchus clarki* site indicate high-energy flood events and the silty micrites suggest post-flood deposition in lakes and ponded, abandoned channels.

The inclusion of the *Heptasuchus clarki* bonebed into a formal stratigraphic unit in the Chugwater Group on the southeastern flank of the Big Horn Mountains has been challenging and debated (Dawley et al. 1979; Lucas et al. 2002). These debates are the result of a number of factors including the lack of continuous outcrops in the area, the unique sedimentology of the unit that the *Heptasuchus clarki* bonebed lies in, the lack of clear lithostratigraphic signatures of other Triassic formations across Wyoming and the lack of unambiguous, and useful fossils for biostratigraphic correlation. It is clear that the *Heptasuchus clarki* type locality lies well above the Red Peak Formation and the Alcova Limestone given that both crop out locally within a kilometer and can be easily mapped. It is also clear that *Heptasuchus clarki* bonebed lies about

50 meters from the top of the Alcova Limestone and ~10 meters below the Jurassic-aged Gypsum Springs Formation (Fig. 1) which crops out on a nearby butte (~30 meters away).

The strata between the Alcova Limestone and the Gypsum Springs Formation have been assigned to a number of stratigraphic units. The Crow Mountain Sandstone lies directly on the Alcova Limestone and consists of sandstones with current crossbedding (Cavaroc and Flores 1991). The fluvial and lacustrine sediments stratigraphically above the Crow Mountain Sandstone, but below the Gypsum Springs Formation, have been assigned to the Popo Agie Formation based on the stratigraphic position and general lithology (Picard, 1978) or by fossil vertebrates from this area (Dawley et al. 1979; Lucas et al. 2002) whereas geologists working in the same area assigned these strata to the 'unnamed red beds' and hypothesize that the Popo Agie Formation in this region was removed by Jurassic erosion and is not present in the area (Cavaroc and Flores 1991; Irmen and Vondra, 2000). The sedimentology and sequence of these strata in question are demonstrably different from that of the Popo Agie Formation further west. High and Picard (1969) and Cavaroc and Flores (1991) interpreted the lenticular and sheet sandstones in the lower portion of the unnamed red beds as channel and splay deposits of a westward prograding fluvial deltaic plain, comparable to equivalent facies of the Jelm Formation (Picard, 1978), specifically the Sips Creek Member of the Jelm Formation of south-central Wyoming (Pipiringos and O'Sullivan 1978; Blakey et al. 1988; Cavaroc and Flores 1991). Cavaroc and Flores (1991) considered the calcareous sandstones, silty micrites and red mudstones of the upper portion of the unnamed red beds to be lake deposits that formed in passive areas of a well-integrated alluvial plain. This juxtaposition of fluvial deltaic in the lower portion and the fossiliferous fluvial - lacustrine facies also characterizes the relationship between the Jelm Formation and vertebrate-bearing lower portion of the Popo Agie Formation in the Wind River Range (High and Picard, 1969, Picard, 1978). The *Heptasuchus clarki* bonebed lies in the fluvial - lacustrine facies in the upper 10 meters of the unnamed red beds and there appears to be a clear color transition located just stratigraphically below the locality. Whether

157 this upper part of the unnamed red beds is equivalent to the Popo Agie Formation or part of the
158 Jelm Formation is not clear.
159
160 Age:
161 The age of the *Heptasuchus clarki* bonebed within the unnamed red beds is poorly
162 constrained because of the lack of both unambiguous correlations and biostratigraphically
163 informative fossils. No direct dating methods have been used in the area, but there is a lower
164 bound and upper bound. The Alcova Limestone from the local area was dated as Spathian or
165 earliest Anisian (Aegean) age as suggested by the position of the 87Sr/86Sr data on the global
166 marine 87Sr/86Sr curve (Lovelace and Doebbert 2015). The sequence is capped by the
167 Gypsum Springs Formation and this has been assigned a Jurassic age (High and Picard 1965;
168 Pipiringos and O'Sullivan 1978). Thus, the Crow Mountain Sandstone and the unnamed red
169 beds are constrained to Middle-Upper Triassic and this has been suggested by many (High and
170 Picard, 1969; Picard, 1978; Pipiringos and O'Sullivan 1978; Blakey et al. 1988; Cavaroc and
171 Flores 1991).
172 Further constraints on the age of the unnamed red beds was based on lithostratigraphic
173 correlation to units with biostratigraphically informative vertebrates. Historically, this region was
174 correlated with the Upper Triassic Popo Agie Formation from the Wind River Range and this
175 formation has a rich vertebrate record comprised of phytosaurs (Lees, 1907, Mehl 1915, Lucas
176 1994; Lucas et al. 2007), metoposaurids (Branson & Mehl, 1929), dicynodonts (Williston, 1904),
177 and a paracrocodylomorph (Mehl, 1915). The presence of metoposaurids and *Parasuchus* has
178 been taken to indicate an early Late Carnian age (*Paleorhinus* Biochron of Lucas 1998; Lucas
179 et al, 2007); however, the general validity of such biochrons is currently a contentious issue
180 (Rayfield, Barrett & Milner, 2009). Regardless, no clear Popo Agie Formation taxa have been
181 found at the *Heptasuchus clarki* bonebed; no phytosaur teeth or osteoderms and large
182 temnospondyl dermal fragments that are common throughout the Popo Agie Formation were

183 found directly at the locality. Metoposaurid dermal bone fragments and phytosaur teeth (UW
184 11571) have been found in the area (~5 km) of the *Heptasuchus clarki* bonebed but it is not
185 clear if these occur in the same stratigraphic unit. Furthermore, a *Hyperodapedon* rhynchosaur
186 was found to the north of the *Heptasuchus clarki* bonebed (Lucas et al. 2002) and the presence
187 of this genus of rhynchosaur was used to argue for an Upper Triassic age for the strata in this
188 area (including the *Heptasuchus clarki* bonebed). However, the correlation of the
189 *Hyperodapedon* locality and the *Heptasuchus clarki* bonebed is not clear and no diagnostic
190 rhynchosaur remains have been found at the *Heptasuchus clarki* bonebed.
191 Using what little age constraints are available, the age of the *Heptasuchus clarki*
192 bonebed could range from Middle to Late Triassic. Our best hypothesis concerning the age is
193 that the upper portion of the unnamed red beds at the *Heptasuchus clarki* type locality is
194 equivalent to, or just older than, that of the early Late Triassic Popo Agie Formation assemblage
195 from western Wyoming.
196
197 Associated assemblage:
198 The *Heptasuchus clarki* bonebed has produced the remains of at least four individuals of
199 *Heptasuchus clarki* (see below) as well as bones of much smaller vertebrates; these specimens
200 are represented in collections at UW (e.g., UW 11568-115670), TMM, USMN, and NMMNH. Of
201 the larger vertebrates, we hypothesize that all of the material pertains to *Heptasuchus clarki,*
202 although none of the postcrania is part of the holotype. The criticism that the material represents
203 a mix of a ‘rauisuchian’ and generically indeterminate phytosaur (Wroblewski 1997) is not
204 supported here given that 1) we have not seen clear evidence that there is more than one
205 ‘rauisuchian’ based on comparisons with *Batrachotomus kupferzellensis* and 2) we have not
206 positively identified any phytosaur crania, teeth, or postcranial material. Of the smaller
207 vertebrates, vertebrae, limb bones, small teeth, and other fragments were abundant on the
208 surface, but nearly all of these elements are broken (e.g., vertebral centra halves, limb bone

209 end). A single lungfish tooth was found at the locality (UW 11567). The identification of this
210 material is ongoing and will be the subject of another publication.
211

## 212 Systematic Paleontology

213 ARCHOSAURIA Cope, 1869 sensu Gauthier 1986
214 SUCHIA Krebs 1976 sensu Sereno et al. 2005
215 *Heptasuchus clarki* Dawley, Zawiskie, and Cosgriff 1979
216 "*Heptasuchus*"; Benton 1986: 298
217 "*Heptasuchus clarki"*; Bonaparte 1984: 213
218 "*Heptasuchus clarki"*; Parrish 1993: 301
219 "*Heptasuchus clarki"*; Juul 1994: 10
220 "*Heptasuchus clarkei"*; Long and Murry 1995: 154
221 "*Heptasuchus clarki"*; Lucas 1998: 364
222 "*Heptasuchus clarki"*; Alcober 2000: 313
223 "*Heptasuchus clarki"*; Gower 2000: 451
224 "*Heptasuchus clarki"*; Lucas et al. 2002: 150
225 "*Heptasuchus*"; Sulej 2005: 85
226 "*Heptasuchus*"; Lucas et al. 2007: 222
227 "*Heptasuchus*"; Peyer et al 2008: 363
228 "*Heptasuchus*"; Brusatte et al. 2010: 10
229 "*Heptasuchus clarki*"; de França et al. 2013: 473
230 "*Heptasuchus clarki*" Nesbitt et al. 2013a: 246
231

232 **Holotype:** UW 11562, partial skull (Figs. 2-7): right premaxilla (UW 11562-A); right maxilla (UW
233 11562-B); left maxilla (UW 11562-C); right jugal (UW 11562-D); left jugal (UW 11562-E); right
234 nasal (UW 11562F); right postfrontal, postorbital, partial frontal, and prefrontal (UW 11562-G);

occiput and braincase (UW 11562-H); left palatine (UW 11562-K); pterygoid? (UW 11562-L); pterygoid fragment (UW 11562-M); fragment of hyoid? (UW 11562-N); unidentified skull fragments (UW 11562-O through -R); loose teeth (UW 11562-AA through -AI). Here, the holotype is restricted to the cranial elements found in situ in quad A-3 (Fig. 2). No skull element is duplicated and the relative similar sizes of the elements suggest that the remains are from a single individual.

**Referred material:** quadrate head (UW 11563-AD); ventral condyles of left quadrate (UW 11563-AF, UW 11563-H); anterior cervical vertebra (UW 11562-T) ; posterior cervical centrum (UW 11564-A); posterior trunk vertebra (TMM 45902-2); neural spine of a cervical-trunk vertebra (UW 11562-CX); presacral neural spine (UW 11562-V); presacral neural spine (UW 11562-CT); anterior caudal vertebra (UW 11562-U); distal caudal vertebra (UW 11562-BW; UW 11563-A-C); osteoderm (TMM 45902-1); right partial scapula (UW 11565-E); right partial scapula (UW 11566-B); partial left coracoid (UW 11566); proximal portion of left humerus (UW 11565-A); left humerus (UW 11563-U); proximal portion of the radius (UW 11562-DM); distal portion of the radius (UW 11562-DI; UW 11562-DF); right ulna (UW 11562-W); left ulna (UW 11562-X); distal ends of ulnae (UW 11563-V; UW 11565-C); left pubis (UW 11562-Y); ilium fragment (UW 11563-Y); pubic peduncle of the right ilium (UW 11563-Z); left pubis (UW 11562-Y); proximal portion of the right ischium (UW 11564-B); proximal portion of a right femur (UW 11563-B); distal portion of the right femur (UW 11563-A); left tibia (UW 11562-Z); proximal portion of a right fibula (UW 11566-S); distal portion of the right fibula (UW 11566-R); proximal end of metatarsals (UW 11562-DH, UW 11562-DHU, UW 11562-DR); ungual (UW 11562-DT).

**Type Locality:** Clark locality; section 2l, TAON, RSQW, E Natrona County, Red Wall Valley, southern Big Horn Mountains, Wyoming, U.S.A.

**Stratigraphic Occurrence:** unnamed red beds of the Chugwater Group. Age = ?Middle Triassic to Upper Triassic (see above for details).

**Differential diagnosis:** *Heptasuchus clarki* differs from all other suchians except for *Batrachotomus kupferzellensis* in possessing the following combination of character states: exit for cranial nerve V within prootic (shared with *Postosuchus*); a depression on the anterolateral surface on the ventral end of the postorbital (character 425- state 1); a deep depression on the posterodorsal portion of the lateral surface of the ventral process of the postorbital (427-1); a distinct fossa with a rim present on the nasal at the posterodorsal corner of the naris (430-1); the anteroventral corner of the maxilla extensively laterally overlaps the posteroventral corner of the premaxilla (431-1); and an anteroposteriorly trending ridge on the lateral side of the jugal that is asymmetrical dorsoventrally where the dorsal portion is more laterally expanded than the ventral portion (433-1). Furthermore, *Heptasuchus clarki* and *Batrachotomus kupferzellensis* share the following two homoplastic characters within Archosauria: Concave anterodorsal margin at the base of the dorsal process of the maxilla (25-1); and dorsolateral margin of the anterior portion of the nasal with distinct anteroposterior ridge on the lateral edge (35-1: Rauisuchidae synapomorphy also).

*Heptasuchus clarki* differs from *Batrachotomus kupferzellensis* in that *Heptasuchus clarki* lacks a division in the fossa between the basitubera and basipterygoid processes (=median pharyngeal recess) of the parabasisphenoid, the presence of large and posteriorly pointed processes on the posterior portion of the basipterygoid processes*; paroccipital processes more broadly expanded distally; no kink in the ventral process of the postorbital (note, not all *Batrachotomus kupferzellensis* specimens have the kink e.g., SMNS 52970); anterior portion of the maxilla is less expanded and has a smaller foramen between maxilla and the premaxilla; palatal process of premaxilla is more expanded medially; palatal process of the maxilla continuous with anterior edge of maxilla (the palatal process is hidden under a flange of

bone laterally in *Batrachotomus kupferzellensis*); and the anterolateral corner of postfrontal of *Heptasuchus clarki* is blunt and squared off in dorsal view*. Asterisks denote autapomorphies of *Heptasuchus clarki*.

**Ontogenetic status**: The ontogenetic stages of the specimens of *Heptasuchus clarki* are difficult to assess given the holotype contains only skull elements and the postcrania of the taxon has poor association with cranial or other postcranial remains. An ontogenetic age assessment based on the skull (e.g., fusion events) is not reliable in archosaurs (Bailleul et al. 2016). With the exception of a complete tibia and nearly complete ulna, no other limb bones, such as the femoral fragments have a midshaft that could be used for histological analysis. Fragments of limb bones are available, even so, identification of the element based on a limb shaft is difficult and the orientation of the fragments and overall size of the limb would be difficult to assess for comparative purposes. Of the few vertebrae recovered, all neurocentral sutures appear to be fully closed (Brochu 1996; Irmis 2007). This is clear in the partial cervicals, trunk and anterior caudal vertebrae. Based on this cursory assessment, the specimens of *Heptasuchus clarki* are not young individuals, but their ontogenetic stage is largely unconstrained with the available evidence.

**Notes**: The original holotype of *Heptasuchus clarki* (Dawley et al.1979) was amended by Zawiskie and Dawley (2003), who restricted it to the in situ cranial material collected in 1977 in quads A-1 and A-2 of the excavation grid at the Clark locality (see grid in Dawley, 1979 or supplementary materials) following the criticism that the taxon may represent a chimera (Wroblewski 1997). Much of the bonebed was weathered and many bone fragments littered the ground and these specimens were collected in 1977-1979 and in 2009-2010. The association of the postcranial elements is not known but are assigned to *Heptasuchus clarki* based on similarity among elements and similarity to the almost completely known anatomy of

313 *Batrachotomus kupferzellensis* (Gower 1999; Gower and Schoch 2009); we are assuming that
314 all of the archosaur material that is similar in comparative size emanates from a single taxon of
315 loricatan. Therefore, we only refer material to the taxon and do not create paratype specimens.
316 The locality has a minimum number of three individuals (MNI =3) of similar size, as deduced
317 from the number of right distal ends of the ulna.
318

## 319 Comparative Morphological Description

320 **General skull:** Most of the skull of the holotype specimen (UW 11562-A through -S) was
321 recovered as separate, disarticulated bones, except for the postorbital-postfrontal-frontal
322 prefrontal section and the braincase-parietal. The total complement of bones is by no means
323 complete and several elements (lacrimal, squamosal, quadratojugal, and quadrate) are not
324 represented on either the right or left side. However, sufficient material is preserved to provide a
325 reconstruction of most areas of the skull (Fig. 3) and skeleton (Fig. 4). Only the quadrate region
326 is totally unknown, and the palate is represented only by a single fragment. We estimate the
327 skull to be about 56 cm long.
328 The following describes the general aspect of the skull and details of each element are
329 included below. The skull is long and narrow with the preorbital (tooth-bearing) length about
330 two-thirds that of the total length. In lateral view (Fig. 3), the lower margin of the skull forms,
331 roughly, an obtuse angle whose apex points ventrally and is located at the level of the sixth
332 maxillary tooth. There are three premaxillary and nine maxillary teeth preserved. A small
333 subnarial fenestra is present between the premaxilla and the maxilla (see more details below),
334 but this area is damaged. Posteriorly, a moderately large antorbital fenestra lies in a recessed
335 antorbital fossa. The orbit is ‘keyhole shaped,’ and this configuration reflects the expansion of
336 the lower part of the enlarged infraorbital fenestra. In the area of the nasal, the lateral borders of
337 the skull roof form a pair of elevated ridges, which flank a shallow depression in the center of

the dorsal surface of the skull roof. The supratemporal fenestra is small, triangular, and surrounded by a supratemporal fossa.

**Premaxilla:** The premaxilla is only known from the right side (UW 11562-A; Fig. 5E-F) and lacks the anterior portion of the first preserved alveolus, the posterior end of the third alveolus, and the entirety of the anterodorsal (=narial) process. *Heptasuchus clarki* was originally described as having three premaxillary teeth, but the tooth-bearing margin is incomplete. At least three premaxillary teeth are present, but the exact number of premaxillary teeth is unknown. The body of the premaxilla is rounded laterally and does not preserve a distinct narial fossa anteroventral to the external naris, a distinct feature of the premaxilla of *Batrachotomus kupferzellensis*. No foramina are apparent on the premaxilla, but this is possibly the result of a highly fractured and partially weathered surface.

Two prominent processes are preserved, a palatal and a posterodorsal (=maxillary) processes. The posterodorsal process is straight, slender, and projects 30$^{o}$ posterodorsally. The posterodorsal edge of the process forms a concave margin that frames part of the posterior margin of the external naris. The relative length of the process compared to the length of the premaxillary body is similar to that of *Postosuchus kirkpatricki* (TTUP 9000) and *Rauisuchus tiradentes* (BSPG AS XXV-60-121), longer than that of *Batrachotomus kupferzellensis* (Gower 1999), and is much shorter than the longer, more robust, and arched subnarial processes present in *Saurosuchus galilei* (PVSJ 32) and *Luperosuchus fractus* (PULR 04; Nesbitt and Desojo 2017). A small foramen is located in the body of the premaxilla ventral to the base of the posterodorsal process. The base of the posterodorsal process is not laterally expanded into a bulge posteroventral of the external naris as in *Rauisuchus tiradentes* (BSPG AS XXV-60-121; Lautenschlager and Rauhut 2015), *Vivaron haydeni* (Lessner et al. 2016), *Postosuchus kirkpatricki* (Weinbaum 2011), and *Polonosuchus silesiacus* (Sulej 2005).

363 The palatal process is a broad, flat, transversely oriented sheet of bone that originates at
364 the dorsal margin of the tooth row and projects medially to contact its antimere. Ventrally, the
365 palatal process forms the base of a ventrally opening fossa. The process forms the anterior
366 edge of the anterior portion of the palate, as in *Saurosuchus galilei* (Alcober 2000). The
367 posterior edge of the process articulates with the vomer.
368
369 **Maxilla:** The posterior two-thirds of the right maxilla (UW 11562-B; Fig. 5C-D) and the anterior
370 half of the tooth-bearing portion of the left maxilla (UW 11562-C; Fig. 5A-B) are present in the
371 holotype of *Heptasuchus clarki*. Only the base of the dorsal (=ascending) process is preserved.
372 The left maxilla preserves the first six alveoli and the preserved portion of the right maxilla
373 preserves eight alveoli. As reconstructed (Fig. 3; Dawley et al. 1979), a complete maxilla would
374 have a minimum of ten teeth, as determined by overlap of the two preserved maxillae; the
375 anteriormost alveolus from the left maxilla fragment is considered to be equivalent to the
376 anteriormost alveolus of the right maxillary fragment. As reconstructed, the maxilla is a massive,
377 rectangular bone with a deep body similar to that of *Fasolasuchus tenax* (PVL 3851),
378 *Batrachotomus kupferzellensis* (SMNS 80260) and *Saurosuchus galilei* (PVSJ 32).
379 The anterior portion of the maxilla is well preserved. The lateral surface is rather flat and
380 not laterally expanded. The anterior margin of the maxilla is convex. A small notch is present
381 where the anterolateral portion of the maxilla meets its palatal process. This notch is similar to
382 that of *Batrachotomus kupferzellensis* (SMNS 52970), *Saurosuchus galilei* (PVSJ 32),
383 *Fasolasuchus tenax* (PVL 3851), and *Postosuchus kirkpatricki* (TTUP 9000). In these taxa, a
384 foramen is formed between the articulation of the premaxilla and maxilla when in articulation;
385 this morphology was discussed at length by Gower (2000) and Nesbitt (2011). *Heptasuchus*
386 *clarki* was originally reported (Dawley et al. 1979) to have an elongated fenestra between the
387 maxilla and premaxilla, similar to what was reported in *Saurosuchus galilei* (PVL 2062; Reig
388 1959) and *Luperosuchus fractus* (PULR 04; Romer 1971). However, it appears that these

389 elongate fenestrae are the result of disarticulation or deformation (see Nesbitt 2011; Nesbitt and
390 Desojo 2017). Therefore, the elongated fenestra reconstructed in *Heptasuchus clarki* (Fig. 2 of
391 Dawley et al. 1979) is likely not present. An anteriorly opening foramen is present within the
392 notch between the lateral side of the maxilla and the palatal process which is also found in
393 *Postosuchus kirkpatricki* (Weinbaum (2011). Another, smaller anteriorly opening foramen is
394 located just posterodorsal to the foramen in the notch. The transition between the lateral side of
395 the maxilla and the palatal process is continuous as in *Postosuchus kirkpatricki* (TTUP 9000)
396 and *Fasolasuchus tenax* (PVL 3851), a condition in contrast to *Batrachotomus kupferzellensis*
397 (SMNS 52970) where there is a distinct step. There is no clear facet on the anterodorsal surface
398 of the maxilla for the posterodorsal process of the premaxilla. Here, the surface is incompletely
399 preserved but appears to be concave in lateral view between the palatal process and the base
400 of the dorsal process, as in *Batrachotomus kupferzellensis* (SMNS 52970). It is unknown if the
401 mediolaterally compressed ridge of bone that forms the anterodorsal margin of the maxilla
402 contributed to the border of the external naris as it does in *Batrachotomus kupferzellensis*
403 (Gower 1999). The base of the dorsal process is oval in cross-section, similar to what is present
404 in *Batrachotomus kupferzellensis* (SMNS 52970) and *Arizonasaurus babbitti* (MSM 4590) rather
405 than the anteroposteriorly elongated cross-sections of taxa such as *Postosuchus kirkpatricki*
406 (TTUP 9000).

407 The entire lateral side of the maxilla ventral to the antorbital fossa is covered in small
408 ridges and shallow grooves much like that in the holotype of *Saurosuchus galilei* (PVL 2062). A
409 slight bank marks the division of the antorbital fossa from the main body of the maxilla as in
410 *Fasolasuchus tenax* (PVL 3851), *Batrachotomus kupferzellensis* (SMNS 52970), and
411 *Saurosuchus galilei* (PVSJ 32) and not separated by a distinct step as in *Polonosuchus*
412 *silesiacus* (ZPAL Ab III/563) and *Postosuchus kirkpatricki* (TTUP 9000). The depth of the
413 antorbital fossa deepens posteriorly in *Heptasuchus clarki* as well as *Fasolasuchus tenax* (PVL
414 3851), *Batrachotomus kupferzellensis* (SMNS 52970), *Saurosuchus galilei* (PVSJ 32), a

specimen referred to *Prestosuchus* (UFRGS-PV 156 T), and in the crocodylomorph *Dromicosuchus grallator* (NCSM 13733). The posterior portion of the maxilla expands dorsally as in *Turfanosuchus dabanensis* (IVPP V33237) and gracilisuchids, unlike most loricatans. The bone that forms the antorbital fossa is thin posteriorly as in *Postosuchus kirkpatricki* (TTUP 9000), *Fasolasuchus tenax* (PVL 3851), *Batrachotomus kupferzellensis* (SMNS 52970) and other archosaurs (e.g., *Xilousuchus sapingensis,* IVPP V6026). The tooth bearing ventral margin is convex for the length of the element as in *Batrachotomus kupferzellensis* (SMNS 52970).

The first alveolus is the smallest in the maxilla as is typical for most taxa classically grouped as “rauisuchians” (Brusatte et al. 2009). The alveoli increase in size posteriorly to the fourth and fifth alveolus then gradually decrease in size posteriorly based on our reconstructed maxilla from the two pieces. All of the alveoli are ovate in ventral view.

In medial view, a step separates the medial surface of the maxilla from the interdental plates. The step in horizontally oriented and extends the length of the preserved section of maxilla. Anteriorly, the step is located in the dorsoventral middle of the body of the maxilla as in *Fasolasuchus tenax* (PVL 3851) and *Batrachotomus kupferzellensis* (SMNS 52970) whereas the step is located in the ventral third of the anteromedial surface of the maxilla of *Postosuchus kirkpatricki* (TTUP 9000). The anteriormost portion of the step disappears posterior to the anterior termination of the maxilla in *Heptasuchus clarki*. The palatal process is horizontally oriented at the anterodorsal portion of the maxilla. The process is thin dorsoventrally as in *Fasolasuchus tenax* (PVL 3851) and *Batrachotomus kupferzellensis* (SMNS 52970) whereas the process is dorsoventrally deeper in *Postosuchus kirkpatricki* (TTUP 9000). A distinct fossa on the ventral surface of the palatal process is present in *Heptasuchus clarki* and a similar deep fossa is on the ventral surface of the palatal process is also present in *Polonosuchus silesiacus* (ZPAL Ab/III 563), *Fasolasuchus tenax* (PVL 3851), *Batrachotomus kupferzellensis* (SMNS 52970), and the crocodylomorph *Sphenosuchus acutus* (SAM 3014), but absent in *Saurosuchus*

(PVSJ 32) and poposauroids (e.g., *Xilousuchus sapingensis*) (see character 426 in the appendix). Along the ventral half of the medial surface of the tooth row, the internal walls of the alveoli are formed by fused interdental plates at least anteriorly. The interdental plates of all *Batrachotomus kupferzellensis* specimens (e.g., SMNS 52970) are unfused and separated as triangular sheets of bone), whereas the interdental plates of *Postosuchus kirkpatricki* (TTUP 9000) and *Teratosaurus suevicus* (NHMUK 38646) are rectangular and meet on their anterior and posterior sides and this contact extends to the ventral extent of the medial side of the the maxilla. A thin line marks the contact of the interdental plates in *Postosuchus kirkpatricki* (Weinbaum 2011; TTUP 9000, 9002) whereas there is no differentiation between the individual plates in *Teratosaurus suevicus* (NHMUK 38646). The loss of the medial surface on the posterior half of the maxilla has exposed the tips of replacement teeth medial to the roots of the fully erupted teeth. Posteriorly, the maxilla separates into two portions, a ventral portion that houses the alveoli and a mediolaterally thin dorsal portion. The ventral portion tapers posteroventrally and expands more posteriorly than the thin dorsal portion. A posteriorly opening foramen lies at the juncture of the ventral and dorsal portions. Here, a faint facet for the articulation with the jugal can be followed posteriorly on the dorsal surface of the maxilla.

**Nasal:** A nearly complete right nasal (UW 11562-F) is known for *Heptasuchus clarki* (Fig. 5G-H); only the anterior portion that meets the anterodorsal (=nasal) process of the premaxilla is missing. The nasal formed the posterodorsal portion of the external nares. The anterior half of the nasal splits into a robust anterior process that would have met the anterodorsal process of the premaxilla, if complete, and a shorter, anteroventrally directed process that lies on the anterodorsal margin of the maxilla. The anterior process bows dorsally to form a “roman nose” similar to that of *Batrachotomus kupferzellensis* (Gower 1999), *Saurosuchus galilei* (PVSJ 32), a skull assigned to *Prestosuchus chiniquensis* (UFRGS T-156), *Luperosuchus fractus* (PULR 04;

Nesbitt and Desojo 2017), and *Decuriasuchus quartacolonia* (França et al. 2011). The lateral surface of the anterior process bears a rugose lateral ridge that continues posteriorly to the articular surface with the lacrimal. This ridge is similar to that in *Postosuchus kirkpatricki* (TTUP 9000) and *Batrachotomus kupferzellensis* (Gower 1999). A distinct fossa is present posterodorsal to the external naris at the junction of the anterior process and the anteroventral process. The fossa is well defined and is similar to that of *Batrachotomus kupferzellensis* (Gower 1999) (see character 430) and an isolated nasal fragment (NMMNH 55779) from the Middle Triassic Moenkopi Formation of New Mexico (Schoch et al. 2010). The anteroventral process tapers just ventral to the posterior extent of the external naris. The location of the anterior termination of this process is not known and it is not clear if the process met the posterodorsal process of the premaxilla, hence excluding the maxilla from the external naris, as in the case in *Batrachotomus kupferzellensis* (Gower 1999).

The nasal articular surfaces with the maxilla and lacrimal lie at the ventrolateral edge and are oriented almost vertically, indicating a nearly perpendicular contact between these bones and the nasal. It appears that the nasal formed the anterodorsal portion of the antorbital fossa in *Heptasuchus clarki* as in *Batrachotomus kupferzellensis* (Gower 1999) but not in *Postosuchus kirkpatricki* (TTUP 9000) or *Saurosuchus galilei* (PVSJ 32). Dorsally, the surface medial to the lateral ridge is dorsoventrally thin and concave at the midline like that of *Postosuchus kirkpatricki* (TTUP 9000, 9002), *Batrachotomus kupferzellensis* (Gower 1999), the crocodylomorph *Sphenosuchus acutus* (Walker 1990) and *Turfanosuchus dabanensis* (IVPP V3237). This concave depression narrows anteriorly until it disappears just posterior to the division of the anterior portion of the nasal.

The medial surface of the nasal bears a dorsoventrally thick midline suture that thins posteriorly. The suture itself bears a series of complex grooves and ridges. The medial surface is largely concave anteriorly and flat posteriorly where the nasal is dorsoventrally thin.

492 **Jugal:** Both the right and left jugals of *Heptasuchus clarki* are represented in the holotype (UW
493 11562-D and -E, respectively; Fig. 6D-F). The right jugal is missing the dorsal end of the
494 ascending process and the posterior portion of the posterior process whereas the left element is
495 missing much of the posterior process. The jugal is a triradiate structure, with two dorsal
496 processes contributing to the ventral portions of the anterior and posterior walls of the orbit and
497 a posterior process forming much of the lower margin of the infratemporal fenestra. The
498 anterodorsal process projects forward at approximately 50° anterodorsally along its contact with
499 the maxilla. Elongated groove and ridges mark the articulation with the maxilla and this
500 articulation terminates posteriorly in an acute angle within the body of the jugal. A similar
501 termination within the jugal is present in *Batrachotomus kupferzellensis* (SMNS 52970) as well
502 as *Revueltosaurus callenderi* (PEFO 34561) and aetosaurs (Nesbitt 2011). The anterodorsal
503 process trends mediolaterally in the dorsal direction where it would meet the lacrimal. The
504 articular surfaces with the maxilla and the lacrimal are separated by a distinct anteroposteriorly
505 trending ridge that continues posteriorly as the laterally expanded jugal ridge. Anteriorly, this
506 ridge is sharp, mediolaterally thin, hides parts of the lateral side of jugal in lateral view, and
507 dorsally forms a small shelf. A similar shelf is present in *Batrachotomus kupferzellensis* (SMNS
508 52970) and definitely absent in *Postosuchus kirkpatricki* (TTUP 9000) and *Saurosuchus galilei*
509 (PVSJ 32). The anterior surface shifts vertically at the anterior edge, and terminates in a sutural
510 surface with the lacrimal. The lacrimal appears to have articulated with the lateral side of the
511 jugal but the details of this articulation are not clear.
512 The prominent jugal ridge on the lateral side of the body of the jugal of *Heptasuchus*
513 *clarki* continues for the length of the jugal. The lateral side of the ridge is covered in small
514 anteroposteriorly trending ridges and lacks the long grooves present in *Batrachotomus*
515 *kupferzellensis* (SMNS 52970). In its anteroposterior center, the lateral ridge is asymmetrical
516 with the dorsal portion more laterally expanded then the ventral portion. This asymmetry is also
517 present *Batrachotomus kupferzellensis* (SMNS 52970) whereas other paracrocodylomorphs

(e.g., *Postosuchus kirkpatricki*, *Saurosuchus galilei*) have a dorsoventrally symmetrical lateral ridge. The posterior process is rectangular in cross-section and the ventral edge of the jugal is nearly straight.

The dorsal process of the jugal arcs posterodorsally at its dorsal termination. The lateral side bears a shallow fossa at the base and on the posterior half of the process. A similar fossa is also present in *Batrachotomus kupferzellensis* (SMNS 52970). The anterior edge of the dorsal process is mediolaterally thin and distinctly convex as in *Batrachotomus kupferzellensis* (SMNS 52970) whereas the anterior edge is typically straight in other loricatans (e.g., *Postosuchus kirkpatricki*; TTUP 9000). The anterior bowing of the anterior edge of the dorsal process of *Heptasuchus clarki* suggests that the ventral portion of the orbit is more anteroposteriorly restricted than the dorsal portion of the orbit. Therefore, it is clear that *Heptasuchus clarki* had a 'keyhole shaped' (sensu Benton and Clark 1988) orbit as with non-crocodylomorph loricatans and other large carnivorous archosaurs (e.g., allosaurids, tyrannosaurids). In *Heptasuchus clarki*, the thin anterior margin hides the articular surface with the postorbital. The concave posterior margin of the process is mediolaterally thin. Overall, the dorsal process is subcircular in cross-section at its base.

Medially, the body of the jugal is convex anteriorly and concave posteriorly. The posterior process bears an anteroposteriorly oriented groove that is also present in the loricatans *Batrachotomus kupferzellensis* (SMNS 52970), *Postosuchus kirkpatricki* (TTUP 9000), some crocodylomorphs (e.g., *Sphenosuchus acutus*, Walker 1990) and in phytosaurs (Stocker 2010; Stocker and Butler 2013). Anteriorly, just ventral to the dorsal process, the groove divides the articular facets for the ectopterygoid. The head of the ectopterygoid likely split into two lateral heads as with *Batrachotomus kupferzellensis* (SMNS 80260), *Postosuchus kirkpatricki* (Weinbaum 2011), and crocodylomorphs (e.g., *Sphenosuchus acutus*, Walker 1990). The dorsal articular surface for the ectopterygoid is round and poorly defined whereas the ventral articulation is well defined and extends to the ventral edge of the jugal. The articular

surface with the postorbital lies on the anteromedial edge of the dorsal process and extends ventrally for much of the length of the dorsal process. Therefore, the anterior edge is mediolaterally thick. Anteriorly, the jugal has a shallow fossa on the ventral edge, opposite the articular facets. A small channel is present between the fossa and the ventral articular surface with the ectopterygoid.

**Skull roof elements:** A large fragment of the skull roof (UW 11562-G) comprises the right prefrontal, postfrontal, frontal, and postorbital (Fig. 6A-C). With the exception of the frontal, the elements are essentially complete, but microfracturing has obscured the sutural contacts between them.

The prefrontal (Fig. 6C) lies on the anterolateral edge of the frontal and forms the anterodorsal corner of the orbit. The lateral margin bears a rugose lateral ridge that could have been continued from the nasal to the lacrimal to the prefrontal as in rauisuchids and *Batrachotomus kupferzellensis*. The posterolateral margin of the prefrontal does not have a clear sutural contact for a supraorbital element or palpebral(s) that are present on the prefrontal in *Saurosuchus galilei* (PVSJ 32) and *Postosuchus kirkpatricki* (TTUP 9000; Weinbaum 2011; Nesbitt et al. 2013b). A rugose articulation with the lacrimal located on the anterior portion of the prefrontal is inset from the lateral margin and rounded posteriorly. The ventral end of the prefrontal is broken.

The anterior and medial parts of the frontal are incomplete (Fig. 6). The frontal clearly contributes to the lateral margin of the orbit. Here, the lateral orbital margin is rounded and slightly rugose. The preserved portion of the dorsal surface of the frontal is smooth, but much of the surface is poorly preserved and fragmented. The suture between the postfrontal and the frontal is clear on the ventral surface of the elements. Posteriorly, it appears that part of the supratemporal fossa is present on the frontal as in crocodylomorphs, dinosaurs, and *Batrachotomus kupferzellensis* (SMNS 80260) (Nesbitt 2011). In *Postosuchus kirkpatricki*

(TTUP 9000), a supratemporal fossa is present anterior to the supratemporal fenestra, but present almost entirely on the postfrontal (Weinbaum 2011; Nesbitt 2011) with only the medial portion of the frontal participating in the fossa. Thus, among non-crocodylomorph loricatans, a fossa on the posterior portion of the frontal seems to be restricted to *Heptasuchus clarki,* *Batrachotomus kupferzellensis,* and *Postosuchus kirkpatricki*. The posterior edge of the frontal appears to contribute to the border of the supratemporal fenestra.

The postfrontal lies at the posterodorsal edge of the orbit (Fig. 6). In dorsal view, the anterolateral corner angle is nearly 90$^{o}$ from the anterior orbital margin to the lateral margin. The anterior and the lateral edges of the element are rounded and have small grooves on them. The body of the postfrontal dorsally overhangs the postorbital where the two elements meet. The medial portion tapers posteromedially between the frontal and the postorbital, and apparently is not part of the supratemporal fossa.

The postorbital is nearly completely preserved (Fig. 6). The postorbital has two components, a dorsal portion, which forms part of the skull table and a ventral process, which separates the orbit and infratemporal fenestra. The dorsal portion is a flat, mediolaterally expanded element which forms the lateral portion of the supratemporal fenestra. The medial side of the postorbital bears a supratemporal fossa that is continuous with the fossa of the frontal. This is also present in *Batrachotomus kupferzellensis* (SMNS 80260) and in *Postosuchus kirkpatricki* (Weinbaum 2011). The fossa shallows posteriorly and disappears at the posterior portion. A posterolaterally directed ridge originates at the border of the supratemporal fenestra and crosses the postorbital to terminate on the lateral edge of both *Heptasuchus clarki* and *Batrachotomus kupferzellensis* (SMNS 80260). The posterior portion of the postorbitals of *Heptasuchus clarki, Batrachotomus kupferzellensis* (SMNS 80260), and *Postosuchus kirkpatricki* (TTUP 9000) are relatively wider than that of *Saurosuchus galilei* (PVSJ 32), a skull assigned to *Prestosuchus chiniquensis* (UFRGS T-156), and *Luperosuchus fractus* (UNLR 04). The posterior portion of the postorbital of *Heptasuchus clarki* appears to

596 overlay the squamosal as in *Batrachotomus kupferzellensis* (SMNS 80260), and *Postosuchus*
597 *kirkpatricki* (TTUP 9000) (see character 428).
598 The laterally oriented, rugose ridge continues from the postfrontal to the postorbital. The
599 ridge splits into ventral and posterior components, with a small gap on the anterior side where
600 the ridges come together (Fig. 6C). The ventral ridge forms the posterior margin of the orbit for
601 the length of the ventral process. Directed ventrally at its origin, the ridge, along with the ventral
602 process, curves gradually anteroventrally creating an arc of nearly 50°. The ridge is rugose and
603 similar to that of *Batrachotomus kupferzellensis* (SMNS 80260) although the degree of rugosity
604 differs among *Batrachotomus kupferzellensis* individuals (SMNS 80260 versus SMNS 52970).
605 Posterior to the dorsal portion of the ridge, a large fossa is present that is roofed by the dorsal
606 portion of the postorbital. This deep fossa is also present in *Batrachotomus kupferzellensis*
607 (SMNS 80260) and also, to a lesser degree in *Saurosuchus galilei* (PVSJ 32), a skull assigned
608 to *Prestosuchus chiniquensis* (UFRGS T-156), and *Postosuchus kirkpatricki* (TTUP 9000). The
609 ridge terminates dorsoventrally in a broad flange that clearly entered the orbit and contributed to
610 the ‘keyhole shape’ of the orbit. Additionally, a deep fossa is present on the anterodorsal side of
611 the ventral termination of the postorbital. This deep fossa, which extends dorsally into the
612 ventral process, is only visible in anterior view. A similar feature is also present in
613 *Batrachotomus kupferzellensis* (SMNS 80260) and was originally considered to be an
614 autapomorphy of the taxon by Gower (1999) (see character 428). However, the fossa in
615 *Batrachotomus kupferzellensis* is located only on the lateral surface whereas the feature in
616 *Heptasuchus clarki* is only on the anterodorsal surface. It is not clear if this difference is the
617 result of crushing in *Heptasuchus clarki*. Moreover, the depth of the fossa differs among
618 *Batrachotomus kupferzellensis* individuals (SMNS 80260 versus SMNS 52970).
619 The ventral process of the postorbital is subrectangular in cross-section for the length of
620 the element. The ventral process lacks the ‘kink’ as seen in *Batrachotomus kupferzellensis*
621 (SMNS 80260), *Postosuchus kirkpatricki* (TTUP 9000), and *Saurosuchus galilei* (PVSJ 32).

However, this ‘kink’ is subtle in taxa with the feature and may be difficult to detect if parts of the posteroventral margin of the ventral process are incomplete. In medial view, a shallow and broad groove posterior to a ridge on the anterior edge of the ventral process marks the articulation with the dorsal process of the jugal. The articular surface with the jugal is restricted to the posteroventral side of the ventral process. A shallow fossa is present at the dorsal margin of the ventral process and may represent the articular surface with the laterosphenoid.

**Parietal:** Only the lateral portion of the occipital process of the right parietal is preserved (Fig. 7). The process remains in articulation with the supraoccipital and possibly touches the paroccipital process posterior laterally. The vertically oriented process forms the dorsal portion of a large post temporal fenestra. A distinct ridge is present on the anterior side of the lateral process.

**Occiput and Braincase:** The three dimensionally preserved braincase (UW 11562-H) is largely complete on the right side and preserves the opisthotic, exoccipital, occipital and parabasisphenoid, prootic, and the right half of the supraoccipital (Fig. 7). The braincase elements are still in articulation with the occipital process of the right parietal. The bone surface is well preserved and details of the morphology of the medial surfaces are readily apparent. The braincase is well ossified and sutures between most elements cannot be distinguished in most cases.

The basioccipital forms the majority of the occipital condyle and the exoccipitals are completely fused to the dorsolateral surfaces (Fig. 7). A small notochordal pit is present on the dorsal portion of the basioccipital. The condylar stalk (=neck) is well expanded and a distinct rim outlines the circumference of the basioccipital. The preserved portion of the foramen magnum is semicircular in shape and its flattened floor extends onto the dorsal surface of the occipital condyle. The basitubera originate at the ventral portion of the occipital condyle and stretch

ventrolaterally. As with *Batrachotomus kupferzellensis* (SMNS 80260), the basitubera are bilobed and are separated from the basitubera of the parabasisphenoid by an unossified gap. The unossified gap of *Heptasuchus clarki* is large like that of *Saurosuchus galilei* (PVSJ 32). The lateral edge of the more lateral lobe of the basitubera is continuous with the lateral ridge (sensu Gower 2002) that originates on the exoccipital. The more medial lobe of *Heptasuchus clarki* is larger and is distinctly convex in contrast to that of the basitubera of *Postosuchus kirkpatricki* (TTUP 9000). There is no division between the basioccipital and the parabasisphenoid at the midline.

Only the right exoccipital is fully preserved (Fig. 7). The exoccipitals meet on the midline similarly to most pseudosuchians other than crocodylomorphs and shuvosaurids (Nesbitt 2011). The lateral side of the exoccipital bears a lateral ridge that obstructs the descending process of the opisthotic in posterior view, similar to that of *Batrachotomus kupferzellensis* (SMNS 80260), *Postosuchus kirkpatricki* (Weinbaum 2011), crocodylomorphs and aetosaurs (Gower and Walker 2002). Two foramina, interpreted as the exits of cranial nerve XII, pierce the medial surface of the exoccipital. However, only one exit cranial nerve XII can be observed on the lateral side of the exoccipital. This exit is located anterior to the lateral ridge and directed into the opening for the metotic opening as with *Batrachotomus kupferzellensis* (Gower 2002). The opisthotic is fused with the exoccipital.

The well-preserved prootic, which separates the parabasisphenoid from the laterosphenoid, is complete (Fig. 7). However, the sutures with the surrounding elements are difficult to discern. The anterolateral surface bears the exits for cranial nerves V and VII. The exit for cranial nerve V appears to lie completely within the prootic as in *Postosuchus kirkpatricki* and Postosuchus alisonae (Weinbaum 2011; Peyer et al. 2008) and not shared with the laterosphenoid as in *Batrachotomus kupferzellensis* (Gower 2002) and *Sphenosuchus acutus* (Walker 1990). A fossa surrounds the opening for cranial nerve V in *Heptasuchus clarki*. Anteriorly, a groove is present linking the exit for cranial nerve V and the anterior edge. A notch

on the anterodorsal edge, just anteromedial to the exit of cranial nerve V, possibly represents the exit of the middle cerebral vein. A slight groove leads anteriorly into this notch. A small ridge located dorsal to the exit of cranial nerve V is interpreted to be the site of attachment for the protractor pterygoidei following Gower and Sennikov (1996) and Gower (2002). There is a vertical ridge on the small anterior portion of the prootic just anteroventral to the exit of cranial nerve V. The pathway of cranial nerve IV appears to pierce the anterior, upturned process of the prootic. This process separates the laterosphenoid from the parabasisphenoid.

The exit for cranial nerve VII is located in a posterolaterally opening slot on the posterolateral portion of the prootic (Fig. 7A-B). The deep pocket for the exit of cranial nerve VII continues ventrally as a groove on the lateral side of the parabasisphenoid. The surface between the exits of cranial nerves V and VII is concave. There is no articular surface on the anterolateral surface of the prootic and the quadrate head as in crocodylomorphs (Gower 2002).

Medially, the surface of the prootic is not well preserved. There is no clear pneumatization of inner ear as in crocodylomorphs as described by Walker (1990). The medial wall of the vestibule appears to be nearly fully ossified as with most suchians (Gower 2002; Gower and Nesbitt 2006), but the center of the wall is broken.

The right opisthotic is completely preserved (Fig. 7). The stapedial groove leading into the fenestra ovalis is shallow and poorly defined anteriorly. The descending process of the opisthotic (=crista interfenestralis) divides the metotic foramen anteriorly from the fenestra ovalis posteriorly. This thin process of the opisthotic is expanded mediolaterally. Nearly all of the descending process of the opisthotic is hidden posteriorly by the lateral ridge on the exoccipital in *Heptasuchus clarki,* as in aetosaurs, *Batrachotomus kupferzellensis, Postosuchus kirkpatricki,* and crocodylomorphs (Gower 2002). There does not appear to be a foramen in the dorsal portion of the metotic opening as there is in *Batrachotomus kupferzellensis* (Gower 2002), but this area is incompletely prepared. The perilymphatic foramen is not fully ossified, but

must have been oriented posteriorly and not laterally as in *Sphenosuchus acutus* (Walker 1990) and other crocodylomorphs (Gower 2002).

Lateral to the foramen magnum, the paroccipital processes of the opisthotics are constricted (to 2.3 cm) at their bases but broaden considerably (to 5.2 cm) to form club-shaped posterolateral expansions (Fig. 7). The processes are directed dorsolaterally at an angle of 35° from the vertical plane of the occiput. The broadness of the lateral portions of the paroccipital processes is greater than that of *Batrachotomus kupferzellensis* (SMNS 80260), but similar to *Postosuchus kirkpatricki* (Weinbaum 2011) and crocodylomorphs (e.g., *Sphenosuchus acutus*). The ventral portion of the process of *Heptasuchus clarki* is nearly straight whereas the dorsal margin is significantly expanded dorsally. The dorsal edge of the process forms the ventral margin of a clear post temporal fenestra. Shallow grooves are present on the ventral surface of the paroccipital process. The lateral edge of the paroccipital is rounded like that of *Batrachotomus kupferzellensis* (SMNS 80260).

The basisphenoid and parasphenoid are fused together to form a parabasisphenoid. The body of the parabasisphenoid is vertically oriented where the basipterygoid processes are extended well ventral of the basitubera. The parabasisphenoid portion of the basitubera project laterally and dorsolaterally at its tips. A deep fossa (=medial pharyngeal recess, =hemispherical fontanelle) is positioned between the basitubera and the midline. This depression is undivided on the midline, whereas there is a distinct lamina of bone dividing the depression in *Batrachotomus kupferzellensis* (Gower 2002) and *Sphenosuchus acutus* (Walker 1990). There is no intertubural plate (Gower and Sennikov 1996) across the midline. The body of the parabasisphenoid is waisted between the basitubera and the basipterygoid processes. The posteriorly directed basipterygoid processes extend ventrally beyond the rest of the braincase. The articular surfaces with the pterygoid are positioned on the anterior portion of the basipterygoid processes. The posterior portions of the processes expand posterodorsally into mediolaterally thin sheets of bone. These processes are autapomorphic (see diagnosis) for

725 *Heptasuchus clarki* and represent a clear difference between *Heptasuchus clarki* and
726 *Batrachotomus kupferzellensis*.
727 Laterally, the entrance of the internal carotid arteries lies in the groove that is continued
728 from the prootic on the lateral side of the parabasisphenoid (Fig. 7). The path of the internal
729 carotid travels anteriorly to exit at the base of the hypophyseal fossa as observed on the broken
730 left lateral side. The articulation of the descending process of the opisthotic with the
731 parabasisphenoid is not distinct. The base of both the metotic fenestra and the fenestra ovalis
732 are broadly rounded and lie on the dorsal portion of the parabasisphenoid. The ventral base of
733 the metotic fenestra is well ventral to the contact between the basioccipital and the exoccipital.
734 The cultriform process is complete, relatively short compared with the braincase, and
735 dorsoventrally expanded posterior to the anteriorly tapering tip (Fig. 7). A dorsoventrally
736 expanded cultriform process is also present in *Batrachotomus kupferzellensis* (Gower 2002)
737 and *Postosuchus kirkpatricki* (Weinbaum 2011). A distinct ventral step is present in the anterior
738 half of the element. There does not appear to be a longitudinal groove on the dorsal surface of
739 the cultriform process as there is in *Arizonasaurus babbitti* (Gower and Nesbitt 2006).
740 Comparisons with the length and dorsoventral depth of the cultriform process are limited among
741 suchians given that this region is not common preserved.
742 Dorsal to the foramen magnum, the vertically inclined face of the supraoccipital extends
743 dorsally to contact the parietal.
744
745 **Quadrate:** The dorsal (UW 11563-AD) and ventral portions (UW 11563-AF, UW 11563-H) of
746 the left quadrate were found among the weathered elements collected at the locality. The dorsal
747 fragment (Fig. 8D) that articulated with the squamosal, is rounded in dorsal view, and the
748 surface is composed of spongy bone circumscribed by a ring of compact bone. There is no
749 posterior hook of the quadrate as there is in *Postosuchus kirkpatricki* (TTUP 9000). The ventral
750 portion consists of the articular facet with the articular (Fig. 8A-C). The convex facet is divided

751 into medial and lateral condyles separated by a shallow fossa. The more medial condyle of the
752 articular surface projects further ventrally than the lateral condyle. The ventral articular surfaces
753 lap dorsally onto the anterior surface. Anteriorly, a small but well-defined ridge originates on the
754 lateral condyle and trends dorsomedially.
755
756 **Palate:** A nearly complete left palatine (UW 11562-K, Fig. 6F) is represented in the type
757 specimen. The thin medial, anterior and posterior portions of the element are incomplete. The
758 body of the palatine is thin for most of the length of the element. The lateral side bears a
759 dorsoventrally expanded, anteroposteriorly straight facet for articulation with the medial side of
760 the maxilla. In dorsal view, the expansion forms a lateral lip on the lateral side of the element.
761 The posterolateral portion forms the anteromedial margin of the suborbital fenestra and the
762 posterior portion tapers posteromedially. Anteriorly, only a portion of the dorsal fossa that holds
763 the pterygoideus muscle (Witmer 1997) is preserved. The portion preserved suggests that the
764 fossa is anteriorly shifted near the choana as in *Batrachotomus kupferzellensis* (Gower 2002)
765 relative to the more posterior position in *Polonosuchus silesiacus* (ZPAL Ab/III 563),
766 *Saurosuchus galilei* (PVSJ 32), aetosaurs (Gower and Walker 2002), and the crocodylomorph
767 *Sphenosuchus acutus* (Walker 1990). The posterior border of the choana is thickened relative to
768 the body in *Heptasuchus clarki* but does not possess a surrounding rim in the same area as in
769 *Polonosuchus silesiacus* (ZPAL Ab/III 563). Ventrally, the surface is nearly flat except for a
770 shallow facet for the articulation with the pterygoid on the posteromedial portion.
771
772 **Pterygoid:** Two elements (UW 11562-L and UW 11562-M; Fig. 8E-H) not readily identified
773 originally were found in situ with the holotype; here we interpret these fragments as parts of the
774 pterygoid. UW 11562-L consists of a thin, plate like element that is possibly part of the lateral
775 process of the pterygoid. All sides except one, presumably the medial side, are broken. The
776 ‘medial’ side is straight with a distinct step at the edge near the middle of the element. Here the

777 bone is rugose and may serve as an articular facet. The essentially flat surfaces are nearly
778 featureless. UW 11562-M is a thin fragment that may pertain to the anterior (=palatine) process
779 of the pterygoid. The element likely tapers anteriorly and between longitudinal ridges on both
780 sides.
781
782 **Dentition:** A single premaxillary tooth (UW 11562-A), the first five teeth of the left maxilla (UW
783 11562-C) and the fourth, sixth, and ninth tooth of the right maxilla (UW 11562-B) are preserved
784 in place in the holotype (Fig. 5). Loose teeth (UW 11562-AA through -AI) found at the locality
785 are referred to *Heptasuchus clarki* based on similarity, but only the teeth found in the tooth
786 bearing bones are described in detail. The roots of the premaxillary and maxillary teeth lie in
787 deep sockets.
788 The only preserved premaxillary tooth, in either tooth position two or three (Fig. 5E-F), is
789 unique among the other teeth preserved in *Heptasuchus clarki* in that its crown is cylindrical in
790 shape and bears no serrations. The tip grades into a distal portion, which is laterally
791 compressed to form a blade similar in shape to the distal tips of the maxillary teeth. The axis of
792 this blade, however, lies at an angle to the blade axis of the maxillary teeth.
793 Generally, the maxillary teeth are ziphodont in that they are mediolaterally compressed,
794 recurved, and bear serrations on the mesial and distal sides. The crowns are long, that of a fully
795 erupted tooth being approximately equal in length to its root. Typically, there are 12 serrations
796 per 5 mm. The left maxilla (Fig. 5A-B), bearing the first five teeth of the maxillary series, clearly
797 shows the pattern of tooth replacement. As in *Saurosuchus galilei* (Sill 1974), the teeth grow
798 and are replaced in two alternating waves. Teeth in positions three and five were newly erupted
799 when the individual was buried whereas teeth in positions two and four are fully erupted. Tooth
800 position two shows especially severe signs of wear, as its tip is badly blunted and the serrations
801 were worn away, likely in life. The right maxilla (Fig. 5C-D), with the medial wall almost entirely
802 removed by erosion also illustrates the process of tooth replacement in *Heptasuchus clarki*;

tooth position six is fully erupted and a replacement tooth lies on its lingual surface within a socket of the fully erupted tooth at the base of its root.

**Postcranial Skeleton**

The postcranial of *Heptasuchus clarki* is only represented by a few complete or nearly complete bones (e.g., pubis, tibia, ulna) whereas most other postcranial elements were found on the surface after extensive surface weathering. It is apparent that much of the shaft of limb bones and delicate parts of vertebrae (e.g., base of the neural arches) were weathered away much more easily than the more robust elements, such as limb bone ends and centra fragments. A few postcranial bones were found in place (e.g., trunk vertebra; Fig. 9A-B), but suffer from poor surface details with few exceptions.

**Vertebrae:** The vertebral column of *H. clarki* is represented by only a few poorly preserved centra, one complete neural spine, and a large number of fragments from neural arches (e.g., diapophyses from trunk vertebrae) along the column. Those centra that are sufficiently preserved to warrant description include parts of three cervicals, a trunk, and parts of caudal centra.

The most anterior vertebra represented among the referred material consists of a fragmentary centrum (UW 11562-T) from approximately the middle of the cervical series (comparing to that of *Postosuchus kirkpatricki* Weinbaum 2013) which retains the anterior and posterior articular surfaces and the length of this centum is a bit less than its height, typical of loricatan taxa with short necks (e.g., *Batrachotomus kupferzellensis*, Gower and Schoch 2009; *Postosuchus alisonae,* Peyer et al. 2008; *Prestosuchus chiniquensis*, Desojo et al. 2020). Between the articular faces, the centrum is constricted in ventral view. Lateral to the anterior articular facet, the parapophyses sit on the ventral half of the centrum and project laterally. They are separated by a ventrally projecting lip, which originates from the ventral portion of the

anterior facet. The ventral surface of the centrum bears a slight ridge (=keel), as typical of most archosauriforms (Nesbitt 2011).

A more posterior cervical centrum is represented by just the anterior portion (UW 11564-A). The anterior articular facet is circular and only slightly concave/amphicoelous. Lateral to the anterior articular facet, the parapophyses lie slightly more dorsally on the centrum than in UW 11562-T. The parapophyses face laterally with a slight posterior component. Just posterior to the anterior articular facet, the centrum constricts rapidly to the point where it has broken, preserving only about half of the total length of the element based on our estimation and comparisons to *Batrachotomus kupferzellensis* (Gower and Schoch 2009) and *Postosuchus alisonae* (Peyer et al. 2008). The marked constriction decreases width from 4.5 cm at the anterior articular facet rim to l.5 cm at the midpoint. A trace of a faint ridge (=keel) is present on the midline of the ventral surface. In this vertebra, as in all those preserved in *Heptasuchus clarki*, the neural canal deeply indents the dorsal portion of the body of the centrum behind the flared rim. This condition "central excavation" is present in archosauriforms outside crown Archosauria *Euparkeria capensis* (Ewer l965), and also within the crown group (e.g., *Arizonasaurus babbitti*, Nesbitt 2005).

A nearly complete trunk centrum (TMM 45902-2; Fig. 9A-B) was excavated from the ground in 2009, but the specimen is poorly preserved and lacks the process of the neural arch. TMM 45902-2 likely represents a mid to posterior trunk vertebra based on the dorsal and posteriorly placed parapophysis based on comparison with other loricatans (e.g., *Batrachotomus kupferzellensis*, Gower and Schoch 2009). The anterior and posterior articular facets of the centrum are nearly circular, with a slightly taller dorsoventral height compared to the mediolateral width. The centrum rims are well pronounced, but slightly weathered, and the centrum is well constricted in both lateral and ventral views between the articular facets. The neurocentral suture is fused and no trace of the suture can be observed. The lateral portions of the diapophyses are broken, but the base is shifted posteriorly and likely connected with the

855 base of the diapophyses. Posteriorly, the neural canal is oval, with a much greater height
856 dorsoventrally than mediolateral width. This width to height to ratio of 0.7 in *Heptasuchus clarki*
857 is much higher than in closely related taxa (e.g., *Batrachotomus kupferzellensis*, Gower and
858 Schoch 2009; *Postosuchus alisonae*, Peyer et al. 2008; *Stagonosuchus nyassicus*, Gebauer
859 2004).

860 A mostly complete caudal vertebra (UW 11562-U; Fig. 9G-H) comprises a nearly
861 complete centrum and part of the neural arch. We interpret this as a more anterior caudal
862 vertebra given that the centrum is about as tall as long, lacks any clear facets for the chevron,
863 and the transverse processes, although broken, are large and similar to those of the anterior
864 caudal vertebrae of *Prestosuchus chiniquensis* (SNSB-BSPG AS XXV 3b; Desojo et al. 2020).
865 The anterior articular facet of the centrum (Fig. 9F) is ellipsoidal with a dorsoventral height of
866 five centimeters compared to a mediolateral width of four centimeters. Additionally, the anterior
867 articular facet is slightly concave, like the other vertebrae throughout the column. The centrum is
868 constricted just posterior to the well-defined rim of the anterior articular facet. Only a small
869 fraction of the posterior articular facet is preserved. The anterior portion of the neural arch is
870 intact, including bases of the prezygapophyses. The articular facets of the prezygapophyses are
871 low, ~20$^{o}$ to the horizontal. Dorsal to the neural canal, the beginnings of the neural spine project
872 dorsally, flanking a deep interspinous cleft (Fig. 9G) as in *Saurosuchus galilei* (Sill, 1974). As in
873 the other vertebrae described, the neural canal expands ventrally into the dorsal surface of the
874 centrum.

875 A number of partial centra of distal caudal vertebrae are preserved (UW 11563-A-C; UW
876 11562-BW; Fig. 9I-J); none preserve the neural spine. The posterior caudal vertebrae are
877 typical of archosaurs (e.g., *Postosuchus alisonae*; NCSM 13731) in that the centra are longer
878 than tall, lack lateral processes, and the middle of the centrum is only slightly constricted relative
879 to the articular facets. The width of the centra (Fig. 9G-H) is similar to those of *Postosuchus*

880 *kirkpatricki* (TTUP 9002), but do not appear to be unique among archosaurs given the paucity of
881 posterior caudal vertebrae associated with diagnostic material.
882 A number of neural spines were found among the surface collected material, but the
883 exact position of each neural spine within the vertebral column cannot be reconstructed
884 precisely. The height of the neural spines are difficult to estimate, but most of a neural spine
885 (UW 11562-V; Fig. 9E) shows that at least some of the neural spines were about twice the
886 height of a trunk centrum. The neural spines are blade-like in anterior and posterior views and
887 clearly bear lateral expansions at the dorsal end of the spine. The lateral expansions are
888 globular in lateral view and obtain their greatest lateral expansion near the anteroposterior
889 center (UW 11562-CT) or slightly posterior to the anteroposterior center. Additionally, the lateral
890 expansions appear to not expand anteriorly or posteriorly compared to the rest of the neural
891 spine. There is clear variation in the sample; the lateral expansions are greater in some
892 specimens (UW 11562-CT) compared to others (UW 11562-V). In dorsal view, some appear
893 nearly circular (UW 11562-CX) whereas others are more 'heart-shaped' with a posterior prong
894 present at the midline (UW 11562-CT). These expansions, referred to as spine tables by some
895 authors (e.g., see Nesbitt 2011), commonly occur in non-crocodylomorph loricatans such as
896 *Batrachotomus kupferzellensis* (Gower and Schoch 2009), *Stagonosuchus nyassicus*, (Gebauer
897 2004), *Saurosuchus galilei* (Trotteyn et al. 2011), *Prestosuchus chiniquensis* (ULBRA-PVT-281;
898 Roberto-Da-Silva et al. 2018), and in the cervical vertebrae of *Postosuchus kirkpatricki*
899 (Weinbaum 2013), and clearly outside the group (e.g., *Nundasuchus songeaensis* Nesbitt et al.
900 2014). The morphology of the lateral expansions of the dorsal portion of the neural spines are
901 abundant enough to support that both the cervical and the trunk vertebrae had the feature, as in
902 *Batrachotomus kupferzellensis* (Gower and Schoch 2009).
903
904 **Osteoderm:** A single osteoderm (Fig. 9K-M) was recovered among the holotype in 2010 (TMM
905 45902-1). The size of the osteoderm is consistent with that of *Heptasuchus clarki*, but it is

906 impossible to conclude that the osteoderm definitely belonged to *Heptasuchus clarki*. The
907 semicircular osteoderm has a nearly flat outer surface covered in small foramina and a few
908 short canals connecting some of the foramina. The ventral surface is nearly smooth with small
909 crisscrossing bone fibers as in most archosauriform osteoderms. In lateral view, the osteoderm
910 is compressed and dorsal and ventral sides are parallel for much of their length, both sides
911 taper toward the edges. The location of the osteoderm on the skeleton is not known and there is
912 no anterior process is present as in most pseudosuchians (Nesbitt 2011).
913
914 **Scapula**: Two partial scapulae, consisting solely of the glenoid region, are known from the
915 accumulation. The larger specimen (UW 11566-B) and smaller specimen (UW 11565-E; Fig.
916 10A) is from the right side. The larger specimen indicates that the coracoid may be partially
917 coossified to the scapula whereas the smaller specimen clearly has a contact surface with the
918 coracoid. The glenoid is well defined by a rim and the glenoid itself is weakly concave. The
919 glenoid opens posteriorly with a lateral component, but the exact angle cannot be determined
920 because the rest of the scapula is not present; the orientation of what is preserved is similar to
921 that of *Batrachotomus kupferzellensis* (SMNS 80271). Just distal to the glenoid on the posterior
922 edge, a rugose scar marks the surface for origin of M. triceps as in other archosaurs (Gower
923 and Schoch, 2009). This scar is rugose and distinct in *Heptasuchus clarki*, but not nearly as
924 laterally expanded compared to that of *Batrachotomus kupferzellensis* (SMNS 80271).
925
926 **Coracoid:** Two fragmentary coracoids (UW 11566; Fig. 10B) were recovered as float during the
927 initial excavation. Both coracoids consist of the more robust glenoid region with a broad
928 articulation surface with the scapula. The laterally concave articulation surface with the humerus
929 (=glenoid) project posterolaterally like that of *Batrachotomus kupferzellensis* (SMNS 80271) and
930 *Postosuchus kirkpatricki* (TTUP 9002). In proximal view, the rugose articulation surface with the
931 scapula is triangular and extends laterally into a small peak. The anterolateral surface just distal

to this articulation surface is striated and flat. A clear coracoid foramen is present anterior to the largest articulation surface with the scapula. The foramen is only partially complete in both specimens; but shows that the foramen nearly contacted the scapula articulation surface on the medial surface. The medial surface is flat. It is not clear if the coracoid of *Heptasuchus clarki* had a postglenoid process.

**Humerus:** A proximal portions of a left humerus (UW 11565-A; Fig. 10C-D) and the proximal portion of a second left humerus (UW 11563-U) are represented among the referred material of *Heptasuchus clarki*. The latter bone, collected outside the quadrant system, is weathered, but clearly indicates the presence of a slightly smaller individual from the locality.

The surfaces of UW 11565-A are well preserved. The overall proportions of the humerus cannot be specifically determined because the shaft and distal end are missing. However, it is clear that the proximal expansion relative to the shaft would have been less in *Heptasuchus* and other forms like *Batrachotomus kupferzellensis* (SMNS 80276), *Postosuchus kirkpatricki* (TTUP 9002), *Ticinosuchus ferox*, and crocodylomorphs rather than the largely expanded proximal portions of *Stagonosuchus nyassicus* (GPIT/RE/3832), and aetosaurs and their close relatives (e.g., *Parringtonia gracilis*, NMT RB426) where the medial and lateral edges diverge at a greater angle proximally. The proximal surface of the bone is rugose, possibly indicating that ossification of the proximal end was not complete at the time of death. The proximal surface lacks a rounded ‘head,’ as present in *Batrachotomus kupferzellensis* (SMNS 80276), *Postosuchus kirkpatricki* (TTUP 9002), and early crocodylomorphs (Nesbitt, 2011). In proximal view, the medial portion expands relative to the narrower middle to lateral portion. In posterior view, the medial portion of the proximal surface is rounded and is deflected distally. More laterally, the proximal surface bears a distinct peak near the origin of the deltopectoral crest. The distinct peak (Fig. 10C-D), which is best observed in posterodorsal view, occurs in *Batrachotomus kupferzellensis* (SMNS 80276) and *Stagonosuchus nyassicus* (GPIT/RE/3832),

958 to a lesser extent in *Mandasuchus tanyauchen* (NHMUK PV R6793), but absent in *Postosuchus*
959 *kirkpatricki* (TTUP 9002) and early crocodylomorphs (Nesbitt, 2011). Broken in UW 11565-A,
960 the deltopectoral crest of UW 11563-U shows that the structure is continuous with the proximal
961 surface, as in *Mandasuchus tanyauchen* (NHMUK PV R6793) and *Batrachotomus*
962 *kupferzellensis* (SMNS 80276) and not distally shifted as in *Postosuchus kirkpatricki* (TTUP
963 9002), and early crocodylomorphs (Nesbitt, 2011). The apex of the deltopectoral crest, which is
964 triangular in lateral view, is located in a similar position as in *Batrachotomus kupferzellensis*
965 (SMNS 80276). The anterior surface of the proximal portion is concave whereas the posterior
966 surface is nearly flat. A weakly defined scar is present on the posterolateral side of the posterior
967 surface and is equivalent to a scar in *Batrachotomus kupferzellensis* (SMNS 80276), interpreted
968 to be the surface for origin of M. triceps (Gower and Schoch, 2009).
969
970 **Ulna:** A complete right ulna (UW 11562-W) and a nearly complete left ulna (UW 11562-X) are
971 included as referred specimens (Fig. 11I-L). Additionally, the distal ends of two other ulnae (UW
972 11563-V and UW 11565-C) are present indicating that at least three individuals were buried
973 together at the locality. UW 11562-W measures 23.5 cm long and is nearly as long as the
974 complete tibia (UW 11562-Z), but the ulna has a much smaller radius throughout the shaft. The
975 ulna has an expanded proximal portion relative to the shaft and the shaft narrows distally for
976 2/3rds the length of element and then slightly expands at the distal end (Fig. 11). The expanded
977 proximal end of the ulna bears a moderately developed olecranon process as demonstrated by
978 UW 11562-X (Fig. 11I-L). It appears that the olecranon process of UW 11562-W was a separate
979 ossification and was not fused onto the proximal surface at the time of death. Comparatively,
980 the olecranon is relatively smaller in *Heptasuchus clarki* than in aetosaurs (e.g., *Stagonolepis*
981 *robertsoni*, Walker 1961), *Postosuchus kirkpatricki* (TTUP 9002), *Batrachotomus kupferzellensis*
982 (SMNS 80275), and crocodylomorphs (e.g., *Hesperosuchus agilis*, Colbert 1952) and is more
983 similar in size to that of *Ticinosuchus ferox* (Krebs 1965) and *Mandasuchus tanyauchen*

(NHMUK PV R6793). The proximal surface is rugose and triangular (Fig. 11E, I) with a distinct radial tuber, but this tuber is not as well expanded as that of *Postosuchus kirkpatricki* (TTUP 9000). The radial tuber extends distally for about 1/3 the length of the ulna. The medial side of the proximal portion is concave, as in *Batrachotomus kupferzellensis* (SMNS 80275). The shaft of the ulna is circular, and the anterior surface of the bone bears a longitudinal ridge, that twists medially toward the distal end, where a narrow groove is formed between it and the medial edge of the bone. This ridge and groove appear to be present in both UW 11562-W and UW 11562-X and is autapomorphic for *Heptasuchus clarki* (see diagnosis). The rugose distal surface is ovoid in outline with a slightly tapered anterolateral end.

**Radius –** Only the ends of the radius have been identified from weathered fragments, but determining which side these elements are from is difficult. The proximal portion is represented by UW 11566-T and UW 11562-DM (Fig. 11AB) and the possible distal ends are represented by UW 11562-DF and UW 11562-DI (Fig. 11CD). The proximal end of the radius is mediolaterally compressed with anterior and posterior tapered ends. A concave surface, in lateral view, lies between the anterior and posterior ends of the proximal surface. The distal end is rounded anteriorly and possibly posteriorly also, but this cannot be confirmed because the posterior portion is broken.

**Ilium:** A fragment consisting of much of the pubic peduncle, and part of the acetabulum is the only positively recognized part of the of the ilium known (UW 11563-Y and UW 11563; Fig. 12F). In anteroventral view, the articulation surface with the pubis is rugose and triangular. The acetabular portion that is preserved is concave and the acetabulum appears to be imperforate, as expected for a non-crocodylomorph pseudosuchian. The surface within the acetabulum is smooth.

**Pubis:** A nearly complete left pubis (UW 11562-Y; Fig. 12A-D) of *Heptasuchus clarki* was recovered; only parts of the thin medial portion of the pubic apron are not preserved. The pubis is ~37 cm in length from the articulation surface with the ilium to the distal surface. In lateral view, the bone is nearly straight along its entire length like that of *Batrachotomus kupferzellensis* (SMNS 80270). The proximal surface of the pubis articulates with the pubic peduncle of the ilium dorsally and ventrally, the proximal portion of the pubis contributes only a minor portion of the edge of the acetabulum, as in *Saurosuchus galilei* (Sill, 1974). Distally, the proximal portion narrows in lateral view and transitions into the shaft laterally and medially with the pubic apron. The lateral surface of the proximal portion bears a fossa surrounded by a rugose surface, as in *Batrachotomus kupferzellensis* (SMNS 80270); this surface marks the hypothesized site of origin of the *M. ambiens* (Gower and Schoch, 2009). Medially, the proximal portion of the apron is broken so that that the exact size of the obturator foramen cannot be determined, but it appears to be small like that of *Batrachotomus kupferzellensis* (Gower and Schoch 2009), rather than the larger opening in *Postosuchus kirkpatricki* (Weinbaum 2013). The anteroposteriorly thickened medial process marks the proximal articulation with its antimere as in nearly all paracrocodylomorphs.

In posterior and anterior views, the shaft bows laterally (Fig. 12B) and a similar morphology is absent in other paracrocodylomorphs. The shaft is rounded laterally and tapers to an anteroposteriorly thinner apron medially. The lateral surface of the shaft is smooth without any ridges.

The distal end expands in the last tenth of the length of the pubis. In lateral view, the anterior end slightly expands at its distalmost margin whereas the posterior edge expands comparatively more to form an asymmetric expansion (or boot). The distal margin, in lateral view, is rounded. In anterior view, the pubis shaft medial to the distal expansion is directed posteromedially where it presumably meets its antimere. Consequently, the posteromedial surface of the pubis is distinctly concave in distal view (Fig. 12D). The configuration is in

contrast to that of *Batrachotomus kupferzellensis* (SMNS 80279), *Arizonasaurus babbitti* (MSM 4590), *Postosuchus alisonae* (NCSM 13731), and *Poposaurus gracilis* (TMM 43683-1), where the apron is orientated directly medially (Nesbitt, 2011). The shape of the distal expansion of *Heptasuchus clarki* is rounded like that of *Batrachotomus kupferzellensis* (SMNS 80279) but not the mediolaterally narrower expansions of poposauroids (Nesbitt, 2011). The distal surface is rugose.

**Ischium:** The proximal portion of the right ischium (UW 11564-B; Fig. 12E) was recovered. The proximal portion of the ischium bears a well-defined ridge that demarcates the posteroventral portion of the acetabulum, as in *Batrachotomus kupferzellensis* (SMNS 52970). The robust proximal portion has two articulation surfaces at its proximal edge, a dorsal one for articulation with the ilium and a ventral one for articulation with the pubis. The dorsal and ventral articular surfaces are divided in lateral view by a portion of the ischium that may not have articulated with either the ilium or the pubis. Therefore, there may have been a slight gap between the ischium, ilium, and pubis, like that reconstructed for *Batrachotomus kupferzellensis* (Gower and Schoch 2009; Figure 6E). Just posterior to the acetabular rim, a clear pit is present on the dorsal edge. This pit occurs in a variety of archosauromorphs (Ezcurra, 2016) although its length and form differ among archosaurs (Gower and Schoch 2009).

The shape of the shaft cannot be determined with the preserved portion. The medial surface of the proximal portion of the ischium is flat and the medial and ventral edges indicate that the ischia contacted each other near the proximal portion, similar to other paracrocodylomorphs (e.g., *Postosuchus kirkpatricki*, Weinbaum 2013; *Batrachotomus kupferzellensis*, SMNS 52970; *Arizonasaurus babbitti*, Nesbitt 2005).

**Femur:** Two badly worn fragments representing the proximal and distal ends of a right femur (UW 11563-B, UW 11563-A, respectively; Fig. 13A-D) were recovered; it is not clear if both

ends belong to the same bone. The proximal surface bears a groove like that of poposauroids and some loricatans (e.g., *Postosuchus kirkpatricki*, Weinbaum 2013) and all three proximal tubera (sensu Nesbitt, 2005; 2011) appear to be present, although the anteromedial tuber is highly eroded (Fig. 13A-D). The preserved portions of the shaft appear to be thin walled like other paracrocodylomorphs (Nesbitt 2011), but the exact ratio of the thickness of the cortex versus the diameter could not be determined. The distal end bears a small crista tibiofibularis crest and a clear depression is located on the distal surface.

**Tibia:** The well preserved and complete left tibia of *Heptasuchus clarki* (UW 11562-Z; Fig. 13E-H) is robust with a wide midshaft compared to the length (= 24.0 cm) of the element. The proximal portion does not expand as much relative to the shaft like in *Batrachotomus kupferzellensis* (SMNS 52970), where the proximal portion is more greatly expanded. The proximal surface (maximum length = 7 cm) is roughly triangular with a short cnemial crest and rounded lateral surface for contact with the fibula. The lateral portion of the proximal surface is depressed like that of suchian archosaurs (Nesbitt, 2011) and this surface is separated from the posterior portion of the tibia by a vertical gap (Fig. 13). The proximal surface is highly rugose.

The shaft of the tibia remains oval in section throughout its length, and like the femur, the tibia is also thin walled. The posterior surface of the entire bone, in contrast to the other faces, is flattened, and exhibits a slight twisting along its length. The distal end of the tibia (maximum width = 6 cm) is expanded less than the proximal end and is triangular in distal view. The differentiation of the distal surface of the tibia for articulation with the astragalus is poor; the ‘cork-screw’ configuration (proximally slanted posterolateral surface and distally expanded anteromedial portion) typical in shuvosaurids (Nesbitt, 2007), aetosaurs (Parrish 1993), *Batrachotomus kupferzellensis* (SMNS 52970) and in rauisuchid taxa like *Postosuchus kirkpatricki* (TTUP 9002) is not present in *Heptasuchus clarki*. Instead the distal surface is flatter

in *Heptasuchus clarki* and is more like that of *Prestosuchus chiniquensis* (von Huene, 1942; Desojo et al. 2020). The distal surface is also rugose.

**Fibula**: The fibula is only represented by the right (?) proximal portion (UW 11566-S) and right distal portion (11566-R) recovered among weathered fragments (Fig. 13I-L). The more robust proximal portion is asymmetrical in lateral view with a tapering posterior portion. The distal end expands anteriorly and posteriorly and possesses an ovate distal surface (with an anteroposteriorly long axis).

**Metatarsals and phalanges:** A number of fragmentary metatarsals (UW 11562, UW 11562-DH, UW 11562-DHU, UW 11562-DR) and phalanges were recovered from the locality and all pes elements consist of weathered proximal or distal ends. Given the difficulty of assigning fragments of metatarsal, we are hesitant to assign anatomical positions to the most fragments, but we have identified a proximal end of a right metatarsal IV (UW 11566; Fig. 13M-N) and possibly a proximal end of a right metatarsal II (UW 11566; Fig. 13O-P) based on comparisons with the pes of *Postosuchus alisonae* (NCSM 13731). The proximal surfaces of the metatarsals have rugose surfaces and are typically rectangular with well-defined faces with squared-off ventral ends of the proximal surfaces. The distal end of the metatarsals poses large articular facets that are about as long as wide. A single ungual (UW 11562-DT; Fig. 13O-P), possibly from the pes, indicates that the unguals were dorsoventrally flattened like that of *Prestosuchus chiniquensis* (von Huene, 1942).

## Phylogenetic Analysis

The phylogenetic position of *Heptasuchus clarki* was assessed using the early archosaur matrix of Nesbitt (2011) as a base followed by the modifications of characters, scores, and

terminal taxa of Butler et al. (2014, 2018), Nesbitt et al. (2014, 2017, 2018), Nesbitt and Desojo (2017), and Desojo et al. (2020) and additions of terminal taxa by von Baczko et al. (2014) and Lacerda et al. (2016; 2018). We added the additional and new characters of Desojo et al. (2020; characters 414 – 422 here), the aphanosaur-centered characters of Nesbitt et al. (2017; characters 434-439 here), a character for rauisuchids and kin from Brusatte et al. (2008; 2010; character 424 here), and nine new characters centered on the relationships of *Heptasuchus clarki* among loricatans (Fig. 14; characters 425-433 here; see appendix 1) for a total of 439 characters. Characters 32, 52, 121, 137, 139, 156, 168, 188, 223, 247, 258, 269, 271, 291, 297, 314 328, 356, 371, 399 and 413 were ordered - 21 total. We ordered characters 314 and 371 based on the character descriptions of Nesbitt (2011) – characters were not listed in the ordered state list in character sampling and methods. The characters were scored in Mesquite (Maddison and Maddison 2015).

Our primary dataset consists of 100 terminal taxa (supplemental information). This dataset now contains the most specimens and species level terminal taxa of paracrocodylomorphs to date. The matrix includes some stem archosaurs, but for better taxon and character sampling of this part of the tree see Ezcurra (2016) and likewise, for better taxon and character sampling for Dinosauria see the dataset of Baron et al. (2017a) and further modifications (e.g., Langer et al. 2017; Baron et al. 2017b).

The matrix was constructed in Mesquite (Madison and Madison 2015) and analyzed with equally weighted parsimony using TNT v. 1.5 (Goloboff and Catalano 2016). Using parsimony, we used new technology search (with the following boxes checked: Sectorial Search, Drift, and Tree Fusing) until 100 hits to the same minimum length. These trees were then run through a traditional search (search trees from RAM option) using TBR branch swapping. *Euparkeria* was set as the outgroup. Zero length branches were collapsed if they lacked support under any of the most parsimonious reconstructions.

We ran the first analysis *a priori* excluding the following terminal taxa: *Lewisuchus admixtus*, *Pseudolagosuchus majori* (combined into *Lewisuchus*/*Pseudolagosuchus* following Nesbitt et al. 2010, Nesbitt 2011, and Ezcurra et al. 2019), '*Prestosuchus loricatus* paralectotype' (Desojo et al. 2020), and collapsed *Prestosuchus chiniquensis* lectotype, *Prestosuchus chiniquensis* paralectotype, *Prestosuchus chiniquensis* type series, UFRGS PV 156 T, UFRGS PV 152 T, CPEZ 239b into a '*Prestosuchus chiniquensis* ALL' (with the addition of scores from ULBRA-PVT-281; Roberto-Da-Silva et al. 2018), added to another description (UFRGS-PV-0629-T; Mastrantonio et al. 2019; see supplemental information). This data matrix resulted in 144 most parsimonious trees (MPTs) of length (1553 steps) (Consistency Index = 0.330; Retention Index = 0.749) (See supplemental information for full tree; S1).

In our main analysis, we also eliminated *Nundasuchus songeaensis* and *Pagosvenator candelariensis* from the final analysis because 1) *Nundasuchus songeaensis* likely is closer to the base of Archosauria (see Nesbitt et al. 2014) and 2) *Pagosvenator candelariensis* is clearly a member of Erpetosuchidae (Lacerda et al. 2018), but because of missing information and some character conflict, the taxon is highly unstable (see Desojo et al. 2020). Both taxa could thus greatly impact the optimizations of character states at the base of and within Paracrocodylomorpha which is the target portion of the Pseudosuchian tree here. This data matrix resulted in 72 most parsimonious trees (MPTs) of length 1529 steps (Consistency Index = 0.335; Retention Index = 0.752) (Fig. 15 for partial tree; See supplemental information for full tree; S2).

## Discussion

**The phylogenetic position of *Heptasuchus clarki* among archosaurs:**

The results of both our analyses (supplemental information) is similar to the original analysis of Nesbitt (2011) where classic 'Rauisuchia' is a paraphyletic group relative to Crocodylomorpha with 'Rauisuchia' divided among loricatans (paracrocodylomorph taxa closer

to Crocodylomorpha), poposauroids (paracrocodylomorph taxa closer to *Shuvosaurus inexpectatus*), and a few taxa just outside Paracrocodylomorpha (e.g., *Mandasuchus tanyauchen*, *Ticinosuchus ferox*) (Fig. 15). Unsurprisingly, this pattern has been retained in most iterations of the Nesbitt (2011) dataset (Butler et al. 2011; 2014; 2018; Baczko et al. 2014; Lacerda et al. 2016; 2018; Nesbitt and Desojo 2017; Nesbitt et al. 2014; 2017; 2018; Desojo et al. 2020). Like these other analyses, the base of Paracrocodylomorpha is poorly supported with the addition or removal of a taxon, a character score change, or the addition of new characters that alter the relationships of early diverging taxa such as *Mandasuchus tanyauchen* and *Stagonosuchus nyassicus*. Within Loricata, *Saurosuchus galilei*, *Prestosuchus chiniquensis*, and *Luperosuchus fractus* consistently are located at the base of the clade. The relationship of these taxa could be a grade (as found here) or in a clade (Nesbitt and Desojo 2017; Desojo et al. 2020) as a consequence of character optimizations for taxa closer to Crocodylomorpha. Moreover, we did not find *Stagonosuchus* (=*Prestosuchus* Desojo et al. 2020) *nyassicus* as the sister taxon of *Prestosuchus chiniquensis* with the addition of our new characters (see appendix), but given that the new characters focus on the skull and *Stagonosuchus nyassicus* is almost entirely represented by postcrania, this instability is not surprising. The relationship within loricatans closer to Crocodylomorpha (e.g., *Batrachotomus kupferzellensis* + *Alligator mississippiensis*) remained unchanged in comparison with Nesbitt (2011).

*Heptasuchus clarki* is well nested within Loricata and firmly supported as the sister taxon of *Batrachotomus kupferzellensis.* The following four unambiguous character states support the sister taxon relationship within Loricata where *Heptasuchus clarki* could be scored: posterior portion of the nasal is concave at the midline in dorsal view (34-1); supratemporal fossa present anterior to the supratemporal fenestra (144-1); ventral surface of palatal process of the maxilla with distinct fossa (426-1); medial side of the posterior process of the jugal with longitudinal groove (429-1). The following nine unambiguous character states are synapomorphies within Loricata and scored for *Batrachotomus kupferzellensis*, but not for *Heptasuchus clarki* because

of missing information: dorsal (=ascending) process of the maxilla remains the same width for its length (29-0); anterior portion of the frontal tapers anteriorly along the mid-line (43-1); squamosal with distinct ridge on dorsal surface along edge of supratemporal fossa (49-1); upper temporal fenestrae of the parietal by a mediolaterally thin strip of flat bone separated (59-1); double-headed ectopterygoid (89-1) (the jugal indicates that the ectopterygoid was likely double-headed, but we chose not to score it because the ectopterygoid was not preserved); articular with dorsomedial projection separated from glenoid fossa by a clear concave surface (156-1); angle between the lateral condyle and the crista tibiofibularis of the femur about a right angle in distal view (319-1); presacral and paramedian osteoderms with a distinct longitudinal bend near lateral edge (404-1); presacral osteoderms dimensions longer than wide (407-1); position of the posterior process of the squamosal below anterior process and set off by distinct step (423-1).

*Heptasuchus clarki* is well supported as the sister taxon of *Batrachotomus kupferzellensis*. The following unambiguous character states support this relationship: anterodorsal margin at the base of the dorsal process of the maxilla concave (25-1); dorsolateral margin of the anterior portion of the nasal with a distinct anteroposteriorly ridge on the lateral edge (35-1); depression on the anterolateral surface of the ventral end of the postorbital (425-1)(also present in *Postosuchus kirkpatricki*); distinct fossa on the posterodorsal portion of the naris on the lateral side of the nasal (430-1); anteroposteriorly trending ridge on the lateral side of the jugal is asymmetrical dorsoventrally where the dorsal portion is more laterally expanded (433-1). The crania of *Heptasuchus clarki* share a number of unique features with *Batrachotomus kupferzellensis*, many of which were once considered autapomorphies of *Batrachotomus kupferzellensis* (Gower 1999). However, we were not able to pinpoint any postcranial character states that *Batrachotomus kupferzellensis* and *Heptasuchus clarki* share exclusively.

**_Heptasuchus clarki_ and _Poposaurus gracilis_:**

When initially described, *Heptasuchus clarki* was considered to be from the Popo Agie Formation, which also contained the remains of another 'rauisuchian' *Poposaurus gracilis*. Long and Murry (1995) hypothesized that *Heptasuchus clarki* may be a poposauroid after comparisons with *Poposaurus gracilis*, *Shuvosaurus* (= 'Chatterjeea') *elegans* and *Postosuchus kirkpatricki*. Soon after, Zawiskie and Dawley (2003) hypothesized that the skull of *Heptasuchus clarki* might belong to the body of *Poposaurus gracilis* based on age proximity and on a few overlapping postcranial bones. After further analyses, we now reject these hypotheses based on a number of lines of evidence. First of all, our robust phylogenetic analysis clearly places *Heptasuchus clarki* and *Batrachotomus kupferzellensis* as close relatives and both are more closely related to crocodylomorphs than poposauroids. Second, the deposits that *Heptasuchus clarki* was found in are likely not the same as the Popo Agie Formation from the western portion of Wyoming and the deposits that *Heptasuchus clarki* was found in are likely older than that of the Popo Agie Formation and hence *Poposaurus gracilis*. Third, with an abundance of new specimens of *Poposaurus gracilis* from partial skeletons (Weinbaum and Hungerbühler 2007) to nearly complete and articulated postcranial remains (Gauthier et al. 2011; Schachner et al. 2019), and comparative skull material (Parker and Nesbitt 2013), it is clear that *Poposaurus gracilis* and *Heptasuchus clarki* are different taxa.

**Further implications of _Heptasuchus clarki_:**

The stratigraphic and temporal occurrence of *Heptasuchus clarki* fills a critical gap in loricatan biogeography within current-day North America and across Pangea. *Heptasuchus clarki* is the only confirmed loricatan taxon from either the late Middle Triassic or the early portion of the Late Triassic (see above) and demonstrates that large paracrocodylomorphs were present from the early portion of the Middle Triassic (i.e., *Arizonasaurus babbitti* and other forms from the Moenkopi Formation; Nesbitt 2003; Schoch et al. 2010) through the end of the

deposition of Upper Triassic strata (*Effigia okeeffeae* 'siltstone member,' *Coelophysis* Quarry, *Redondavenator quayensis* Nesbitt et al. 2005). Furthermore, *Heptasuchus clarki* fills a 'phylogenetic gap' in that it is the only named loricatan from current-day North America that does not fit into Poposauroidea (Ctenosauriscidae or Shuvosauridae), Rauisuchidae (e.g. *Postosuchus*, *Viviron haydeni*), or Crocodylomorpha and links these disparate clades present in current-day North America to forms from current-day South America and Europe. The presence of a 'mid-grade' loricatan in current-day North America hints that earlier diverging loricatans known from current-day South America (*Prestosuchus chiniquensis*, *Luperosuchus fractus*, *Saurosuchus galilei*) may have had close relatives in current-day North America, but equivalently-aged deposits in North America are lacking.

The sister taxon relationship of *Heptasuchus clarki* and *Batrachotomus kupferzellensis* demonstrates the first biotic link between current-day North America in the Middle to early Late Triassic and the Middle Triassic (Ladinian Stage) of current-day Germany. Although the assemblage from the *Heptasuchus clarki* bonebed has not been studied in detail (see above), there are no other overlapping species or genus-level taxa that are present from the *Heptasuchus clarki* bonebed and the *Batrachotomus kupferzellensis* locality (= Kupferzell = Lagerstätte Kupferzell-Bauersbach), let alone major clades (e.g., the temnospondyls *Gerrothorax*, *Plagiosuchus*, *Mastodontosaurus*, *Kupferzellia*, *Trematolestes*, the chronosuchian *Bystrowiella schumanni*, Choristodera, the sauropterygian *Nothosaurus*; Hagdorn et al. 2015 and a variety of smaller tetrapods represented by jaw material or tooth distinct morphologies; Schoch et al. 2018). Moreover, the clades present in the Ladinian-aged Kupferzell locality of current-day Germany are either completely absent or rare in North America during the entire Triassic Period (e.g., the temnospondyl clades from the Lagerstätte Kupferzell-Bauersbach, chronosuchian). The similarity of just the large carnivorous archosaurs between current day North America and Germany in highly differentiated vertebrate assemblages implies that the larger archosaurs may have had significant flexibility in their paleoenvironments across Pangea

through the Middle to Upper Triassic. This notion is further supported by the evidence presented by Nesbitt et al. (2009) suggesting that carnivorous archosaurs (e.g., dinosaurs and crocodylomorphs) may have had greater distribution in the environments across Pangea.

The holotype locality of *Heptasuchus clarki* contains a minimum of four individuals and this occurrence appears to be common with paracrocodylomorph archosaurs, at least in the Triassic Period. The exact number of individuals is not known because of the heavily weathered bonebed, but it is clear that some individuals were highly scattered and disarticulated whereas some other individuals, including the holotype, were closely associated. The closest relative of *Heptasuchus clarki, Batrachotomus kupferzellensis* was also found in a similar condition: associated and disarticulated individuals across a bonebed (i.e., Lagerstätte Kupferzell-Bauersbach; Gower 1999). Finding non-crocodylomorph paracrocodylomorphs (or 'rauisuchians') in bonebeds with more than one individual appears common across the clade from the Middle to Upper Triassic across Pangea. For example, multiple individuals of *Heptasuchus clarki, Batrachotomus kupferzellensis*, *Postosuchus kirkpatricki*, *Effigia okeeffeae*, *Shuvosaurus inexpectatus*, and *Decuriasuchus quartacolonia* have been found together in the same deposits. The preservation of these paracrocodylomorphs ranges from nearly complete skeletons to disarticulated, but associated skeletons. The implications of the association of these individuals to behavior must be carefully considered on a variety of anatomical, taphonomic and sedimentalogical data (França et al. 2011), but the repeated co-occurrence of individuals of paracrocodylomorphs is intriguing and may suggest that these reptiles were typically in groups (França et al. 2011) and that this behavior was maintained through much of their evolutionary history.

## Institutional Abbreviations

**ALM**, refers to 'Alili n'yifis' locality near the village of Alma. Specimens stored at Museum National d'Histoire Naturelle, Paris, France (MNHN); **BPI**, Evolutionary Studies Institute (formerly Bernard Price Institute for Palaeontological Research), University of the Witwatersrand, Johannesburg, South Africa; **CPEZ**, Coleção de Paleontologia do Museu Paleontológico Arqueológico Walter Ilha, São Pedro do Sul, Brazil; **GPIT**, Institut und Museum für Geologie und Paläontologie, Universität Tübingen, Germany; **IVPP**, Institute of Vertebrate Paleontology and Paleoanthropology, Beijing, China; **MSM**, Arizona Museum of Natural History, Mesa, Arizona, USA; **NCSM**, North Carolina Museum of Natural Sciences, Raleigh, North Carolina, USA; **NHMUK** (formerly BMNH), Natural History Museum, London, U.K.; **NMMNH**, New Mexico Museum of Natural History and Science, Albuquerque, New Mexico, USA; **NMT**, National Museum of Tanzania, Dar es Salaam, Tanzania; **PEFO**, Petrified Forest National Park, Arizona, USA; **PULR**, Paleontología, Universidad Nacional de La Rioja, La Rioja, Argentina; **PVL**, Paleontología de Vertebrados, Instituto "Miguel Lillo", San Miguel de Tucumán, Argentina; **PVSJ**, División de Paleontología de Vertebrados del Museo de Ciencias Naturales y Universidad Nacional de San Juan, San Juan, Argentina; **SAM**, Iziko South African Museum, Cape Town, South Africa; **SMNS**, Staatliches Museum für Naturkunde, Stuttgart, Germany; **SNSB-BSPG**, Staatliche Naturwissenschaftliche Sammlungen Bayerns, Bayerische Staatssammlung für Paläontologie und Geologie, Munich, Germany; **TMM**, Texas Vertebrate Paleontology Collections, The University of Texas at Austin, Texas, USA; **TTU**, Texas Tech University Museum, Lubbock, Texas, USA; **UFRGS-PV**, Laboratório de Paleovertebrados, Universidade Federal do Rio Grande do Sul, Porto Alegre, Brazil; **ULBRA-PVT**, Paleovertebrate Collection of the Universidade Luterana do Brasil, Canoas, Rio Grande do Sul, Brazil; **USNM**, National Museum of Natural History (formerly United States National Museum), Smithsonian

Institution, Washington, DC, USA; **UW**, University of Wyoming, Laramie, Wyoming, USA; **ZPAL**, Institute of Paleobiology, Polish Academy of Sciences, Warsaw, Poland.

## Acknowledgements

We especially thank Michelle Stocker for conversations about Wyoming geology, Triassic rocks of the western US, and Triassic assemblages. We thank the many insightful conversations about 'rauisuchian' relationships and anatomy with David J. Gower and Julia B. Desojo. We thank Brent Breithaupt for help tracking down BLM permit numbers in challenging times. Laura A. Vietti helped locate and curate *Heptasuchus clarki* material from the UW collection and J. Chris Sagebiel curated the TMM *Heptasuchus clarki* material. Reviews by Andrew Heckert, Thomasz Sulej, and Jonathon Weinbaum greatly improved the paper. We thank the Willi Henning Society for free access to TNT software.

## References

Alcober, O. 2000. Redescription of the skull of *Saurosuchus galilei* (Archosauria: Rauisuchidae). Journal of Vertebrate Paleontology 20:302-316.

Bailleul, A. M., J. B. Scannella, J. R. Horner, and D. C. Evans. 2016. Fusion patterns in the skulls of modern archosaurs reveal that sutures are ambiguous maturity indicators for the Dinosauria. PLoS One 11: e0147687.

Baron, M. G., D. B. Norman, and P. M. Barrett. 2017a. A novel hypothesis of dinosaur relationships and early dinosaur evolution. Nature 543:501–506.

Baron, M. G., D. B. Norman, and P. M. Barrett. 2017b. Baron et al. reply. Nature 551:E4-E5.

Benton, M. J. 1986. The Late Triassic reptile *Teratosaurus* - A rauisuchian, not a dinosaur. Palaeontology 29:293-301.

1337 Benton, M. J., and J. M. Clark. 1988. Archosaur phylogeny and the relationships of the
1338 Crocodylia; pp. 295-338 in M. J. Benton (ed.), The Phylogeny and Classification of the
1339 Tetrapods. Vol 1: Amphibians and Reptiles. Clarendon Press, Oxford.
1340 Bittencourt, J. S., A. B. Arcucci, C. A. Marsicano, and M. C. Langer. 2015. Osteology of the
1341 Middle Triassic archosaur *Lewisuchus admixtus* Romer (Chañares Formation,
1342 Argentina), its inclusivity, and relationships amongst early dinosauromorphs. Journal of
1343 Systematic Palaeontology 13:189-219.
1344 Blakey, R.C., F. Peterson, and G. Kocurek. 1988. Synthesis of late Paleozoic and Mesozoic
1345 eolian deposits of the Western Interior of the United States. Sedimentary Geology 56:3-
1346 125.
1347 Bonaparte, J. F. 1984. Locomotion in rauisuchid thecodonts. Journal of Vertebrate Paleontology
1348 3:210-218.
1349 Brochu, C. A. 1996. Closure of neurocentral sutures during crocodilian ontogeny: implications
1350 for maturity assessment in fossil archosaurs. Journal of Vertebrate Paleontology 16:49-
1351 62.
1352 Brusatte, S. L., M. J. Benton, J. B. Desojo, and M. C. Langer. 2010. The higher-level phylogeny
1353 of Archosauria (Tetrapoda: Diapsida). Journal of Systematic Palaeontology 8:3-47.
1354 Brusatte, S. L., M. J. Benton, M. Ruta, and F. T. Lloyd. 2008. Superiority, competition, and
1355 opportunism in the evolutionary radiation of dinosaurs. Science 321:1485-1488.
1356 Brusatte, S. L., R. J. Butler, T. Sulej, and G. Niedzwiedzki. 2009. The taxonomy and anatomy of
1357 rauisuchian archosaurs from the Late Triassic of Germany and Poland. Acta
1358 Palaeontologica Polonica 54:221-230.
1359 Butler, R. J., S. L. Brusatte, M. Reich, S. J. Nesbitt, R. R. Schoch, and J. J. Hornung. 2011. The
1360 sail-backed reptile *Ctenosauriscus* from the latest Early Triassic of Germany and the
1361 timing and biogeography of the early archosaur radiation. PLoS One 6:1-28.

1362 Butler, R. B., C. Sullivan, M. D. Ezcurra, J. Liu, A. Lecuona, and R. B. Sookias. 2014. New clade
1363 of enigmatic early archosaurs yields insights into early pseudosuchian phylogeny and
1364 the biogeography of the archosaur radiation. BMC Evolutionary Biology 14:1-16.
1365 Butler, R. J., S. L. Brusatte, M. Reich, S. J. Nesbitt, R. R. Schoch, and J. J. Hornung. 2011. The
1366 sail-backed reptile ctenosauriscus from the latest Early Triassic of Germany and the
1367 timing and biogeography of the early archosaur radiation. PLoS One 6:1-28.
1368 Butler, R. J., S. J. Nesbitt, A. J. Charig, D. J. Gower, and P. M. Barrett. 2018. *Mandasuchus*
1369 *tanyauchen* gen. et sp. nov., a pseudosuchian archosaur from the Manda Beds of
1370 Tanzania; pp. 96–121 in C. A. Sidor, and S. J. Nesbitt (eds.), Vertebrate and climatic
1371 evolution in the Triassic rift basins of Tanzania and Zambia. Society of Vertebrate
1372 Paleontology Memoir 17, Journal of Vertebrate Paleontology 37 (6, supplement).
1373 Cavaroc, V. V., and R. M. Flores. 1991. Red beds of the Triassic Chugwater Group,
1374 Southwestern Powder River Basin, Wyoming. US. Geological Survey Bulletin 1917-E,
1375 17.
1376 Chatterjee, S. 1985. *Postosuchus*, a new thecodontian reptile from the Triassic of Texas and the
1377 origin of tyrannosaurs. Philosophical Transactions of the Royal Society of London B
1378 309:395-460.
1379 Clark, J. M., and H.-D. Sues. 2002. Two new basal crocodylomorph archosaurs from the Lower
1380 Jurassic and the monophyly of the Sphenosuchia. Zoological Journal of the Linnean
1381 Society 136:77-95.
1382 Colbert, E. H. 1952. A pseudosuchian reptile from Arizona. Bulletin of the American Museum of
1383 Natural History 99:561-592.
1384 Colbert, E. H. 1989. The Triassic dinosaur *Coelophysis*. Bulletin of the Museum of Northern
1385 Arizona 57:1-174.
1386 Cope, E. D. 1869. Synopsis of the extinct Batrachia, Reptilia, and Aves of North America.
1387 Transactions of the American Philosophical Society 40:1-252.

1388 Dawley, R. M., J. M. Zawiske, and J. W. Cosgriff. 1979. A rauisuchid thecodont from the Upper
1389 Triassic Popo Agie Formation of Wyoming. Journal of Paleontology 53:1428-1431.
1390 de França, M. A. G., J. Ferigolo, and M. C. Langer. 2011. Associated skeletons of a new Middle
1391 Triassic “Rauisuchia” from Brazil. Naturwissenschaften 98:389-395.
1392 de França, M. A. G., M. C. Langer, and J. Ferigolo. 2013. The skull anatomy of *Decuriasuchus*
1393 *quartacolonia* (Pseudosuchia: Suchia: Loricata) from the middle Triassic of Brazil; pp.
1394 469-501 in S. J. Nesbitt, J. B. Desojo, and R. B. Irmis (eds.), Anatomy, Phylogeny and
1395 Palaeobiology of Early Archosaurs and their Kin. Geological Society, London, Special
1396 Publications, London.
1397 Desojo, J. B., M. B. Von Baczko, and O. W. M. Rauhut. 2020. Anatomy, taxonomy and
1398 phylogenetic relationships of *Prestosuchus chiniquensis* (Archosauria: Pseudosuchia)
1399 from the original collection of von Huene, Middle-Late Triassic of southern Brazil.
1400 Palaeontologia Electronica 23:a04. https://doi.org/10.26879/1026palaeo-
1401 electronica.org/content/2020/2917-type-materials-of-prestosuchus.
1402 Ewer, R. F. 1965. The anatomy of the thecodont reptile *Euparkeria capensis* Broom.
1403 Philosophical Transactions of the Royal Society of London, Series B 248:379-435.
1404 Ezcurra, M. D. 2016. The phylogenetic relationships of basal archosauromorphs, with an
1405 emphasis on the systematics of proterosuchian archosauriforms. PeerJ:4:e1778.
1406 Ezcurra, M. D., S. J. Nesbitt, L. E. Fiorelli, and J. B. Desojo. 2019. New specimen sheds light on
1407 the anatomy and taxonomy of the early Late Triassic dinosauriforms from the Chañares
1408 Formation, NW Argentina. Anatomical Record: DOI: 10.1002/ar.24243.
1409 Gauthier, J. A. 1986. Saurischian monophyly and the origin of birds. Memoirs of the California
1410 Academy of Science 8:1-55.
1411 Gauthier, J. A., S. J. Nesbitt, E. Schachner, G. S. Bever, and W. G. Joyce. 2011. The bipedal
1412 stem crocodilian *Poposaurus gracilis*: inferring function in fossils and innovation in
1413 archosaur locomotion. Bulletin of the Peabody Museum of Natural History 52:107-126.

1414 Gebauer, E. V. I. 2004. Neubeschreibung von *Stagonosuchus nyassicus* v. Huene, 1938
1415 (Thecodontia, Rauisuchia) from the Manda Formation (Middle Triassic) of southwest
1416 Tanzania. Neues Jahrbuch für Geologie und Paläeontologie, Abhandlungen 231:1-35.
1417 Goloboff, P. A., and S. A. Catalano. 2016. TNT version 1.5, including a full implementation of
1418 phylogenetic morphometrics. Cladistics 32:221-238.
1419 Gower, D. J. 1999. The cranial and mandibular osteology of a new rauisuchian archosaur from
1420 the Middle Triassic of southern Germany. Stuttgarter Beitraege zur Naturkunde Serie B
1421 (Geologie und Palaeontologie) 280:1-49.
1422 Gower, D. J. 2000. Rauisuchian archosaurs (Reptilia, Diapsida): An overview. Neues Jahrbuch
1423 für Geologie und Paläontologie Abhandlungen 218:447-488.
1424 Gower, D. J. 2002. Braincase evolution in suchian archosaurs (Reptilia: Diapsida): Evidence
1425 from the rauisuchian *Batrachotomus kupferzellensis*. Zoological Journal of the Linnean
1426 Society 136:49-76.
1427 Gower, D. J., and S. J. Nesbitt. 2006. The braincase of *Arizonasaurus babbitti*- further evidence
1428 of the non-monophyly of Rauisuchia. Journal of Vertebrate Paleontology 26:79-87.
1429 Gower, D. J., and R. Schoch. 2009. Postcranial anatomy of the rauisuchian archosaur
1430 *Batrachotomus kupferzellensis*. Journal of Vertebrate Paleontology 29:103-122.
1431 Gower, D. J., and A. G. Sennikov. 1996. Braincase morphology in early archosaurian reptiles.
1432 Palaeontology 39:883-906.
1433 Gower, D. J., and A. D. Walker. 2002. New data on the braincase of the aetosaurian archosaur
1434 (Reptilia: Diapsida) *Stagonolepis robertsoni* Agassiz. Zoological Journal of the Linnean
1435 Society 136:7-23.
1436 Hagdorn, H., R. Schoch, D. Seegis, and R. Werneburg. 2015. Wirbeltierlagerstätten im
1437 Lettenkeuper; pp. 325–358 in H. Hagdorn, R. R. Schoch, and G. Schweigert (eds.), Der
1438 Lettenkeuper – Ein Fenster in die Zeit vor den Dinosauriern. Staatliches Museum für
1439 Naturkunde Stuttgart, Stuttgart.

1440 High Jr, L. R., and M. D. Picard. 1969. Stratigraphic relations within upper Chugwater group
1441 (Triassic), Wyoming. American Association of Petroleum Geologists Bulletin
1442 53:1091-1104.
1443 Huene, F. v. 1942. Die fossilen Reptilien des Südamerikanischen Gondwanalandes.
1444 Ergebnisse der Sauriergrabungen in Südbrasilien 1928/29. 332 pp. C.H. Beck,
1445 München, Germany.
1446 Irmen, A., and C. Vondra. 2000. Aeolian sediments in Lower to Middle (?) Triassic rocks of
1447 central Wyoming. Sedimentary Geology 132:69-88.
1448 Irmis, R. B. 2007. Axial skeleton ontogeny in the parasuchia (Archosauria: Pseudosuchia) and
1449 its implications for ontogenetic determination in archosaurs. Journal of Vertebrate
1450 Paleontology 27:350-361.
1451 Jalil, N.-E., and K. Peyer. 2007. A new rauisuchian (Archosauria, Suchia) from the Upper
1452 Triassic of the Argana Basin, Morocco. Palaeontology 50:417-430.
1453 Johnson, E. A. 1993. Depositional History of Triassic Rocks in the Area of the Powder River
1454 Basin, Northeastern Wyoming, and Southeastern Montana. US Government Printing
1455 Office.
1456 Juul, L. 1994. The phylogeny of basal archosaurs. Palaeontologia Africana 31:1-38.
1457 Krebs, B. 1976. Pseudosuchia; pp. 40-98 in O. Kuhn (ed.), Handbuch Palaoherpetology. Gustav
1458 Fischer Verlag, Stuttgart.
1459 Lacerda, M. B., M. A. de França, and C. L. Schultz. 2018. A new erpetosuchid (Pseudosuchia,
1460 Archosauria) from the Middle–late Triassic of Southern Brazil. Zoological Journal of the
1461 Linnean Society 184:804-824.
1462 Lacerda, M. B., B. M. Mastrantonio, D. C. Fortier, and C. L. Schultz. 2016. New insights on
1463 *Prestosuchus chiniquensis* Huene, 1942 (Pseudosuchia, Loricata) based on new
1464 specimens from the “Tree Sanga” Outcrop, Chiniquá Region, Rio Grande do Sul, Brazil.
1465 PeerJ 4:e1622.

1466 Langer, M. C., M. D. Ezcurra, O. W. Rauhut, M. J. Benton, F. Knoll, B. W. McPhee, F. E. Novas,
1467 D. Pol, and S. L. Brusatte. 2017. Untangling the dinosaur family tree. Nature 551:E1-E3.
1468 Lautenschlager, S., and J. B. Desojo. 2011. Reassessment of the Middle Triassic rauisuchian
1469 archosaurs *Ticinosuchus ferox* and *Stagonosuchus nyassicus*. Paläontologische
1470 Zeitschrift 85:357-381.
1471 Lautenschlager, S., and O. W. M. Rauhut. 2015. Osteology of *Rauisuchus tiradentes* from the
1472 Late Triassic (Carnian) Santa Maria Formation of Brazil, and its implications for
1473 rauisuchid anatomy and phylogeny. Zoological Journal of the Linnean Society 173:55-
1474 91.
1475 Lessner, E. J., M. R. Stocker, N. D. Smith, A. H. Turner, R. B. Irmis, and S. J. Nesbitt. 2016. A
1476 new taxon of rauisuchid (Archosauria, Pseudosuchia) from the Upper Triassic of New
1477 Mexico increases the diversity and temporal range of the clade. PeerJ 4:e2336.
1478 Long, R. A., and P. A. Murry. 1995. Late Triassic (Carnian and Norian) tetrapods from the
1479 southwestern United States New Mexico Museum of Natural History and Science
1480 Bulletin 4:1-254.
1481 Lovelace, D. M., and A. C. Doebbert. 2015. A new age constraint for the Early Triassic Alcova
1482 Limestone (Chugwater Group), Wyoming. Palaeogeography, Palaeoclimatology,
1483 Palaeoecology 424:1-5.
1484 Lucas, S.G. 1994. The beginning of the age of dinosaurs in Wyoming. Wyoming Geological Association
1485 Guidebook, 44:105-113.
1486 Lucas, S. G. 1998. Global Triassic tetrapod biostratigraphy and biochronology.
1487 Palaeogeography, Palaeoclimatology, Palaeoeocology 143:347-384.
1488 Lucas, S. G., A. B. Heckert, and N. Hotton III. 2002. The rhynchosaur *Hyperodapedon* from the
1489 Upper Triassic of Wyoming and its global biochronological significance. Bulletin of the
1490 New Mexico Museum of Natural History and Science 21:149-156.

1491 Lucas, S. G., A. B. Heckert, and L. Rinehart. 2007. A giant skull, ontogenetic variation and
1492 taxonomic validity of the Late Triassic phytosaur *Parasuchus*. Bulletin of the New Mexico
1493 Museum of Natural History and Science 41:222-227.
1494 Maddison, W. P., and D. R. Maddison. 2015. Mesquite: a modular system
1495 for evolutionary analysis (version 3.02). Available at http://mesquiteproject.org
1496 Mastrantonio, B. M., M. B. Von Baczko, J. B. Desojo, and C. L. Schultz. 2019. The skull
1497 anatomy and cranial endocast of the pseudosuchid archosaur *Prestosuchus*
1498 *chiniquensis* from the Triassic of Brazil. Acta Palaeontologica Polonica 64:171-198.
1499 Nesbitt, S. J. 2003. *Arizonasaurus* and its implications for archosaur divergences. Proceedings
1500 of the Royal Society of London, B 270(Supplement 2):S234-S237.
1501 Nesbitt, S. J. 2005. The osteology of the Middle Triassic pseudosuchian archosaur
1502 *Arizonasaurus babbitti*. Historical Biology 17:19-47.
1503 Nesbitt, S. J. 2007. The anatomy of *Effigia okeeffeae* (Archosauria, Suchia), theropod
1504 convergence, and the distribution of related taxa. Bulletin of the American Museum of
1505 Natural History 302:1-84.
1506 Nesbitt, S. J. 2011. The early evolution of Archosauria: relationships and the origin of major
1507 clades. Bulletin of the American Museum of Natural History 352:1-292.
1508 Nesbitt, S. J., S. L. Brusatte, J. B. Desojo, A. Liparini, D. J. Gower, M. A. G. d. França, and J. C.
1509 Weinbaum. 2013a. “Rauisuchia”; pp. 241-274 in S. J. Nesbitt, J. B. Desojo, and R. B.
1510 Irmis (eds.), Anatomy, Phylogeny, and Palaeobiology of Early Archosaurs and their Kin.
1511 Geological Society, London, Special Volume.
1512 Nesbitt, S. J., R. J. Butler, M. D. Ezcurra, P. M. Barrett, M. R. Stocker, K. D. Angielczyk, R. M.
1513 H. Smith, C. A. Sidor, G. Niedźwiedzki, A. Sennikov, and A. J. Charig. 2017. The earliest
1514 bird-line archosaurs and assembly of the dinosaur body plan. Nature 544:484-487.
1515 Nesbitt, S. J., R. J. Butler, M. D. Ezcurra, A. J. Charig, and P. M. Barrett. 2018. The anatomy of
1516 *Teleocrater rhadinus*, an early avemetatarsalian from the lower portion of the Lifua

1517 Member of the Manda Beds (~Middle Triassic); pp. 142-177 in C. A. Sidor, and S. J.
1518 Nesbitt (eds.), Vertebrate and climatic evolution in the Triassic rift basins of Tanzania
1519 and Zambia. Society of Vertebrate Paleontology Memoir 17, Journal of Vertebrate
1520 Paleontology 37 (6, supplement).
1521 Nesbitt, S. J., and J. B. Desojo. 2017. The osteology and phylogenetic position of *Luperosuchus*
1522 *fractus* (Archosauria: Loricata) from the latest Middle Triassic or earliest Late Triassic of
1523 Argentina. Ameghiniana 54:261–282.
1524 Nesbitt, S. J., R. B. Irmis, S. G. Lucas, and A. P. Hunt. 2005. A giant crocodylomorph from the
1525 upper Triassic of New Mexico. Palaeontologische Zeitschrift 79/4:471-478.
1526 Nesbitt, S. J., J. Liu, and C. Li. 2011. A sail-backed suchian from the Heshanggou Formation
1527 (Early Triassic: Olenekian) of China. Earth and Environmental Science Transactions of
1528 the Royal Society of Edinburgh 101:271-284.
1529 Nesbitt, S. J., C. A. Sidor, K. D. Angielczyk, R. M. H. Smith, and L. A. Tsuji. 2014. A new
1530 archosaur from the Manda beds (Anisian: Middle Triassic) of southern Tanzania and its
1531 implications for character optimizations at Archosauria and Pseudosuchia. Journal of
1532 Vertebrate Paleontology 34:1357-1382.
1533 Nesbitt, S. J., C. A. Sidor, R. B. Irmis, K. D. Angielczyk, R. M. H. Smith, and L. A. Tsuji. 2010.
1534 Ecologically distinct dinosaurian sister-group shows early diversification of Ornithodira.
1535 Nature 464:95-98.
1536 Nesbitt, S. J., N. D. Smith, R. B. Irmis, A. H. Turner, A. Downs, and M. A. Norell. 2009. A
1537 complete skeleton of a Late Triassic saurischian and the early evolution of dinosaurs.
1538 Science 326:1530-1533.
1539 Nesbitt, S. J., A. H. Turner, and J. C. Weinbaum. 2013b. A survey of skeletal elements in the
1540 orbit of Pseudosuchia and the origin of the crocodylian palpebral. Earth and
1541 Environmental Science Transactions of the Royal Society of Edinburgh 103:365-381.

1542 Parker, W. G., and S. J. Nesbitt. 2013. Cranial remains of *Poposaurus gracilis* (Pseudosuchia:
1543 Poposauroidea) from the Upper Triassic, the distribution of the taxon and its implications
1544 for poposauroid evolution; pp. 503-523 in S. J. Nesbitt, J. B. Desojo, and R. B. Irmis
1545 (eds.), Anatomy, Phylogeny, and Palaeobiology of Early Archosaurs and their Kin.
1546 Geological Society, London, Special Volume.
1547 Parrish, J. M. 1993. Phylogeny of the Crocodylotarsi, with reference to archosaurian and
1548 crurotarsan monophyly. Journal of Vertebrate Paleontology 13:287-308.
1549 Peyer, K., J. G. Carter, H.-D. Sues, S. E. Novak, and P. E. Olsen. 2008. A new suchian
1550 archosaur from the Upper Triassic of North Carolina. Journal of Vertebrate Paleontology
1551 28:363-381.
1552 Picard, M. D. 1978. Stratigraphy of Triassic rocks in west-central Wyoming. Wyoming
1553 Geological Association Resources of the Wind River Basin; 30th Annual Field
1554 Conference Guidebook: 101-130.
1555 Roberto-Da-Silva, L., R. T. Müller, M. A. G. d. França, S. F. Cabreira, and S. Dias-Da-Silva.
1556 2018. An impressive skeleton of the giant top predator *Prestosuchus chiniquensis*
1557 (Pseudosuchia: Loricata) from the Triassic of Southern Brazil, with phylogenetic
1558 remarks. Historical Biology:1-20.
1559 Romer, A. S. 1971. The Chañares (Argentina) Triassic reptile fauna. VIII. A fragmentary skull of
1560 a large thecodont, *Luperosuchus fractus*. Breviora 373:1-8.
1561 Schachner, E. R., R. B. Irmis, A. K. Huttenlocker, S. J. Nesbitt, R. K. Sanders, and R. L. Cieri.
1562 2019. Osteology of the Late Triassic bipedal archosaur *Poposaurus gracilis*
1563 (Archosauria: Pseudosuchia). Anatomical Record:DOI: 10.1002/ar.24298.
1564 Schoch, R. R., and J. B. Desojo. 2016. Cranial anatomy of the aetosaur *Paratypothorax*
1565 *andressorum* Long & Ballew, 1985, from the Upper Triassic of Germany and its bearing
1566 on aetosaur phylogeny. Neues Jahrbuch für Geologie und Paläontologie-Abhandlungen
1567 279:73-95.

1568 Schoch, R., S. J. Nesbitt, J. Muller, M. Fastnacht, S. G. Lucas, and J. A. Boy. 2010. The reptile
1569 assemblage from the Moenkopi Formation (Middle Triassic) of New Mexico. Neues
1570 Jahrbuch für Geologie und Paläontologie, Abhandlungen 255:245-369.
1571 Schoch, R. R., F. Ullmann, B. Rozynek, R. Ziegler, D. Seegis, and H.-D. Sues. 2018. Tetrapod
1572 diversity and palaeoecology in the German Middle Triassic (Lower Keuper) documented
1573 by tooth morphotypes. Palaeobiodiversity and Palaeoenvironments 98:615-638.
1574 Sereno, P. C., S. McAllister, and S. L. Brusatte. 2005. TaxonSearch: a relational database for
1575 suprageneric taxa and phylogenetic definitions. PhyloInformatics 8:1-21.
1576 Sill, W. D. 1974. The anatomy of *Saurosuchus galilei* and the relationships of the rauisuchid
1577 thecodonts. Bulletin of the Museum of Comparative Zoology 146:317-362.
1578 Stocker, M. R. 2010. Clarification of the skeletal anatomy of phytosaurs based on comparative
1579 anatomy and the most complete specimen of *Angistorhinus*. Journal of Vertebrate
1580 Paleontology, Program and Abstracts 2010:170A.
1581 Stocker, M. R., and R. J. Butler. 2013. Phytosauria; pp. 91-117 in S. J. Nesbitt, J. B. Desojo,
1582 and R. B. Irmis (eds.), Anatomy, Phylogeny and Palaeobiology of Early Archosaurs and
1583 their Kin. The Geological Society of London, London.
1584 Sulej, T. 2005. A new rauisuchian reptile (Diapsida: Archosauria) from the Late Triassic of
1585 Poland. Journal of Vertebrate Paleontology 25:78-86.
1586 Trotteyn, M. J., J. B. Desojo, and O. Alcober. 2011. Nuevo material postcraneano de
1587 *Saurosuchus galilei* Reig (Archosauria: Crurotarsi) del Triasico Superior del centro-oeste
1588 de Argentina. Ameghiniana 48:605-620.
1589 von Baczko, M. B., and J. B. Desojo. 2016. Cranial anatomy and palaeoneurology of the
1590 archosaur *Riojasuchus tenuisceps* from the Los Colorados Formation, La Rioja,
1591 Argentina. PLoS One 11: e0148575
1592 von Baczko, M. B., J. B. Desojo, and D. Pol. 2014. Anatomy and phylogenetic position of
1593 *Venaticosuchus rusconii* Bonaparte, 1970 (Archosauria, Pseudosuchia), from the

1594 Ischigualasto Formation (Late Triassic), La Rioja, Argentina. Journal of Vertebrate
1595 Paleontology 34:1342-1356.
1596 von Baczko, M. B., and M. D. Ezcurra. 2013. Ornithosuchidae: a group of Triassic archosaurs
1597 with a unique ankle joint; pp. 187-202 in S. J. Nesbitt, J. B. Desojo, and R. B. Irmis
1598 (eds.), Anatomy, Phylogeny and Palaeobiology of Early Archosaurs and their Kin.
1599 Geological Society, London, Special Publications, London.
1600 Walker, A. D. 1990. A revision of *Sphenosuchus acutus* Haughton, crocodylomorph reptile from
1601 the Elliot Formation (Late Triassic or Early Jurassic) of South Africa. Philosophical
1602 Transactions of the Royal Society of London B 330:1-120.
1603 Weinbaum, J. C. 2011. The skull of *Postosuchus kirkpatricki* (Archosauria: Paracrocodyliformes)
1604 from the Upper Triassic of the United States. PaleoBios 30:18-44.
1605 Weinbaum, J. C. 2013. Postcranial skeleton of *Postosuchus kirkpatricki* (Archosauria:
1606 Paracrocodylomorpha), from the Upper Triassic of the United States; pp. 525-553 in S.
1607 J. Nesbitt, J. B. Desojo, and R. B. Irmis (eds.), Anatomy, Phylogeny and Palaeobiology
1608 of Early Archosaurs and their Kin. Geological Society, London, Special Publications,
1609 London.
1610 Weinbaum, J. C., and A. Hungerbühler. 2007. A revision of *Poposaurus gracilis* (Archosauria:
1611 Suchia) based on two new specimens from the Late Triassic of the southwestern U.S.A.
1612 Paläontologische Zeitschrift 81/2:131-145.
1613 Witmer, L. M. 1997. The evolution of the antorbital cavity of archosaurs: a study in soft-tissue
1614 reconstruction in the fossil record. Journal of Vertebrate Paleontology Memoir 3:1-73.
1615 Wroblewski, A. F.-J. 1997. Mixed assemblages and the birth of a chimera: an example from the
1616 Popo Agie Formation (Upper Triassic), Wyoming. Journal of Vertebrate Paleontology 17
1617 (suppliment to 3):86A.

Zawiskie, J. M., and R. M. Dawley. 2003. On the skull and holotype of *Heptasuchus clarki* (Rauisuchia, Poposauridae) from the Upper Triassic Popo Agie Formation, Natrona Co. Wyoming. Southwest Paleontological Symposium 2003 Guide to Presentations.

## Figure Captions

Figure 1. Distribution of Chugwater Group strata in Wyoming near the location of the type locality of *Heptasuchus clarki*. Stratigraphic section at the type locality of *Heptasuchus clarki* in the upper portion of the unnamed red beds of the upper portion of the Chugwater Group, Big Horn Mountains and a detailed stratigraphic section through the bonebed. Abbreviations: cm, centimeters; GSF, Gypsum Springs Formation; J, Jurassic; LS, limestone; SS, sandstone. [1 column]

Figure 2. The holotype skull of *Heptasuchus clarki* (UW 11562) as found in the field. Image credit: Robert M Dawley. Abbreviations: bc, braincase; j, jugal; l., left; mx, maxilla; n, nasal; pmx, premaxilla; po, postorbital; r., right; sp?, splenial?. Scale = 20 cm [1 column]

Figure 3. Reconstruction of the skull of *Heptasuchus clarki* in right lateral view illustrating the material recovered (light red) from the type locality. Skull reconstruction based on *Batrachotomus kupferzellensis* from Gower (1999). Abbreviations: fr, frontal; j, jugal, la, lacrimal; mx, maxilla, na, nasal; pmx, premaxilla; po, postorbital; pof, postfrontal; prf, prefrontal; q, quadrate; qj, quadratojugal; sq, squamosal. Scale = 5 cm. [1 column]

Figure 4. Reconstruction of the skeleton of *Heptasuchus clarki* in lateral view illustrating the material recovered from the type locality. Skeleton reconstruction based on *Postosuchus*

*kirkpatricki* (Nesbitt et al. 2013a) and skull reconstruction based on Figure 3. Scale = 50 cm. [2 columns]

Figure 5. Skull elements of *Heptasuchus clarki* (UW 11562): left maxilla (UW 11562-C) in lateral (A) and medial (B) views; right maxilla (UW 11562-B) in medial (C) and lateral (D) views; right premaxilla (UW 11562-A) in lateral (E) and medial (F) views; right nasal (UW 11562-F) in lateral (G) and medial (H) views. Abbreviations: a., articulates with; al, alveolus; anf, antorbital fenestra; anfo, antorbital fossa; apn, anterior process of nasal; d, depression; dp, dorsal process; en, external naris; f, fossa; for, foramen; fr, frontal; j, jugal; la, lacrimal; ms, midline suture; mx, maxilla; mpn, maxillary process of nasal; nf, narial fossa; pd, posterodorsal process; plp, palatal process of the premaxilla; plm, palatal process of the maxilla; pmx, premaxilla; r, ridge; rt, replacement tooth; t, tooth; tr, tooth root. Broken surfaces indicated in hash marks. Arrows indicate anterior direction. Scales = 5 cm. [2 columns]

Figure 6. Skull elements of *Heptasuchus clarki* (UW 11562): right postorbital, postfrontal, and frontal (UW 11562-G) in dorsal (A), medial (B) and, with the reattached prefrontal in lateral (C) views; right jugal (UW 11562-D) in lateral (D) and medial (E) views; left palatine (UW 11562-K) in dorsal (F) view. Abbreviations: a., articulates with; d, depression; ec, ectopterygoid; f, fossa; fr, frontal; g, groove; la, lacrimal; ltf, lower temporal fenestra; mx, maxilla; o, orbit; pa, parietal; pf, postfrontal; po, postorbital; prf; prefrontal; sqm squamosal; r, ridge; stf; supratemporal fenestra; stfo, surpratemporal fossa. Broken surfaces indicated in hash marks. Arrows indicate anterior direction. Scales = 5 cm. [2 columns]

Figure 7. The braincase of *Heptasuchus clarki* (UW 11562-H) in right lateral (A), posterolateral (B), medial (C) and posterior (D) views. Abbreviations: bt, basitubera; bpt, basipterygoid process; ci, crista interfenestralis; cp, cultriform process; f, fossa; fo, fenestra ovalis; g., groove

for; ic, entrance of the internal carotid; lr, lateral ridge; mf, metotic foramen; np, notochoral pit; oc, occipital condyle; pa, parietal; pbs, parabasisphenoid; pp, paroccipital process of the otoccipital; ppt; ridge possibly for attachment of protractor pterygoidei; ptf, posttemporal fenestra; so, supraoccipital; ug, unossified gap; V, exit of cranial nerve V (trigeminal); VI, exit of cranial nerve VI (abducens); VII, exit of cranial nerve VII (facial); XII, exit of cranial nerve XII (hypoglossal). Broken surfaces indicated in hash marks. Arrows indicate anterior direction. Scales = 5 cm. [2 columns]

Figure 8. Fragmentary skull elements of *Heptasuchus clarki:* ventral portion of the left quadrate (UW 11563-AF + UW 11563-H, labeled before putting together) in posterior (A), anterior (B), and ventral (C) views; dorsal head of the quadrate (side unknown; UW 11562) in lateral? (D) view; possible fragments of the pterygoid (UW 11562-M) in two (E-F) views; possible fragment of the pterygoid (UW 11562-L) in two (G-H) views. Arrows indicate anterior direction. Scales = 1 cm. [1 column]

Figure 9. Axial elements of *Heptasuchus clarki*: posterior trunk vertebra (TMM 45902-2) in right lateral (A) and posterior (B) views; neural spine of a cervical-trunk vertebra (UW 11562-CX) in dorsal (C) and posterior (D) views; presacral neural spine (UW 11562-V) in lateral (E) view; presacral neural spine (UW 11562-CT) in lateral (F) view; anterior caudal vertebra in lateral (G) and anterior (H) views; distal caudal vertebra (UW 11562-BW) in ventral (I) and posterior (J) views; osteoderm (TMM 45902-1) in three views; anterior caudal vertebra in dorsal (K), ventral (L), and lateral (M) views. Arrows indicate anterior direction. Scales = 1 cm. [1 column]

Figure 10. Pectoral elements and incomplete humerus of *Heptasuchus clarki*: right incomplete scapula (UW 11565-E) in lateral (A) view; incomplete left coracoid (UW 11566) in lateral (B) view; proximal portion of left humerus (UW 11565-A) in proximal (C) and posterior (D) views.

Arrows indicate anterior direction. Abbreviations: cf, coracoid foramen; dp, deltopectoral crest; gl, glenoid; tu, tuber. Scales = 1 cm. [1 column]

Figure 11. Forelimb elements of *Heptasuchus clarki*: proximal portion of the radius (UW 11562-DM) in proximal (A), and lateral (B) views and the distal portion of the radius (UW 11562-DI) in ?anterior (C) and distal (D) views; right ulna (UW 11562-W) in proximal (E), medial (F), posterior (G), and distal (H) views; left ulna (UW 11562-X) in proximal (I), posterior (J), anterior (K), and distal (L) views. Abbreviations: gr, groove; lr, lateral ridge; op, olecranon process; r, ridge. Scales = 1 cm in A-D and 5 cm in E-L. [1 column]

Figure 12. Pelvic elements of *Heptasuchus clarki*: left pubis (UW 11562-Y) in lateral (A), anterior (B), medial (C), and distal (D) views; proximal portion of the right ischium (UW 11564-B) in lateral (E) view; pubic peduncle of the right ilium (UW 11563) in lateral (F) view. Abbreviations: a., articulates with; as, acetabulum; il, ilium; pa, pubic apron; pb, pubic boot; pit, pit; pp, pubic peduncle; pu, pubis. Arrows indicate anterior direction. Scales = 5 cm in A-B and 1 cm in E-F. [1 column]

Figure 13. Hindlimb elements of *Heptasuchus clarki*: proximal portion of a right femur (UW 11563-B) in proximal (A) and anterolateral (B) views and the distal portion of the right femur (UW 11563-A) in anterior (C) and distal (D) views; left tibia (UW 11562-Z) in proximal (E), posterior (F), anterior (G), and distal (H) views; proximal portion of a right fibula (UW 11566-S) in proximal (I) and anterolateral (J) views and the distal portion of the right fibula (UW 11566-R) in anterior (K) and distal (L) views. Right proximal portion of metatarsal IV (UW 11566) in proximal (M) and ventrolateral (N) views. Possible right metatarsal II (UW 11562DU) in proximal (O) and dorsomedial (P) views. Possible pedal ungual (UW 11562DT) in proximal (Q) and dorsal (R) views. Abbreviations: alc, anterolateral tuber; amt, anteromedial tuber; cc, cnemial

1720 crest; ctf, crista tibiofibularis; lc, lateral condyle; mc, medial condyle; plt, posterolateral tuber.
1721 Arrows indicate anterior direction. Scales = 1 cm in A-D, I-R and = 5 cm in E-H. [1 column]
1722
1723 Figure 14. New illustrated character states for paracrocodylomorph archosaurs: (A) skull
1724 referred to *Prestosuchus chiniquensis* (ULBRA-PVT-281) in right lateral view; (B) right
1725 postorbital of *Batrachotomus kupferzellensis* (SMNS 52970) in dorsal (top) and lateral (bottom)
1726 view; (C) left postorbital of *Heptasuchus clarki* (UW 11562) in lateral view; (D) left maxilla of
1727 *Batrachotomus kupferzellensis* (SMNS 52970) in medial view; (E) right maxilla of *Heptasuchus*
1728 *clarki* (UW 11562) in medial view; (F) right nasal of *Batrachotomus kupferzellensis* (SMNS
1729 52970) in lateral view; (G) right nasal of *Heptasuchus clarki* (UW 11562) in lateral view; (H) left
1730 maxilla of *Xilousuchus sapingensis* (IVPP V6026) in medial view; (I) right premaxilla of
1731 *Heptasuchus clarki* (UW 11562) in lateral view; (J) left premaxilla of *Postosuchus kirkpatricki*
1732 (TTUP 9000) in lateral view; (K) left premaxilla of *Xilousuchus sapingensis* (IVPP V6026) in
1733 lateral view; (L) right jugal of *Heptasuchus clarki* (UW 11562) in lateral view; (M) right jugal of
1734 *Heptasuchus clarki* (UW 11562) in medial view; (N) left jugal of *Batrachotomus kupferzellensis*
1735 (SMNS 52970) in lateral view; (O) left jugal of *Batrachotomus kupferzellensis* (SMNS 52970) in
1736 medial view. Numbers refer to character number separated by a dash from the state. Scales in
1737 10 cm in A, 5 cm in C-G, I, L-M, and 1 cm in B, H, J-K, N-O. [2 columns]
1738
1739 Figure 15. Partial phylogenetic tree focused on pseudosuchian relationships with *Heptasuchus*
1740 *clarki* included. *Heptasuchus clarki* was found as a loricatan as the sister-taxon of
1741 *Batrachotomus kupferzellensis*. Tree derived from 72 most parsimonious trees (MPTs) of length
1742 (1529 steps) (Consistency Index = 0.335; Retention Index = 0.752)(see supplemental
1743 information figure S2). [1 column]
1744
1745 Appendix: New character descriptions and illustrations:

425. Postorbital, ventral end, depression on the anterolateral surface: (0) - absent; (1) - present. (new; Fig. 14)

The plesiomorphic condition, state 0, in stem archosaurs and within Archosauria is to have a tapering ventral end of the postorbital that fits onto the anterodorsal edge of the dorsal process of the jugal and this condition is clear in the following exemplary taxa: *Euparkeria capensis* (Ewer 1965); *Lewisuchus admixtus* (Bittencourt et al. 2015); *Gracilisuchus stipanicicorum* (MCZ 4117), *Paratypothorax andressorum* (SMNS 19003; Schoch and Desojo 2016) and *Luperosuchus fractus* (PULR 04). In a number of loricatan taxa (e.g., *Batrachotomus kupferzellensis*, SMNS 80260; *Heptasuchus clarki*, UW 11562; and to a lesser degree *Postosuchus kirkpatricki*, TTUP 9000), the ventral end of the postorbital extends anteriorly into the orbit (Benton and Clark 1988; Juul, 1994; Benton, 1999; Alcober, 2000; Benton and Walker, 2002; Brusatte et al. 2010; Nesbitt 2011 Character 65). Out of these taxa, the ventral end of the postorbital is flat or nearly flat whereas a depression on the ventrolateral portion of the distal end of the postorbital is present in both *Batrachotomus kupferzellensis* (SMNS 80260), *Postosuchus kirkpatricki* TTUP 9000, and *Heptasuchus clarki* (UW 11562) – state 1. Gower (1999) listed the depression as a possible autapomorphy of *Batrachotomus kupferzellensis*. The ventrolateral depression in *Heptasuchus clarki* is much deeper and much of the depth is hidden in lateral view compared to *Batrachotomus kupferzellensis* and *Postosuchus kirkpatricki*.

426. Maxilla, medial side, ventral surface of palatal process: (0) flat; (1) - depression present. (new; Fig. 14)

The palatal process of the maxilla is horizontal in most archosauriforms and the ventral surface of the palatal process is typically flat or slightly concave. Within Pseudosuchia, the ventral surface of the palatal process is flat in *Xilousuchus sapingensis* (Nesbitt et al. 2011), *Revueltosaurus callenderi* (PEFO 34561) and in the ornithosuchid *Riojasuchus tenuisceps* (PVL 3827; von Baczko and Desojo 2016). In contrast, a dorsally extended depression at the

posteroventral side of the palatal process of the maxilla is present in *Postosuchus kirkpatricki* (TTUP 9000), *Polonosuchus silesiacus* (ZPAL Ab III/543), *Fasolasuchus tenax* (PVL 3851), *Heptasuchus clarki* (UW 11562). *Batrachotomus kupferzellensis* (SMNS 80260), *Arganosuchus dutuit* (ALM 1; Jalil and Peyer 2007) and possibly in *Sphenosuchus actus* (SAM 3014). It appears that the depression is not present in any of the *Prestosuchus chiniquensis* specimens where the palatal process is visible (Mastrantonio et al. 2019). In some taxa (e.g., *Postosuchus kirkpatricki,* TTUP 9000) the depression is much deeper in that the depression extends well dorsal to the dorsal extent of the palatal process whereas in *Sphenosuchus actus*, the depression is rather shallow but occurs in the same position as that of other loricatans. The function of the depression is not clear. Chatterjee (1985) hypothesized that the depression could serve as the area for Jacobson's organ. However, Weinbaum (2011) points out that Jacobson's organ is not present in crocodylians and avians and thus unlikely that this depression was for housing Jacobson's organ. The depression is located too far medially and, in most taxa, dorsally to represent a depression for accepting an enlarged dentary tooth.

427. Postorbital, lateral side, posterodorsal portion of the ventral process: (0) – smooth; (1) – slight depression, usually ventral to a rounded knob or ridge. (new; Fig. 14)

The posterior side of the postorbital is typically bowed or flat similar to the anterior and lateral sides of the base of the ventral process. Examples of taxa with this plesiomorphic condition include *Euparkeria capensis* (Ewer 1965); *Lewisuchus admixtus* (Bittencourt et al. 2014); *Gracilisuchus stipanicicorum* (MCZ 4117), and *Paratypothorax andressorum* (SMNS 19003; Schoch and Desojo 2016). Within Paracrocodylomorpha, *Luperosuchus fractus* (PULR 04), and *Xilousuchus sapingensis* (Nesbitt et al. 2011) have state 0. In *Prestosuchus chiniquensis* (UFRGS-PV-0629-T; Mastrantonio et al. 2019), *Postosuchus kirkpatricki* (TTUP 9000), *Batrachotomus kupferzellensis* (SMNS 80260), *Heptasuchus clarki* (UW 11562), *Arizonasaurus babbitti* (MSM 4590), and *Sphenosuchus actus* (SAM 3014) have a clear

depression on the posterior side of the ventral process of the postorbital near its base (i.e., near the contact with the squamosal. The taxa scored as state 1 typically have a vertical ridge, sometimes rugose, that divide the anterior part of the ventral process of the postorbital from the posterior portion.

428. Squamosal - postorbital articulation: (0) - postorbital fits into a groove on the lateral side of the squamosal; (1) - the postorbital lies on the dorsal surface of the squamosal; (2) - the squamosal largely lies on the dorsal surface of the postorbital. (new; Fig. 14)

In stem archosaurs and most members of Archosauria, the posterior portion of the postorbital fits into a clear slot into the lateral side of the squamosal. Clear examples of this articulation include *Euparkeria capensis* (Ewer 1965), *Arizonasaurus babbitti* (MSM 4590), *Paratypothorax andressorum* (SMNS 19003; Schoch and Desojo 2016), and *Riojasuchus tenuisceps* (PVL 3827; von Baczko and Desojo 2016). In most loricatans, the anterior process of the squamosal largely fits on the dorsal surface of the postorbital (state 1). As noted by Gower (1999) for *Batrachotomus kupferzellensis*, much of the squamosal of the taxon dorsally overlaps the postorbital, but there is some complexity to this articulation; a small part of the posteromedial portion of the postorbital is underlapped by the squamosal, and this results in the postorbital lying in a small notch of the squamosal. Early diverging loricatans *Luperosuchus fractus* (Nesbitt and Desojo 2017), *Prestosuchus chiniquensis* (UFRGS-PV-0629-T), and *Saurosuchus galilei* (PVSJ 32) appear to have state 1, although it is a bit difficult to see the articulation in the specimens represented by partially articulated or fully articulated skulls. State 1 is clearly present in *Batrachotomus kupferzellensis* (SMNS 80260), *Heptasuchus clarki* (UW 11562), and *Postosuchus kirkpatricki* (TTUP 9000). Within Crocodylomorpha, state 2 appears to be present across the clade where the postorbital largely lies over the squamosal and this is clear in early members of crocodylomorphs like *Dromicosuchus grallator* (NCSM 13733), *Dibothrosuchus elaphros* (IVPP V 7907), and *Litargosuchus leptorhynchus* (Clark and Sues

2002). Crocodyliforms appear to have an interdigitating suture between the postorbital and squamosal so these taxa are scored as ?.

429. Jugal, posterior process, medial side, longitudinal groove: (0) – absent; (1) - present. (new; Fig. 14)

Typically, the medial surface of the posterior process of the jugal of stem archosaurs (e.g., *Euparkeria capensis*) and members of Archosauria (e.g., *Arizonasaurus babbitti*, MSM 4590; *Effigia okeeffeae*; Nesbitt, 2007) are smooth. A clear groove, that parallels the ventral edge is present for nearly the entire length of the jugal in *Batrachotomus kupferzellensis* (SMNS 52970), *Postosuchus kirkpatricki* (TTUP 9000), *Polonosuchus silesiacus* (ZPAL Ab III/543), *Heptasuchus clarki* (UW 11562), and *Sphenosuchus actus* (SAM 3014).

430. Nasal, posterodorsal corner of the naris: (0) - smooth or slight fossa; (1) - distinct fossa with a rim present. (new; Fig. 14)

The anterior portion of the nasal of archosaurs typically splits into a process that lies dorsal to the external naris and one that extends anteroventrally posterior of the external naris (=descending process of some). In the juncture of the two anterior processes, the surface is typically flat. This is the case in most loricatans (e.g., *Postosuchus kirkpatricki*; TTUP 9000; specimens referred to *Prestosuchus chiniquensis*). In *Batrachotomus kupferzellensis* (SMNS 52970) and *Heptasuchus clarki* (UW 11562), there is a clear narial fossa (sensu Gower 1999) between the two anterior processes. Ventral to this fossa, a ridge framing the fossa is present on the anteroventral process in these taxa. This depression is not the fully the consequence of the ridge present dorsally (character 35, state 1) given that *Postosuchus kirkpatricki* (TTUP 9000) possesses that ridge, but not the fossa. A Moenkopi form (NMMNH 55779; Schoch et al. 2010) also possesses state 1.

431. Maxilla, anteroventral corner: (0) - abuts premaxilla; (1) - extensively laterally overlaps the posteroventral corner of the premaxilla. (new; Fig. 14)

Within stem archosaurs and within Archosauria, the juncture between the maxilla and premaxilla at their ventral borders is either separated by a gap (e.g., *Riojasuchus tenuisceps*, von Baczko and Desojo 2016; *Coelophysis bauri*, Colbert 1989), or is loosely connected (e.g., *Euparkeria capensis*, Ewer 1965; *Turfanosuchus dabanensis*, IVPP V3237). In loricatans, there is a medially extended articulation surface between the maxilla and premaxilla. Here, the anterolateral portion of the maxilla lies onto a clear articulation surface on the posterolateral side of the premaxilla. This character state (1) is present in *Saurosuchus galilei* (PVSJ 32), *Batrachotomus kupferzellensis* (SMNS 52970), *Heptasuchus clarki* (UW 11562), *Polonosuchus silesiacus* (ZPAL Ab III/543), *Postosuchus kirkpatricki* (TTUP 9000), and *Fasolasuchus tenax* (PVL 3851). The state in crocodylomorphs is not clear.

This character is difficult to score in articulated skulls because the targeted surfaces cannot be seen so we recommend only scoring the character if the maxilla and premaxilla are disarticulated and the anterior end of the maxilla is complete. Fine surface preservation is typically required also. Additionally, it is possible that this character is correlated with larger sizes; that is, it is easier to see in larger specimens.

432. Premaxilla, base of the posterodorsal process (maxillary process): (0) - flat with the body of the premaxilla; (1) - laterally bulging from the main body. (new; Fig. 14)

The base of the posterodorsal process of the premaxilla is typically continuous with the lateral surface of the body of the premaxilla in stem archosaurs (e.g., *Euparkeria capensis*, Ewer 1965; *Erythrosuchus africanus*, BPI 4526). Within Archosauria, state 0 is typical of avemetatarsalians (e.g., *Silesaurus opolensis*; Dzik 2003; *Coelophysis bauri*, Colbert 1989) and occurs throughout early diverging Pseudosuchia (e.g., *Xilousuchus sapingensis*, IVPP V6026; *Paratypothorax andressorum*, SMNS 19003; *Riojasuchus tenuisceps*, PVL 3827). In Loricata,

*Prestosuchus chiniquensis* (ULBRA-PVT-281), *Saurosuchus galilei* (PVSJ 32), *Heptasuchus clarki* (UW 11562), *Postosuchus kirkpatricki* (TTUP 9000), *Fasolasuchus tenax* (PVL 3850), and *Polonosuchus silesiacus* (ZPAL Ab III/543) all have laterally expanded base of the posterodorsal process of the premaxilla. The bulge is much clearer in some taxa (e.g., *Postosuchus kirkpatricki* TTUP 9000) than others (e.g., *Saurosuchus galilei,* PVSJ 32). Early crocodylomorphs (e.g., *Dromicosuchus grallator,* NCSM 13733) appear to also have state 1.

433. Jugal, lateral surface, anteroposteriorly trending ridge: (0) - symmetrical dorsoventrally; (1) - asymmetrical dorsoventrally where the dorsal portion is more laterally expanded. (new; Fig. 14)

The lateral surface of the jugal of archosaurs is either smooth or bears a ridge that parallels the ventral edge (character 75 of Nesbitt, 2011). The form of the ridge varies across Archosauria and can be a sharp ridge, broad, or laterally extended as a rugose and broad ridge. Most loricatans have some kind of ridge, but *Heptasuchus clarki* (UW 11562) and *Batrachotomus kupferzellensis* (SMNS 52970) share a clear expanded ridge that is asymmetrical dorsoventrally where the dorsal portion is more laterally expanded. Taxa without ridges on the lateral side of the jugal (taxa scored as 75-0) are scored as inapplicable (-) for this character.

# Figure 1

Distribution of Chugwater Group strata in Wyoming near the location of the type locality of *Heptasuchus clarki*

Stratigraphic section at the type locality of *Heptasuchus clarki* in the upper portion of the unnamed red beds of the upper portion of the Chugwater Group, Big Horn Mountains and a detailed stratigraphic section through the bonebed. Abbreviations: cm, centimeters; GSF, Gypsum Springs Formation; J, Jurassic; LS, limestone; SS, sandstone. [1 column]

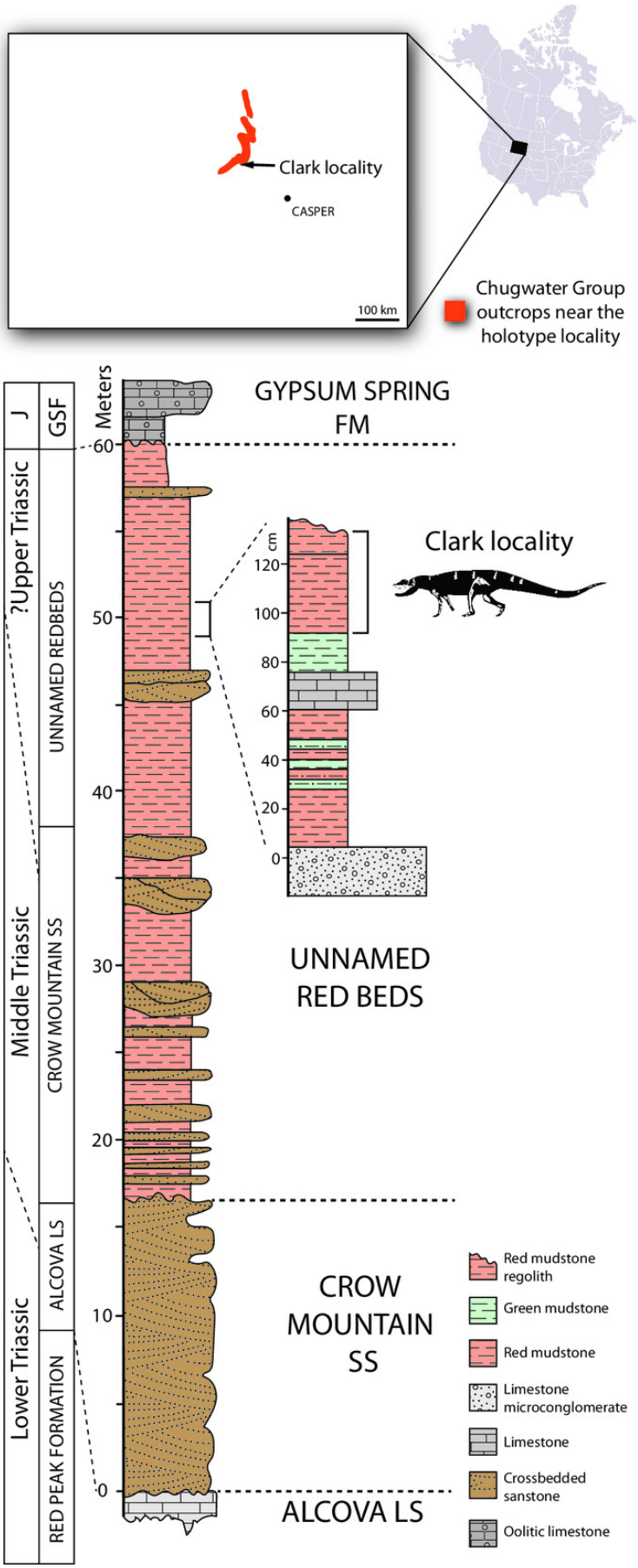
Clark locality
CASPER
100 km
Chugwater Group outcrops near the holotype locality
Meters
GYPSUM SPRING FM
Clark locality
cm
UNNAMED RED BEDS
CROW MOUNTAIN SS
ALCOVA LS
Red mudstone regolith
Green mudstone
Red mudstone
Limestone microconglomerate
Limestone
Crossbedded sanstone
Oolitic limestone
Lower Triassic
Middle Triassic
?Upper Triassic
J
GSF
UNNAMED REDBEDS
CROW MOUNTAIN SS
ALCOVA LS
RED PEAK FORMATION

# Figure 2

The holotype skull of *Heptasuchus clarki* (UW 11562) as found in the field

Image credit: Robert M Dawley. Abbreviations: bc, braincase; j, jugal; l., left; mx, maxilla; n, nasal; pmx, premaxilla; po, postorbital; r., right; sp?, splenial?. Scale = 20 cm [1 column]

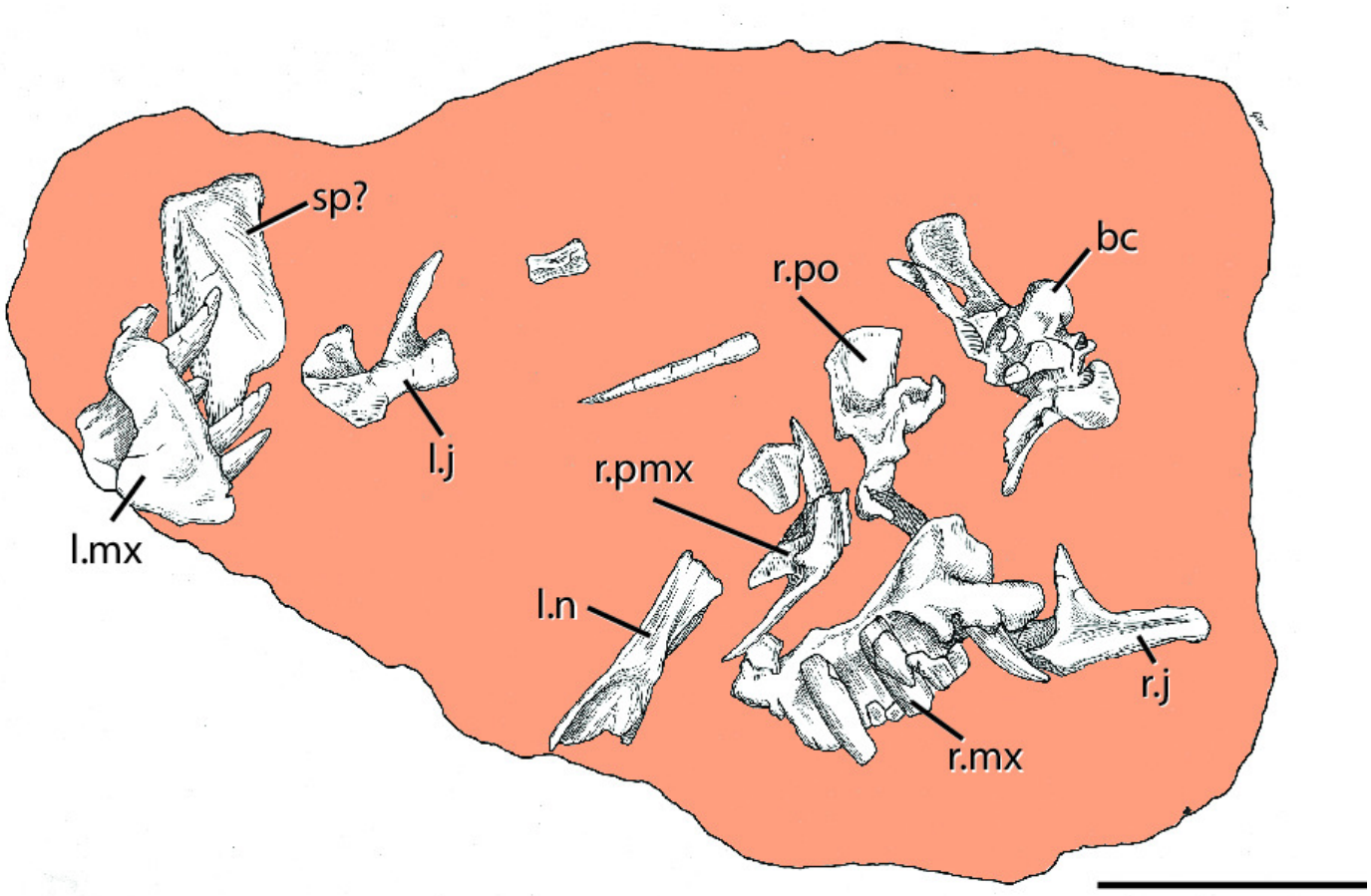

# Figure 3

Reconstruction of the skull of *Heptasuchus clarki* in right lateral view illustrating the material recovered (light red) from the type locality

Skull reconstruction based on *Batrachotomus kupferzellensis* from Gower (1999).

Abbreviations: fr, frontal; j, jugal, la, lacrimal; mx, maxilla, na, nasal; pmx, premaxilla; po, postorbital; pof, postfrontal; prf, prefrontal; q, quadrate; qj, quadratojugal; sq, squamosal.

Scale = 5 cm. [1 column]

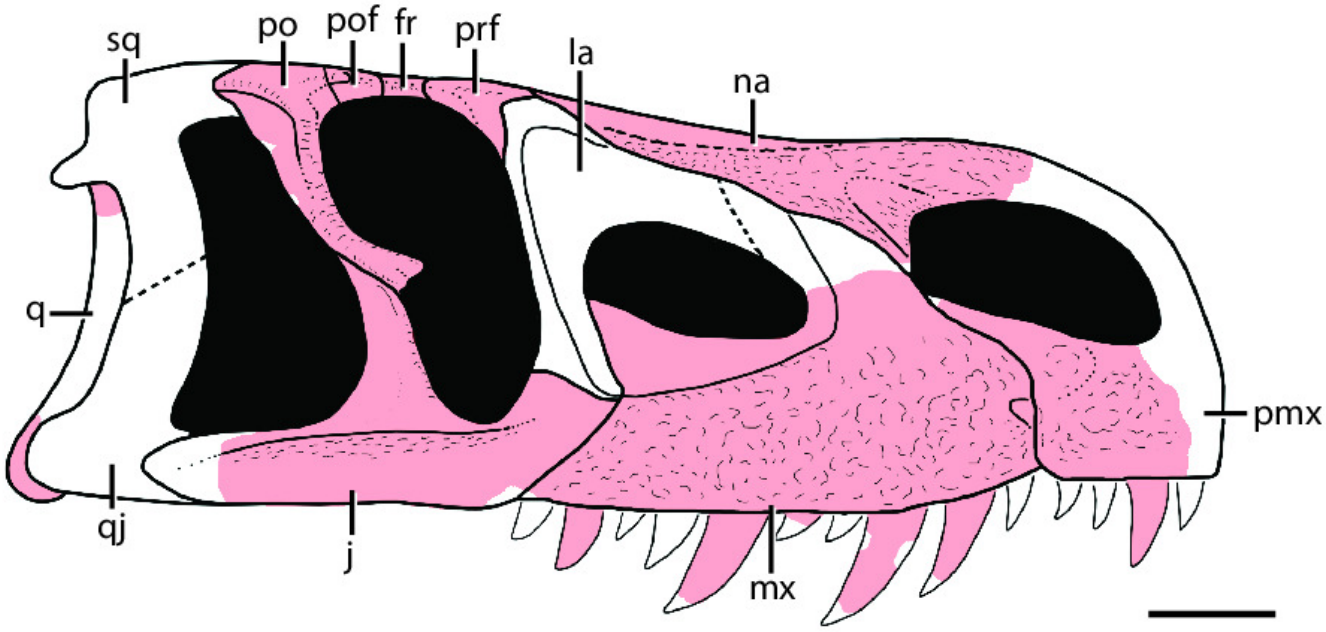

# Figure 4

Reconstruction of the skeleton of *Heptasuchus clarki* in lateral view illustrating the material recovered from the type locality

Skeleton reconstruction based on *Postosuchus kirkpatricki* (Nesbitt et al. 2013) and skull reconstruction based on Figure 3. Scale = 50 cm. [2 columns]

# Figure 5

Skull elements of *Heptasuchus clarki* (UW 11562):

left maxilla (UW 11562-C) in lateral (A) and medial (B) views; right maxilla (UW 11562-B) in medial (C) and lateral (D) views; right premaxilla (UW 11562-A) in lateral (E) and medial (F) views; right nasal (UW 11562-F) in lateral (G) and medial (H) views. Abbreviations: a., articulates with; al, alveolus; anf, antorbital fenestra; anfo, antorbital fossa; apn, anterior process of nasal; d, depression; dp, dorsal process; en, external naris; f, fossa; for, foramen; fr, frontal; j, jugal; la, lacrimal; ms, midline suture; mx, maxilla; mpn, maxillary process of nasal; nf, narial fossa; pd, posterodorsal process; plp, palatal process of the premaxilla; plm, palatal process of the maxilla; pmx, premaxilla; r, ridge; rt, replacement tooth; t, tooth; tr, tooth root. Broken surfaces indicated in hash marks. Arrows indicate anterior direction. Scales = 5 cm. [2 columns]

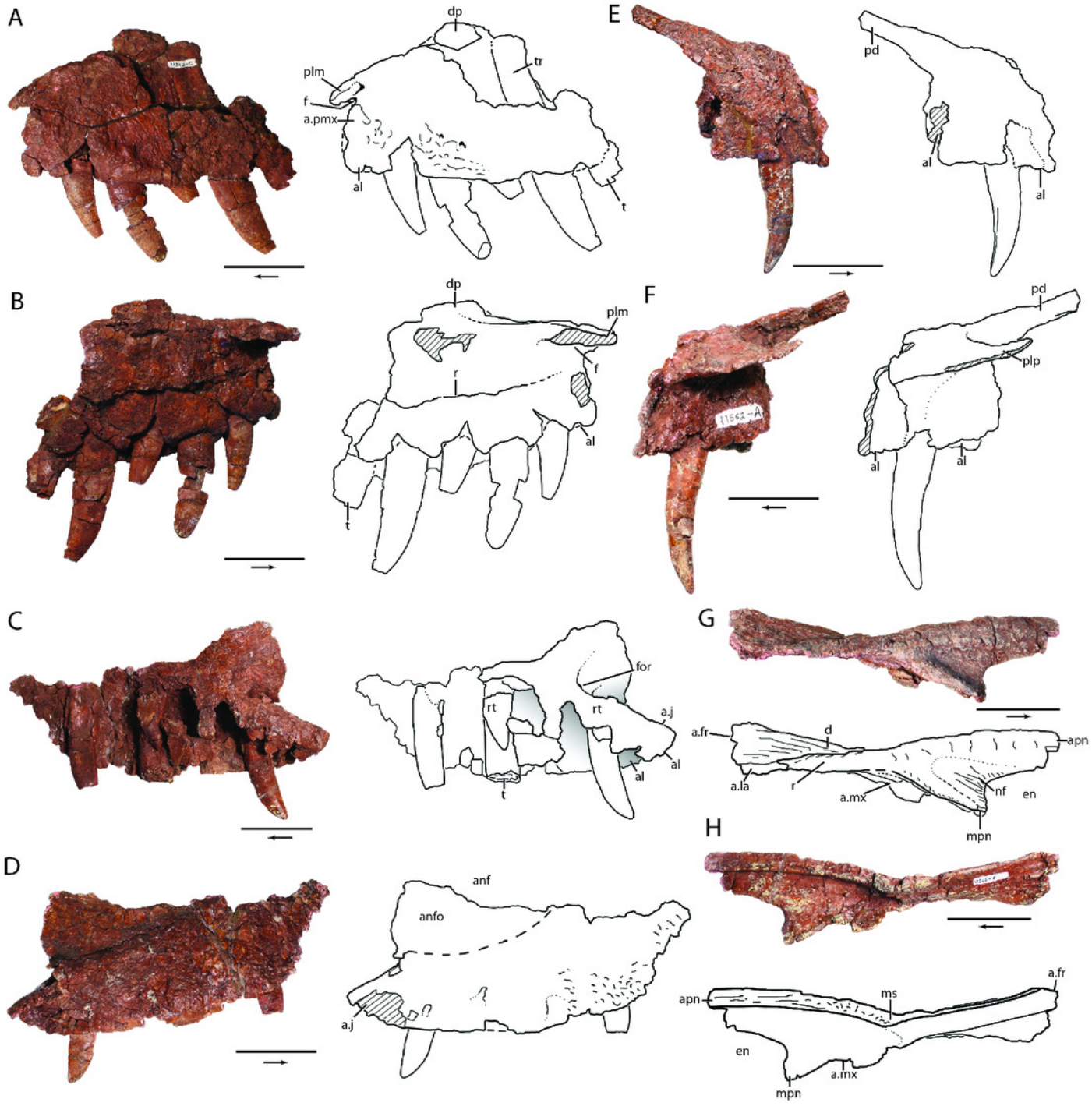
A
dp
plm
f
a.pmx
tr
al
t
E
pd
al
al
B
dp
plm
f
f
al
t
F
pd
plp
11562-A
al
al
C
for
rt
rt
a.j
al
al
t
G
a.fr
d
apn
a.la
r
a.mx
nf
en
mpn
D
anf
anfo
a.j
H
a.fr
ms
apn
en
a.mx
mpn

# Figure 6

Skull elements of *Heptasuchus clarki* (UW 11562):

right postorbital, postfrontal, and frontal (UW 11562-G) in dorsal (A), medial (B) and, with the reattached prefrontal in lateral (C) views; right jugal (UW 11562-D) in lateral (D) and medial (E) views; left palatine (UW 11562-K) in dorsal (F) view. Abbreviations: a., articulates with; d, depression; ec, ectopterygoid; f, fossa; fr, frontal; g, groove; la, lacrimal; ltf, lower temporal fenestra; mx, maxilla; o, orbit; pa, parietal; pf, postfrontal; po, postorbital; prf; prefrontal; sqm squamosal; r, ridge; stf; supratemporal fenestra; stfo, surpratemporal fossa. Broken surfaces indicated in hash marks. Arrows indicate anterior direction. Scales = 5 cm. [2 columns]

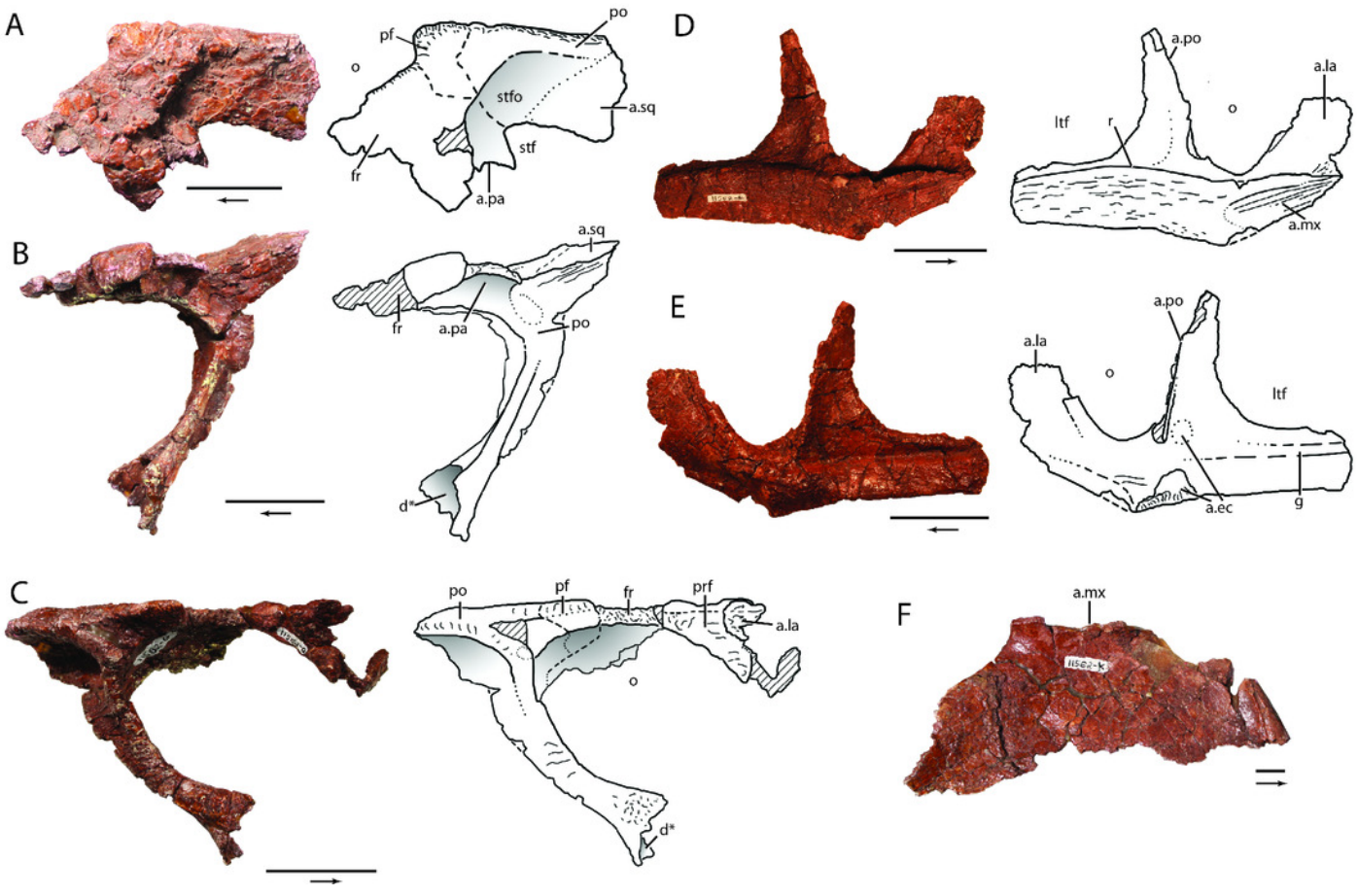

# Figure 7



The braincase of *Heptasuchus clarki* (UW 11562-H) in right lateral (A), posterolateral (B), medial (C) and posterior (D) views.

Abbreviations: bt, basitubera; bpt, basipterygoid process; ci, crista interfenestralis; cp, cultriform process; f, fossa; fo, fenestra ovalis; g., groove for; ic, entrance of the internal carotid; lr, lateral ridge; mf, metotic foramen; np, notochoral pit; oc, occipital condyle; pa, parietal; pbs, parabasisphenoid; pp, paroccipital process of the otoccipital; ppt; ridge possibly for attachment of protractor pterygoidei; ptf, posttemporal fenestra; so, supraoccipital; ug, unossified gap; V, exit of cranial nerve V (trigeminal); VI, exit of cranial nerve VI (abducens); VII, exit of cranial nerve VII (facial); XII, exit of cranial nerve XII (hypoglossal). Broken surfaces indicated in hash marks. Arrows indicate anterior direction. Scales = 5 cm. [2 columns]

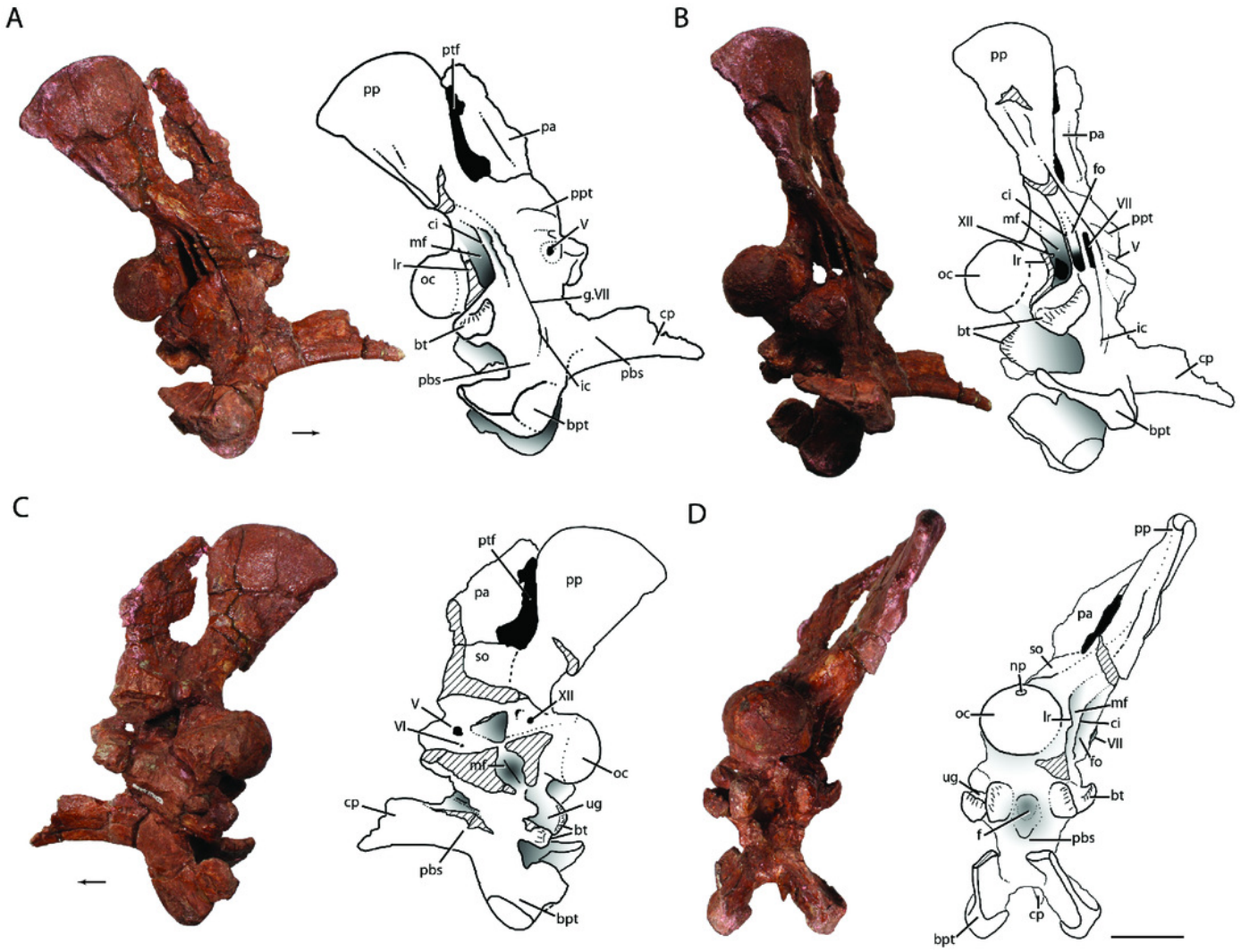
A
ptf
pp
pa
ppt
ci
V
mf
lr
oc
g.VII
cp
bt
pbs
ic
pbs
bpt
B
pp
pa
fo
ci
VII
XII
mf
ppt
V
lr
oc
bt
ic
cp
bpt
C
ptf
pp
pa
so
V
XII
VI
mf
oc
cp
ug
bt
pbs
bpt
D
pp
pa
so
np
oc
lr
mf
ci
VII
fo
ug
bt
f
pbs
cp
bpt

# Figure 8

Fragmentary skull elements of *Heptasuchus clarki:*

ventral portion of the left quadrate (UW 11563-AF + UW 11563-H, labeled before putting together) in posterior (A), anterior (B), and ventral (C) views; dorsal head of the quadrate (side unknown; UW 11562) in lateral? (D) view; possible fragments of the pterygoid (UW 11562-M) in two (E-F) views; possible fragment of the pterygoid (UW 11562-L) in two (G-H) views. Arrows indicate anterior direction. Scales = 1 cm. [1 column]

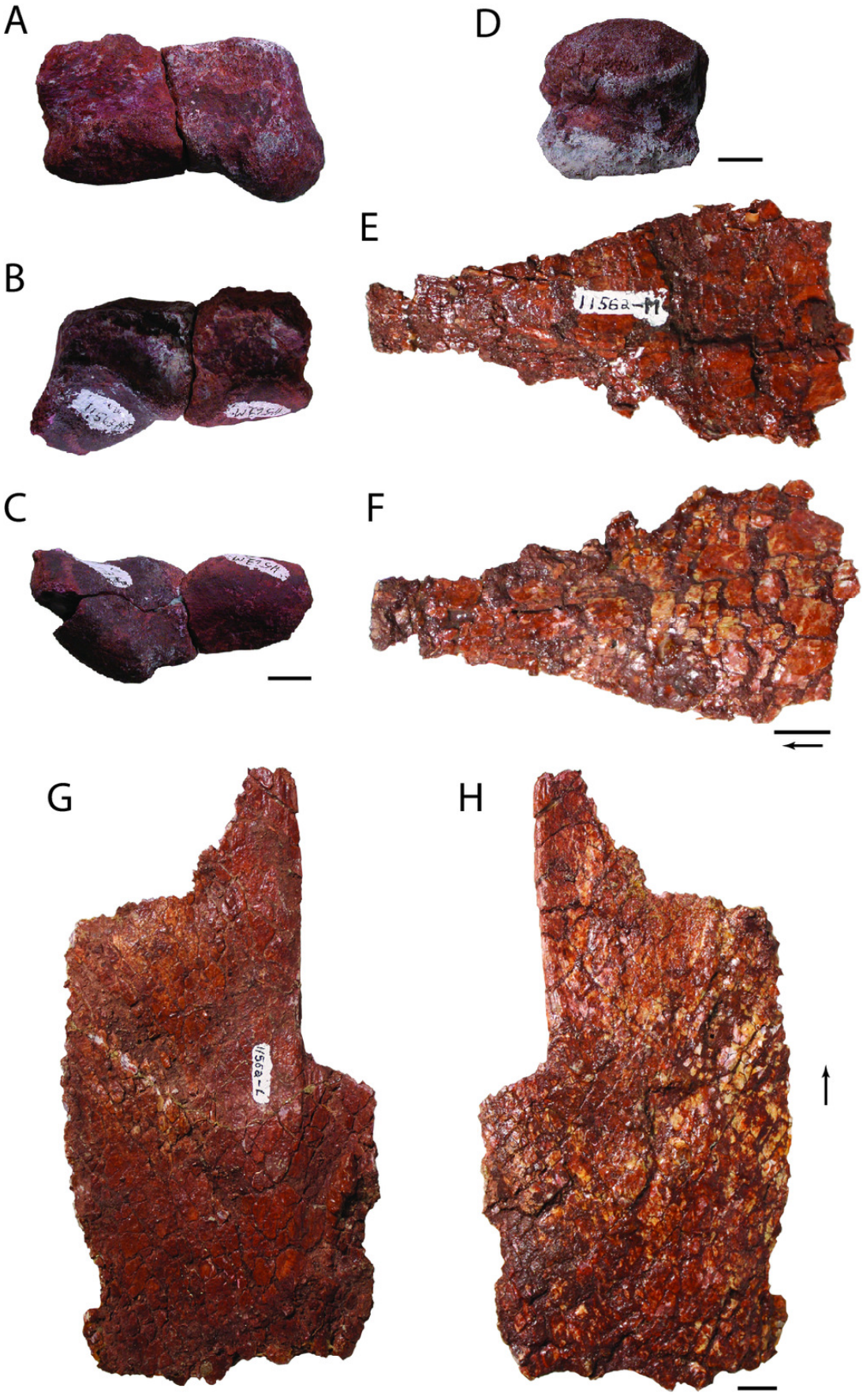
A
D
E
B
11562-M
C
F
G
H
11598-7

# Figure 9

Axial elements of *Heptasuchus clarki*:

posterior trunk vertebra (TMM 45902-2) in right lateral (A) and posterior (B) views; neural spine of a cervical-trunk vertebra (UW 11562-CX) in dorsal (C) and posterior (D) views; presacral neural spine (UW 11562-V) in lateral (E) view; presacral neural spine (UW 11562-CT) in lateral (F) view; anterior caudal vertebra in lateral (G) and anterior (H) views; distal caudal vertebra (UW 11562-BW) in ventral (I) and posterior (J) views; osteoderm (TMM 45902-1) in three views; anterior caudal vertebra in dorsal (K), ventral (L), and lateral (M) views. Arrows indicate anterior direction. Scales = 1 cm. [1 column]

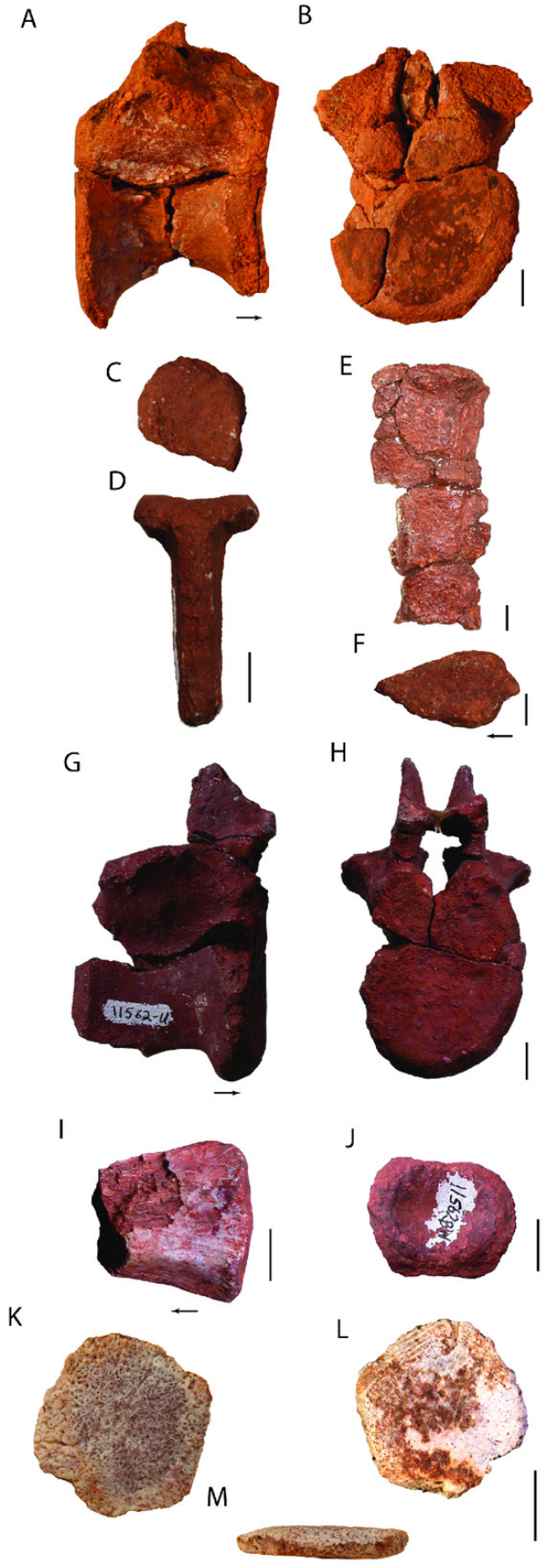
A
B
C
D
E
F
G
H
I
J
K
L
M

# Figure 10

Pectoral elements and incomplete humerus of *Heptasuchus clarki:*

right incomplete scapula (UW 11565-E) in lateral (A) view; incomplete left coracoid (UW 11566) in lateral (B) view; proximal portion of left humerus (UW 11565-A) in proximal (C) and posterior (D) views. Arrows indicate anterior direction. Abbreviations: cf, coracoid foramen; dp, deltopectoral crest; gl, glenoid; tu, tuber. Scales = 1 cm. [1 column]

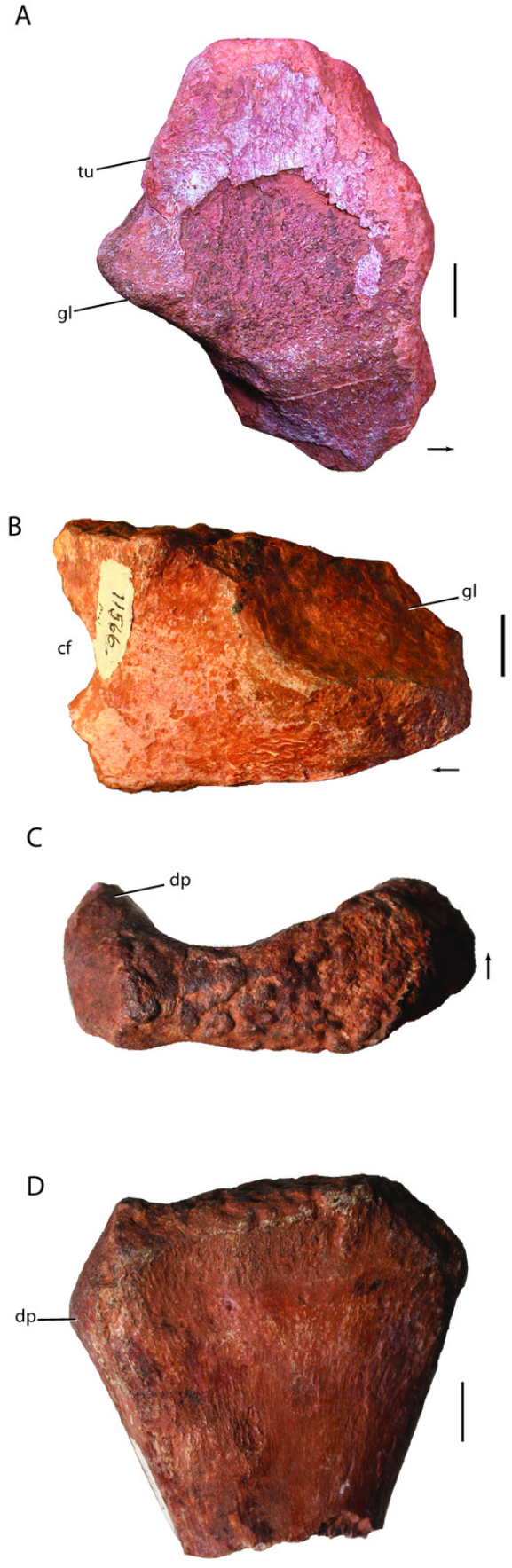
A
tu
gl
B
gl
cf
C
dp
D
dp

# Figure 11

Forelimb elements of *Heptasuchus clarki*:

proximal portion of the radius (UW 11562-DM) in proximal (A), and lateral (B) views and the distal portion of the radius (UW 11562-DI) in ?anterior (C) and distal (D) views; right ulna (UW 11562-W) in proximal (E), medial (F), posterior (G), and distal (H) views; left ulna (UW 11562-X) in proximal (I), posterior (J), anterior (K), and distal (L) views. Abbreviations: gr, groove; lr, lateral ridge; op, olecranon process; r, ridge. Scales = 1 cm in A-D and 5 cm in E-L. [1 column]

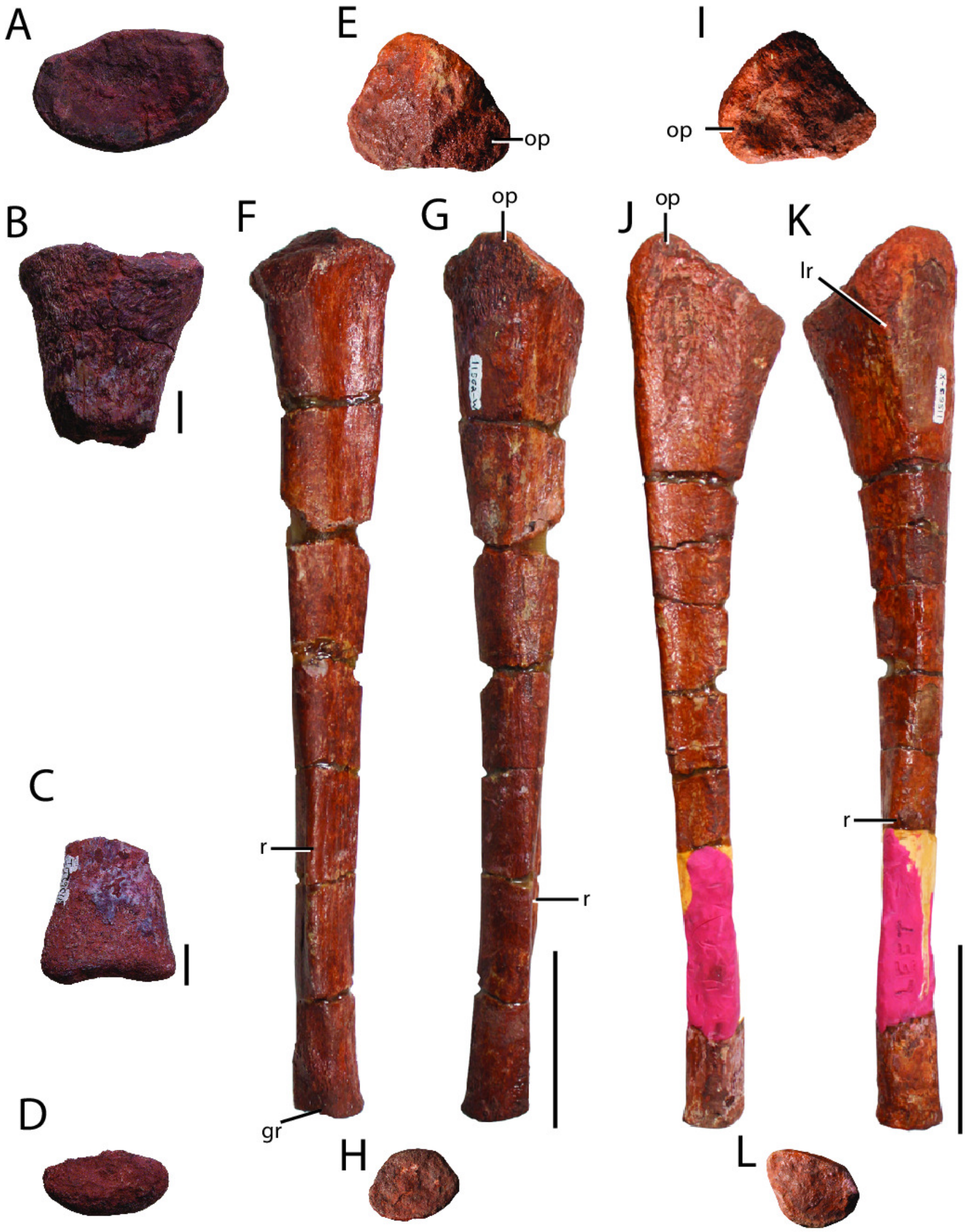
A
E
op
I
op
B
F
G
op
J
op
K
lr
r
r
r
gr
C
D
H
L

# Figure 12

Pelvic elements of *Heptasuchus clarki*:

left pubis (UW 11562-Y) in lateral (A), anterior (B), medial (C), and distal (D) views; proximal portion of the right ischium (UW 11564-B) in lateral (E) view; pubic peduncle of the right ilium (UW 11563) in lateral (F) view. Abbreviations: a., articulates with; as, acetabulum; il, ilium; pa, pubic apron; pb, pubic boot; pit, pit; pp, pubic peduncle; pu, pubis. Arrows indicate anterior direction. Scales = 5 cm in A-B and 1 cm in E-F. [1 column]

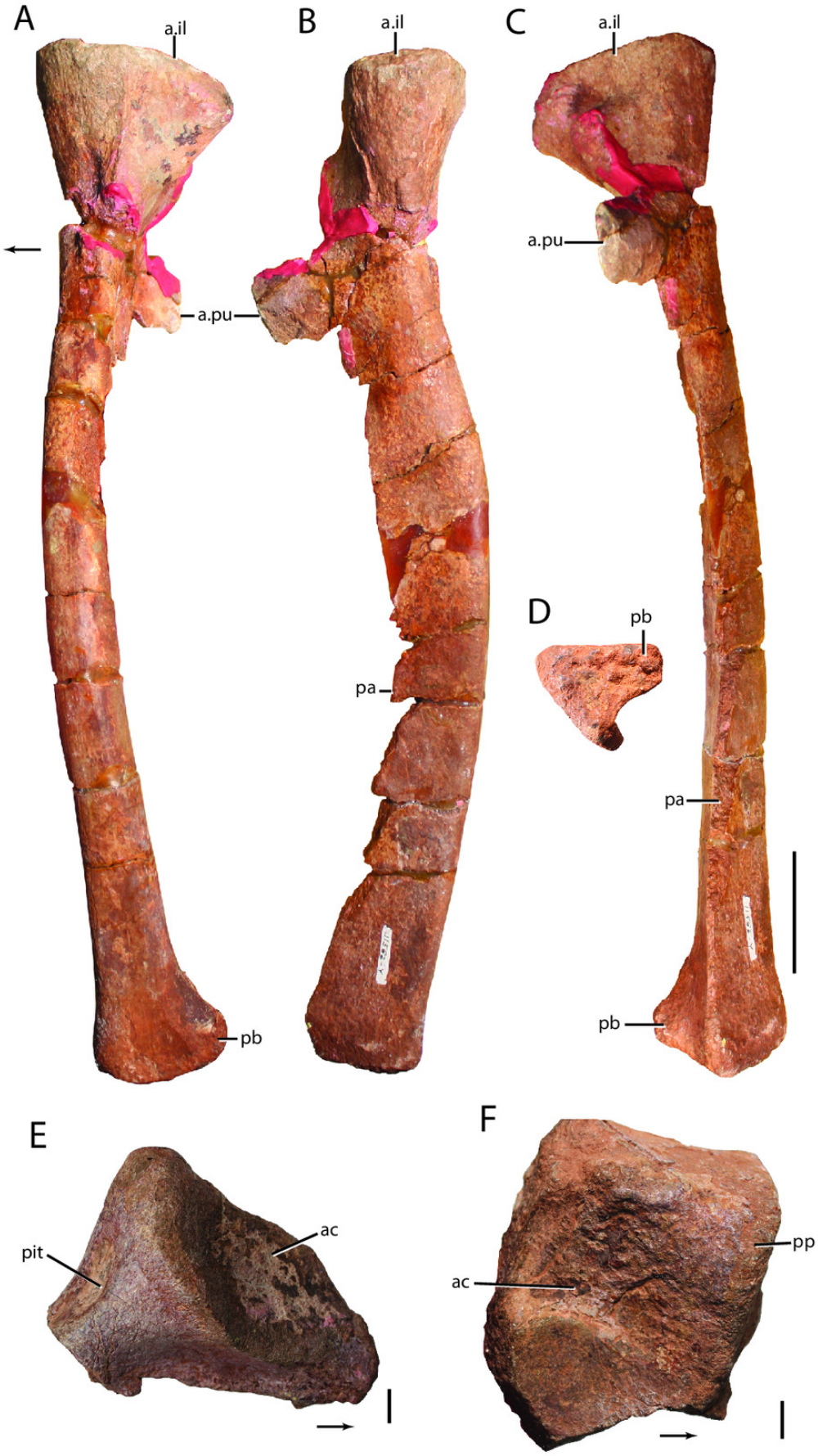
A
a.il
a.pu
pb
B
a.il
pa
C
a.il
a.pu
D
pb
pa
pb
E
pit
ac
F
pp
ac

# Figure 13

Hindlimb elements of *Heptasuchus clarki*:

proximal portion of a right femur (UW 11563-B) in proximal (A) and anterolateral (B) views and the distal portion of the right femur (UW 11563-A) in anterior (C) and distal (D) views; left tibia (UW 11562-Z) in proximal (E), posterior (F), anterior (G), and distal (H) views; proximal portion of a right fibula (UW 11566-S) in proximal (I) and anterolateral (J) views and the distal portion of the right fibula (UW 11566-R) in anterior (K) and distal (L) views. Right proximal portion of metatarsal IV (UW 11566) in proximal (M) and ventrolateral (N) views. Possible right metatarsal II (UW 11562DU) in proximal (O) and dorsomedial (P) views. Possible pedal ungual (UW 11562DT) in proximal (Q) and dorsal (R) views. Abbreviations: alc, anterolateral tuber; amt, anteromedial tuber; cc, cnemial crest; ctf, crista tibiofibularis; lc, lateral condyle; mc, medial condyle; plt, posterolateral tuber. Arrows indicate anterior direction. Scales = 1 cm in A-D, I-R and = 5 cm in E-H. [1 column]

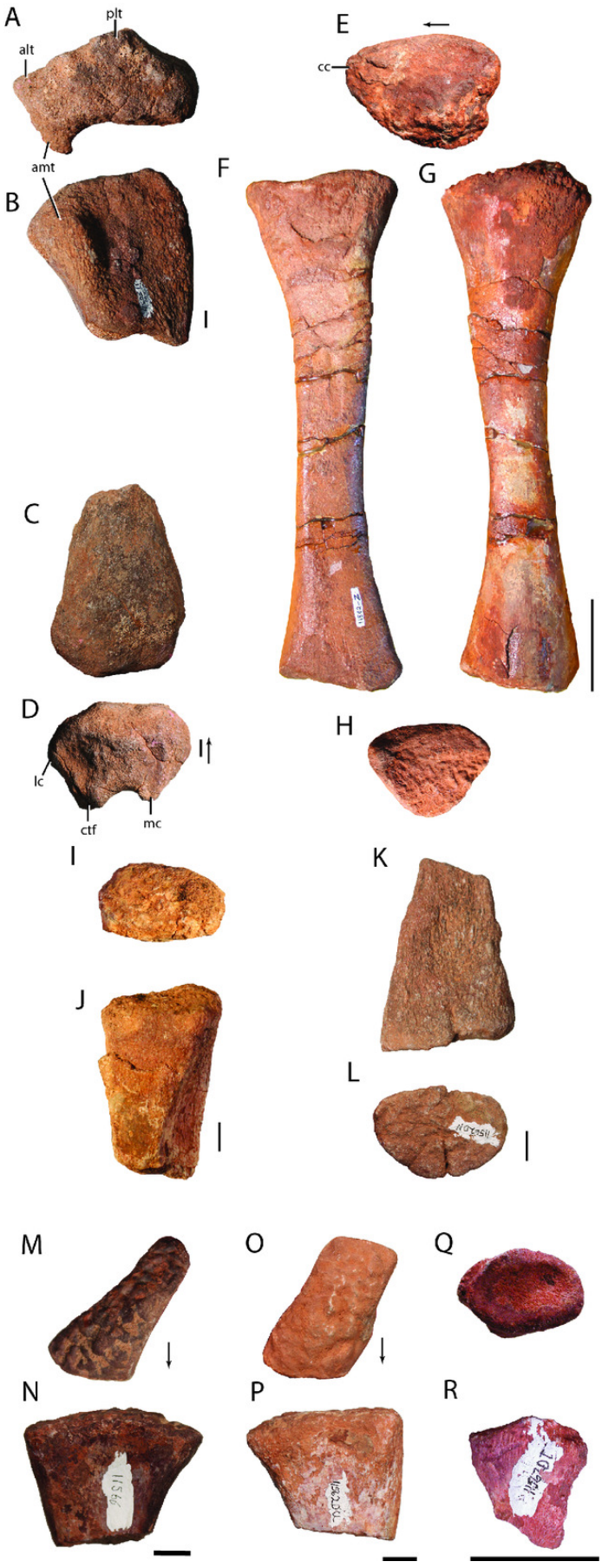
A
plt
alt
amt
B
I
E
cc
F
G
C
D
lc
ctf
mc
H
I
K
J
L
M
O
Q
N
P
R

# Figure 14

New illustrated character states for paracrocodylomorph archosaurs:

(A) skull referred to *Prestosuchus chiniquensis* (ULBRA-PVT-281) in right lateral view; (B) right postorbital of *Batrachotomus kupferzellensis* (SMNS 52970) in dorsal (top) and lateral (bottom) view; (C) left postorbital of *Heptasuchus clarki* (UW 11562) in lateral view; (D) left maxilla of *Batrachotomus kupferzellensis* (SMNS 52970) in medial view; (E) right maxilla of *Heptasuchus clarki* (UW 11562) in medial view; (F) right nasal of *Batrachotomus kupferzellensis* (SMNS 52970) in lateral view; (G) right nasal of *Heptasuchus clarki* (UW 11562) in lateral view; (H) left maxilla of *Xilousuchus sapingensis* (IVPP V6026) in medial view; (I) right premaxilla of *Heptasuchus clarki* (UW 11562) in lateral view; (J) left premaxilla of *Postosuchus kirkpatricki* (TTUP 9000) in lateral view; (K) left premaxilla of *Xilousuchus sapingensis* (IVPP V6026) in lateral view; (L) right jugal of *Heptasuchus clarki* (UW 11562) in lateral view; (M) right jugal of *Heptasuchus clarki* (UW 11562) in medial view; (N) left jugal of *Batrachotomus kupferzellensis* (SMNS 52970) in lateral view; (O) left jugal of *Batrachotomus kupferzellensis* (SMNS 52970) in medial view. Numbers refer to character number separated by a dash from the state. Scales in 10 cm in A, 5 cm in C-G, I, L-M, and 1 cm in B, H, J-K, N-O. [2 columns]

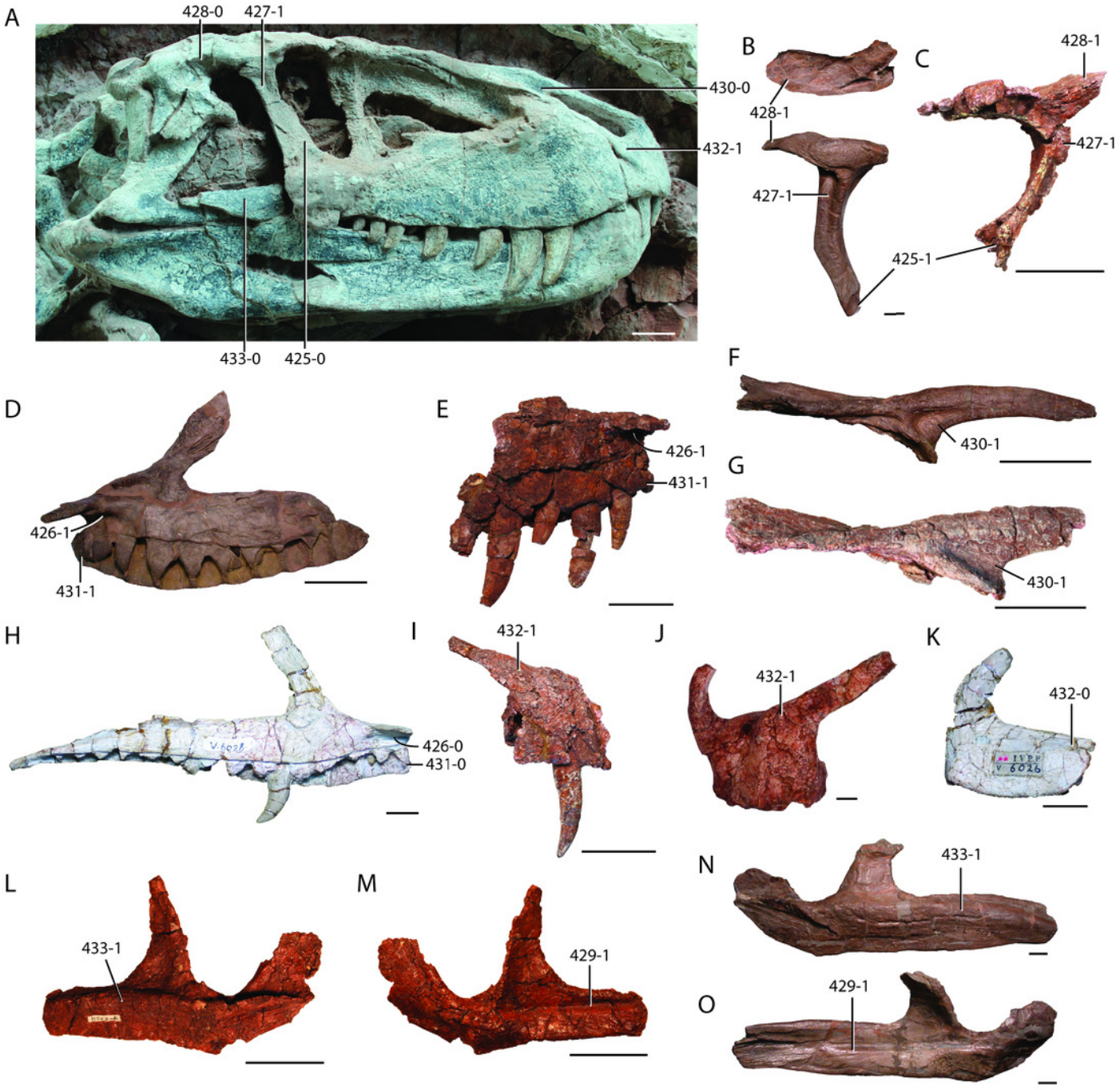
A
428-0
427-1
430-0
432-1
433-0
425-0
B
428-1
427-1
C
428-1
427-1
425-1
D
426-1
431-1
E
426-1
431-1
F
430-1
G
430-1
H
426-0
431-0
I
432-1
J
432-1
K
432-0
L
433-1
M
429-1
N
433-1
O
429-1

# Figure 15

Partial phylogenetic tree focused on pseudosuchian relationships with *Heptasuchus clarki* included

*Heptasuchus clarki* was found as a loricatan as the sister-taxon of *Batrachotomus kupferzellensis*. Tree derived from 72 most parsimonious trees (MPTs) of length (1529 steps) (Consistency Index = 0.335; Retention Index = 0.752)(see supplemental information figure S2). [1 column]

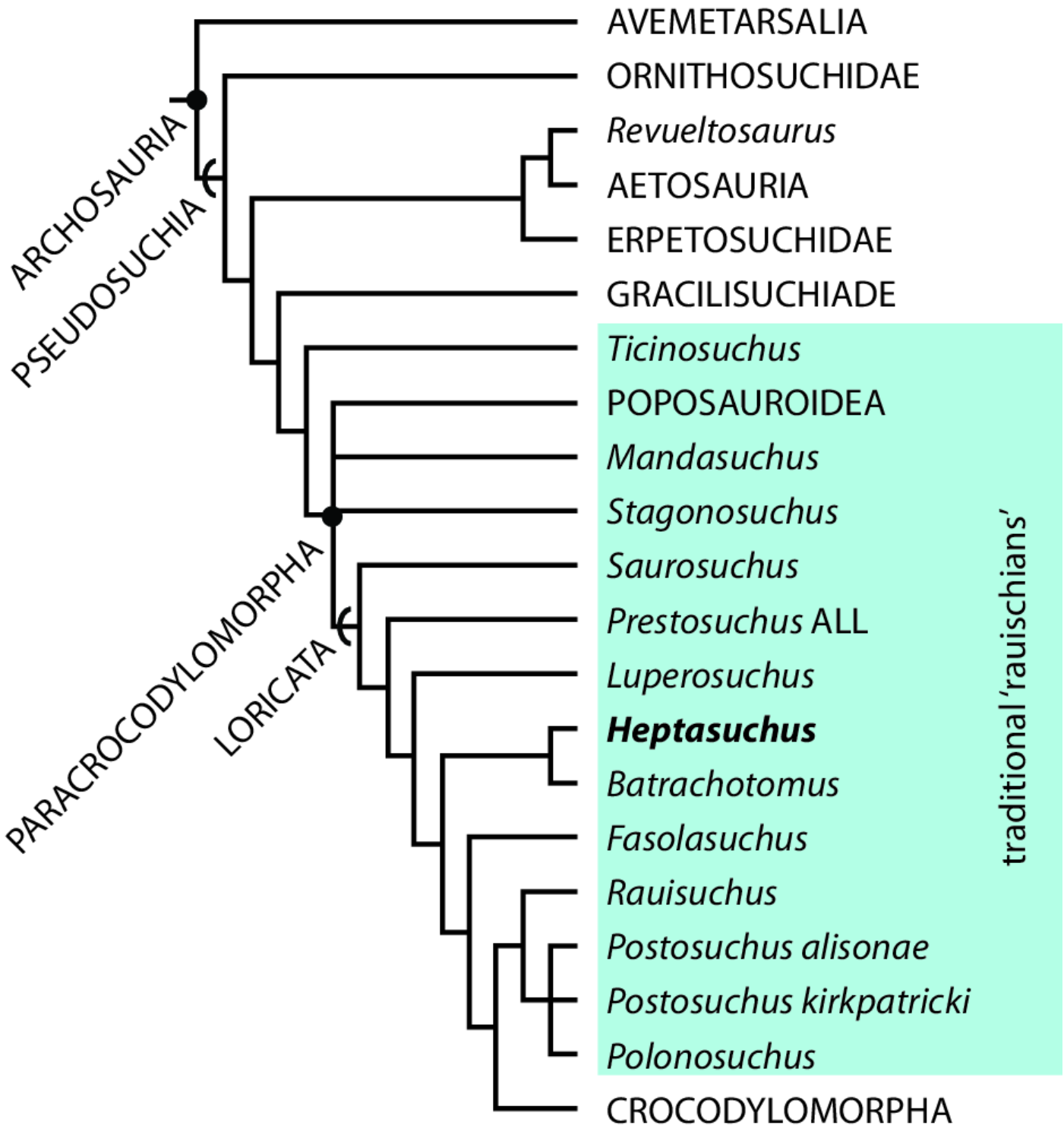
AVEMETARSALIA
ORNITHOSUCHIDAE
Revueltosaurus
AETOSAURIA
ERPETOSUCHIDAE
GRACILISUCHIADE
Ticinosuchus
POPOSAUROIDEA
Mandasuchus
Stagonosuchus
Saurosuchus
Prestosuchus ALL
Luperosuchus
Heptasuchus
Batrachotomus
Fasolasuchus
Rauisuchus
Postosuchus alisonae
Postosuchus kirkpatricki
Polonosuchus
CROCODYLOMORPHA
ARCHOSAURIA
PSEUDOSUCHIA
PARACROCODYLOMORPHA
LORICATA
traditional 'rauischians'